INFORMATION TO USERS

This material was produced from a microfilm copy of the original document. While the most advanced technological means to photograph and reproduce this document have been used, the quality is heavily dependent upon the quality of the original submitted.

The following explanation of techniques is provided to help you understand markings or patterns which may appear on this reproduction.

1. The sign or "target" for pages apparently lacking from the document photographed is "Missing Page(s)". If it was possible to obtain the missing page(s) or section, they are spliced into the film along with adjacent pages. This may have necessitated cutting thru an image and duplicating adjacent pages to insure you complete continuity.

2. When an image on the film is obliterated with a large round black mark, it is an indication that the photographer suspected that the copy may have moved during exposure and thus cause a blurred image. You will find a good image of the page in the adjacent frame.

3. When a map, drawing or chart, etc., was part of the material being photographed the photographer followed a definite method in "sectioning" the material. It is customary to begin photoing at the upper left hand corner of a large sheet and to continue photoing from left to right in equal sections with a small overlap. If necessary, sectioning is continued again — beginning below the first row and continuing on until complete.

4. The majority of users indicate that the textual content is of greatest value, however, a somewhat higher quality reproduction could be made from "photographs" if essential to the understanding of the dissertation. Silver prints of "photographs" may be ordered at additional charge by writing the Order Department, giving the catalog number, title, author and specific pages you wish reproduced.

5. PLEASE NOTE: Some pages may have indistinct print. Filmed as received.

University Microfilms International
300 North Zeeb Road
Ann Arbor, Michigan 48106 USA
St. John's Road, Tyler's Green
High Wycombe, Bucks, England HP10 8HR

Heat transfer during malignant hyperthermia in swine

by

Shui Man Yip

A Dissertation Submitted to the
Graduate Faculty in Partial Fulfillment of
The Requirements for the Degree of
DOCTOR OF PHILOSOPHY

Major: Biomedical Engineering

Approved:

Signature was redacted for privacy.

In Charge of Major Work

Signature was redacted for privacy.

Professor-in-charge,
Program in
Biomedical Engineering

Signature was redacted for privacy.

For the Graduate College

Iowa State University
Ames, Iowa
1977

TABLE OF CONTENTS

LIST OF SYMBOLS

A	Area, cm^2
C_p	Heat capacity, cal/gm ^oC
CB	Convective effect of blood flow, cal/min
h	Heat transfer coefficient, cal/cm^2 min ^oC
H	Rate of heat loss to the environment from the skin by radiation and free convection, cal/min
k	Thermal conductivity, cal/min ^oC cm
L	Length, cm
M	Metabolic heat generation, cal/min
Q	Heat flow rate into or out of a layer by conduction, cal/min
r	Radius, cm
R	Geometric radius of a layer bounded by radius r, cm
RESP	Heat loss rate by respiration, cal/min
T	Temperature, ^oC
V	Volume, cm^3
w	Blood flow rate, ml/min
β	Correction term for calculation of heat transfer coefficient associated with true surface temperature, dimensionless
ϵ	Emissivity, dimensionless
ρ	Density, gm/cm^3
σ	Stefan-Boltzmann constant, 1.355×10^{-12} cal/sec cm^2 ^oK

μ	The true mean value of a variable

Subscripts:

a	Ambient environment
b	Blood
c	Core layer
m	Muscle layer
$\dot{m}$	Malignant hyperthermia susceptible animal
s	Skin layer
n	Normal animal
ss	True skin surface
o	Initial steady-state condition
rad	Radiation
con	Conduction and convection for free convection condition
1	Head core
2	Head muscle
3	Head fat
4	Head skin
5	Trunk core
6	Trunk muscle
7	Trunk fat
8	Trunk skin
9	Hind leg core
10	Hind leg muscle

11	Hind leg fat
12	Hind leg skin
13	Hind foot core
14	Hind foot muscle
15	Hind foot fat
16	Hind foot skin
17	Front leg core
18	Front leg muscle
19	Front leg fat
20	Front leg skin
21	Front foot core
22	Front foot muscle
23	Front foot fat
24	Front foot skin

INTRODUCTION

Normally, the central core temperature of a mammal stays very close to a set point. Large temperature variations in the environment can be tolerated by most healthy domesticated animals.

The body maintains its temperature distribution in steady-state by balancing heat production and heat loss. Heat is normally generated by the body through the process of metabolism. Thermal energy is either stored in the body, which leads to a rise in temperature, or conducted away through the tissues to the environment. Heat transfer from one part of the body to another depends not only on conduction, but also on the convective circulation of blood. Conduction, convection, radiation and evaporation from the body surfaces are all responsible for heat loss to the environment. By varying the metabolic rates and blood flows in parts of the body, different temperature distributions can be achieved. If for any reason, the heat generated by metabolism and carried by blood circulation is not balanced by the heat loss at any location, the temperature at that location will change. If heat generation and loss is not balanced for the body as a whole, the overall body temperature will change.

In man, the syndrome of "malignant hyperthermia"

produces rapid temperature elevation when a malignant hyperthermia susceptible (MHS) individual is anesthetized with certain kinds of anesthetic agents. The syndrome is rare, but the mortality of about 64% is relatively high.

In swine, there are similar syndromes: the "porcine stress syndrome" (81), the "pale, soft and exudated pork syndrome" and the anesthetic-induced "malignant hyperthermia syndrome" (54). An individual subject undergoing hyperthermia in any of the syndromes mentioned above usually experiences a very rapid rise in body temperature.

The objectives of this study were to develop a flexible mathematical model of a mammalian thermoregulatory system and to test its ability to simulate relatively rapid temperature changes. Experiments were conducted to determine the local temperature behavior with time in both normal and malignant hyperthermia susceptible pigs during the administration of the anesthetic drug halothane. A mathematical model was developed to describe the hyperthermic temperature changes from the start of the syndrome until an hour post-mortem. The purpose of the model was to test the basic hypotheses regarding thermoregulation mechanisms in the system.

It must be recognized that the thermoregulatory system is affected by many factors, some of which are very

complicated and almost impossible to describe quantitatively. Any attempt to model a physiological system must greatly simplify the conditions involved. Many assumptions must be made. Such conceptual models will undoubtedly be less flexible than the biological system in producing the phenomenon of interest.

The experimental part of this research involved measuring temperatures and relative blood flow for swine under anesthesia with halothane. A set of differential equations were derived to describe the temperature changes. They were solved numerically by a digital computer to produce simulated data that were in turn compared with the experimental results. This modeling process was carried out in an attempt to develop a more sound understanding of the quantitative aspects of malignant hyperthermia.

LITERATURE REVIEW

Malignant Hyperthermia

History

Malignant hyperthermia, a condition characterized by a sharp rise in body temperature often associated with muscle rigor, has been described in humans by many authors (7,44). The syndrome has also been described in anesthetized pigs by Topel et al. (81) and others (1,45,79).

Probably the first reported cases of malignant hyperthermia were given by Guedel in 1937 (37). Later, other instances were reported by Brown (11), Davies et al. (17), Denborough and Lovell (24), and many others (7,71).

Discussion of the syndrome has appeared in leading articles in the British Medical Journal many times (59,60,61), and international symposia on the subject have been held twice.

Before 1970, a lot of effort was put into case reporting and into investigation of the relation between myopathy and malignant hyperthermia (21,56,71,76).

Recently, more effort is being directed into investigation of the etiology and drug management in pigs (4,14,34,36,41,84), which seem to experience the same malignant hyperthermia syndrome as occurs in man (45,70) and thus are available as models of the human abnormality.

Screening for malignant hyperthermia

Because of the fact that serum creatine phosphokinase (CPK) concentrations are usually elevated in MHS individuals (50,57), serum CPK level has been used as a measure for the identification of MHS individuals. However, Ellis et al. (25,26) and King et al. (57) found that CPK evaluation occasionally gave false results.

Another way of screening for malignant hyperthermia is by the testing of skeletal muscle specimens for halothane-induced contracture in vitro. However, Kalow et al. (56) did not obtain halothane-induced muscle contracture in skeletal muscle specimens from MHS individuals while Moulds and Denborough (65) stated that all individuals with normal CPK level were found to have normal muscle contracture in vitro. Ellis et al. (26) reported that widely differing CPK values were found in different times in the same people. Nelson et al. (69) found that halothane-induced muscle contracture was temperature dependent. They also stated that it would be advisable to test the contracture response to a variety of pharmacological agents.

In swine, the screening is usually done by giving a small dose of the anesthetic agent directly to the animal and watching for temperature and rigidity response (36).

Clinical observation of malignant hyperthermia

The onset of the observable phenomena is rapid (10 to 15 minutes after administration of halothane), although it varies for different anesthetic agents and for different individuals (7). Skeletal muscle rigidity is usually the first sign of malignant hyperthermia (50), although this does not always occur (7).

Temperature rise usually follows muscle rigidity. The rate of rise varies for individuals. In humans, the body temperature may reach a maximum of 43°C, and the rate of rise varies between 1 to 5°C per hour with a mean of 4°C per hour (7,59). In swine, the core and muscle temperatures may rise to 45°C from 39°C within 30 minutes after halothane administration (4,14). The rate of increase of temperature has been observed to be as great as 0.2°C per minute in the core or muscle (45).

Sometimes tachypnea is observed (8,51,71). Rates of up to 125 breaths per minute have been recorded (45). Occasionally apnea develops as a consequence of skeletal muscle rigidity of the muscles of respiration (7).

Tachycardia usually occurs as an early sign of the syndrome (8,45,51,71). In some recorded cases, the heart rate increased, then decreased before increasing again terminally (55). In man, heart rates of up to 200 beats

per minute have been reported (7). Arrhythmias have also been observed by some researchers (7,55). Working with swine, Williams et al. (84) found that blood pressure increased, while Jones et al. (55) reported declining arterial blood pressure during the syndrome. Cardiac output was reported to decrease (84), as was blood flow to the skin.

In swine, blotchy cyanosis was often observed. Skin temperature was reported to be variable to the touch, some regions increasing, while others decreased (55).

The metabolic rate was found to increase approximately tenfold during the syndrome of malignant hyperthermia in swine (83). Oxygen consumption of hind limb muscles has been reported to increase up to threefold while the whole body oxygen consumption increased twofold (36).

Laboratory findings on malignant hyperthermia

Increase in arterial CO_2 partial pressure ($PaCO_2$) occurs soon after the initial onset of the syndrome (45,55). Arterial $PaCO_2$ can increase to 100mm of mercury (7,23). Maximal $PaCO_2$ occurs terminally in some swine, while in some others the degree of hypercapnia declines prior to death (45). Arterial PaO_2 has been reported to decline during malignant hyperthermia despite the administration

per minute have been reported (7). Arrhythmias have also been observed by some researchers (7,55). Working with swine, Williams et al. (84) found that blood pressure increased, while Jones et al. (55) reported declining arterial blood pressure during the syndrome. Cardiac output was reported to decrease (84), as was blood flow to the skin.

In swine, blotchy cyanosis was often observed. Skin temperature was reported to be variable to the touch, some regions increasing, while others decreased (55).

The metabolic rate was found to increase approximately tenfold during the syndrome of malignant hyperthermia in swine (83). Oxygen consumption of hind limb muscles has been reported to increase up to threefold while the whole body oxygen consumption increased twofold (36).

Laboratory findings on malignant hyperthermia

Increase in arterial CO_2 partial pressure ($PaCO_2$) occurs soon after the initial onset of the syndrome (45,55). Arterial $PaCO_2$ can increase to 100mm of mercury (7,23). Maximal $PaCO_2$ occurs terminally in some swine, while in some others the degree of hypercapnia declines prior to death (45). Arterial PaO_2 has been reported to decline during malignant hyperthermia despite the administration

of oxygen-rich gas mixtures (4,45). Jones et al. (55) reported that the arterial pH declined to 7.0 and below. Acidosis usually is profound with both gross metabolic and respiratory components in malignant hyperthermia. Blood lactate concentration increases markedly (79), as that of pyruvate (55) and glucose (4), though not to as large an extent as that of lactate. Allen et al. (1) also reported similar findings about plasma glucose level. Lucke et al. (62) found elevated catacholamine concentration in plasma during malignant hyperthermia.

Berman et al. (4) observed a shift of water into the intracellular space as indicated by an increase of sodium ion and total protein concentration. They also reported the shift of calcium and magnesium ions into the intracellular space. Jones et al. (55) also reported an increase of plasma inorganic phosphorus. Allen et al. (1) found an increase of plasma inorganic phosphorus of up to 100% in Pietrain pigs. Plasma potassium concentration increase has been found in some individuals but not in others by many groups (1,45,55).

Sybesma and Eikelenboom (79) noted the increase of lactic acid dehydrogenase and serum glutamic oxalic transaminase concentration in blood during malignant hyperthermia. They also reported the decline of adenosine triphosphate

(ATP) level in muscle. Allen et al. (1) and Britt and Kalow (7) reported similar results. Elevated creatine phosphokinase (CPK) level during malignant hyperthermia has been reported by many groups (21,51,71,88).

Histological findings of malignant hyperthermia

Various types of muscle pathology have been described in malignant hyperthermia. Steers et al. (76), Barnes (3), King et al. (57) and Denborough et al. (21) all indicated that there might be a relation between malignant hyperthermia and some type of myopathy. la Cour et al. (58) reported the presence of excessive nuclei in muscle fibers and of fibers of abnormal size and shape. They also found signs of degeneration of the intramuscular nervous system. Isaacs et al. (52) found fiber degeneration with marked lymphocytic infiltration. They also reported abnormal mitochondria and membrane changes consistent with neuropathy. They pointed out that destruction of muscle, swelling of fibers and interestitial edema would occur in an episode of malignant hyperthermia. Isaacs and Heffron (53) reported similar findings thought to be an indication for the presence of neuropathic myopathy associated with malignant hyperthermia.

Etiology

Cody (15) suggested that malignant hyperthermia may be an early manifestation of myotonia dystrophica. Harrison et al. (45) observed a fall in muscle ATP during the syndrome. It has been suggested that malignant hyperthermia may be due to insufficient ATP production secondary to the absence of muscle phosphorylase (8). Wilson et al. (85) and Isaacs et al. (52) noted the similarity between malignant hyperthermia and the uncoupling of oxidative phosphorylation which can be produced by poisoning with dinitrophenol (DNP). However, Wang et al. (82) pointed out that this alone was not adequate to account for the large amount of heat output in malignant hyperthermia. They noted that sustained muscular hyperactivity could increase metabolic rate to twenty times the basal level.

Clark et al. (14) pointed out that an abnormal quantity of heat could be produced by accelerated substrate cycling of fructose-6-phosphate. Britt et al. (6,9) found that halothane inhibited calcium uptake by the sarcoplasmic reticulum (SR) of MHS individuals. Isaacs and Heffron (53) suggested the possibility of decreased mitochondrial ATP synthesis resulting in gross inefficient restitution of the resting concentration of phosphocreatine and ATP.

Since ATP is needed for maintenance of normal sarcoplasmic calcium concentration, if demand for ATP is increased, ATP would soon be depleted and increased calcium concentration would lead to rigor of muscle. Denborough (20) pointed out that halothane induced a large release of calcium into the myoplasm of MHS individuals. Heffron et al. (47) reported that the uptake of calcium by MHS sarcoplasmic reticulum was lower than normal SR. It has been suggested that the syndrome could be due to a lesion of the excitation-contraction coupling mechanism (67).

Triggering pharmacological agents

Succinylcholine is often given to assist intubation. It has been found that this drug produces prolonged rigidity in MHS individuals (7). Hall et al. (39) found that the injection of suxamethonium with halothane-induced anesthesia produced hyperthermia. Denborough et al. (23) claimed that ether and trichlorethylene could trigger malignant hyperthermia. They also suspected methoxyfluorane, cyclopropane and chloroform to be triggering agents. Harrison et al. (45) had similar findings. Hall et al. (39) found that anesthetizing animals with nitrous oxide did not produce hyperthermia, whereas Ellis et al. (25) reported in some cases nitrous oxide did produce hyperthermia.

Treatment of malignant hyperthermia

Hall et al. (39) reported that anesthesia with thiopentane sodium could block the triggering of malignant hyperthermia. Harrison reported that alfadione appeared to block initiation of malignant hyperthermia by halothane (42). However, these drugs did not relieve the symptoms once the syndrome had been established (39,42).

Harrison (42) suggested that procaine hydrochloride could be used for treating the syndrome, whereas Hall et al. (39) pointed out that pretreatment with procaine hydrochloride prevented the onset of the syndrome, but the drug had no effect once muscle rigidity was present. Ellis et al. (25) reported that steroids of the dexamethasone could be used to treat the syndrome. Harrison (43) reported that dantrolene sodium pretreatment of MHS pigs blocked the initiation of hyperthermia. Gronert et al. (35) reported that dantrolene reversed the hyperventilation, hyperkalemia, and the increase of lactate, catecholamines and temperature. Anderson et al. (2) found that dantrolene sodium actually increased the rate of relaxation of halothane-induced contraction of MHS muscles.

Other steps for treatment of the syndrome include discontinuation of anesthesia, correction of acidosis, correction of hyperkalemia and aggressive cooling (39,41).

Gjessing et al. (29) suggested peritoneal dialysis with cooled dialysate could be used as a means for rapid cooling.

Mathematical Models of Temperature Changes

In the past few years, several mathematical models for simulating the temperature regulatory system in animals have been constructed. Reviews (28,49,75) have been written to classify the models.

Poppendiek et al. (73) measured the thermal conductivities of biological tissues. The experimental values were compared with values obtained by using a mathematical heat conduction model. The predicted values and experimental values differed by ±3% or less.

Stolwijk and Hardy (77) experimented on human skin temperature during irradiation of the body with thermal radiation. He divided the skin into eight layers and was able to simulate the changes fairly well with an analog computer.

Wyndham and Atkins (89) approximated the body with a cylinder of three layers; a core of bone and organs, a middle layer of muscle and fat, and a skin layer.

Crosbie et al. (16) used an analog computer to simulate the temperature regulation of a nude human during periods

of excercising and following environmental temperature shifts. The mean body temperature, T_b, which was obtained by weighting the temperatures of the different layers was the regulated variable. The thermal conductivities, heat generation and evaporative loss were all functions of T_b.

Wissler (86) divided the human body conceptually into six parts (torso, head, two arms and two legs). Each part was assumed to be a cylinder of three layers, the bone and core tissue, the fat layer and the skin layer; each supplied with arterial blood. The model gave analytical results that were consistent with experimental data. Wissler's improved model (87) had fifteen elements (head, thorax, abdomen, and the proximal, medial, and distal segments of the two arms and two legs). The blood supply to each segment was approximated by an arterial pool. The equations were solved by using the Crank-Nicholson's implicit finite difference method.

Stolwijk and Hardy (78) proposed a model that divided the body into three parts. The trunk consisted of three layers, while the head and the extremities each had two layers. Heat flows between adjacent layers were by conduction. All seven elements exchanged heat with the central blood compartment convectively. Temperature control was by a signal affected by the temperature deviation in

the brain and the average skin temperature. The signal activated a complicated regulatory system.

More recently, mathematical models were constructed and their performance tested by finite difference methods. The predicted results were often compared with experimental data obtained from animals subject to environmental temperature shifts.

Chan et al. (13) used the finite difference technique to investigate the temperature distribution in layers of tissue. The model consisted of three plane layers each containing a thermal source function which was produced from an electromagnetic or ultrasonic source and a cooling function which was the power per unit volume carried out by circulation.

Miller and Seagrave (64) divided the body conceptually into fifteen cylinders and developed a model for humans immersed in time-temperature varying water baths. The 21 simultaneous differential equations were solved numerically with a digital computer.

Gordon and Roemer (31,32) investigated the effect of radial nodal spacing on the performance of a mathematical model of temperature regulation. They found that a four-node model (i.e., a model in which each segmental element has four homogeneous tissue bands) gave

satisfactory results for mild, warm, or cold stresses. For large step environmental temperature changes (±5°C), a ten-node model was adequate. They later used a further developed model (33) to investigate transient cold exposure responses. The control mechanism which altered the individual tissue metabolism and blood flow rate was a complicated system that was affected by the head core temperature, individual skin temperatures and the skin heat flux.

Huckaba *et al.* (48) also investigated dynamic temperature distributions in the human body during environmental cooling with a forty-five-node model.

MATERIALS AND METHODS

Experimental Animals

Swine susceptible to malignant hyperthermia were identified by screening tests involving the inhalation of halothane for a short duration (81). Subjects were observed for signs of muscle rigidity and temperature rise. The screening was done when an animal weighed between 25 to 35 kg.

Six MHS and six normal Yorkshire pigs, all weighing between 50 to 80 kg were selected for this study.

Experimental Apparatus

Temperature measuring devices

Wheatstone bridge Tele-thermometers (Model 43TF)[1] were used to make temperature measurements in the animals. Temperatures of the skin layers were measured with hypodermic needle thermistors made from 18-gage needles and GB34L1 thermistors[2]. Temperatures of muscle and fat layers were measured with four-inch long 20-gage hypodermic needle thermistors[3]. Rectal temperatures were measured with a

---

[1]Yellow Springs Instrument Co., Yellow Springs, Ohio.

[2]Fenwal Electronics Inc., Framingham, Mass.

[3]Model YSI513, Yellow Springs Instrument Co., Yellow Springs, Ohio.

rectal probe thermistor (Model YSI401)[1].

Air temperatures were measured with an ordinary mercury thermometer.

Figure 1 shows the arrangement of the temperature measuring apparatus. The output of the battery-operated Wheatstone bridge Tele-thermometer was connected to a differential amplifier which consisted of two operational amplifiers (80). The output from the differential amplifier was then displayed as a voltage on a digital voltmeter. The thermistors used for temperature measurement at different locations in the animal were connected to a Wheatstone bridge thermometer temperature display unit. During the procedure of temperature measurement, a different thermistor would be connected to the display unit for each switch position. This process of recording seven different temperatures took less than half a minute.

All thermistors were calibrated with a mercury thermometer which was graduated in tenths of a degree Centigrade. The calibration was done in a water bath in temperature steps of 0.8°C. Temperature versus voltage data were plotted for each thermistor tested. These plots were used for obtaining temperature data from voltage recordings

---

[1]Yellow Springs Instrument Co., Yellow Springs, Ohio.

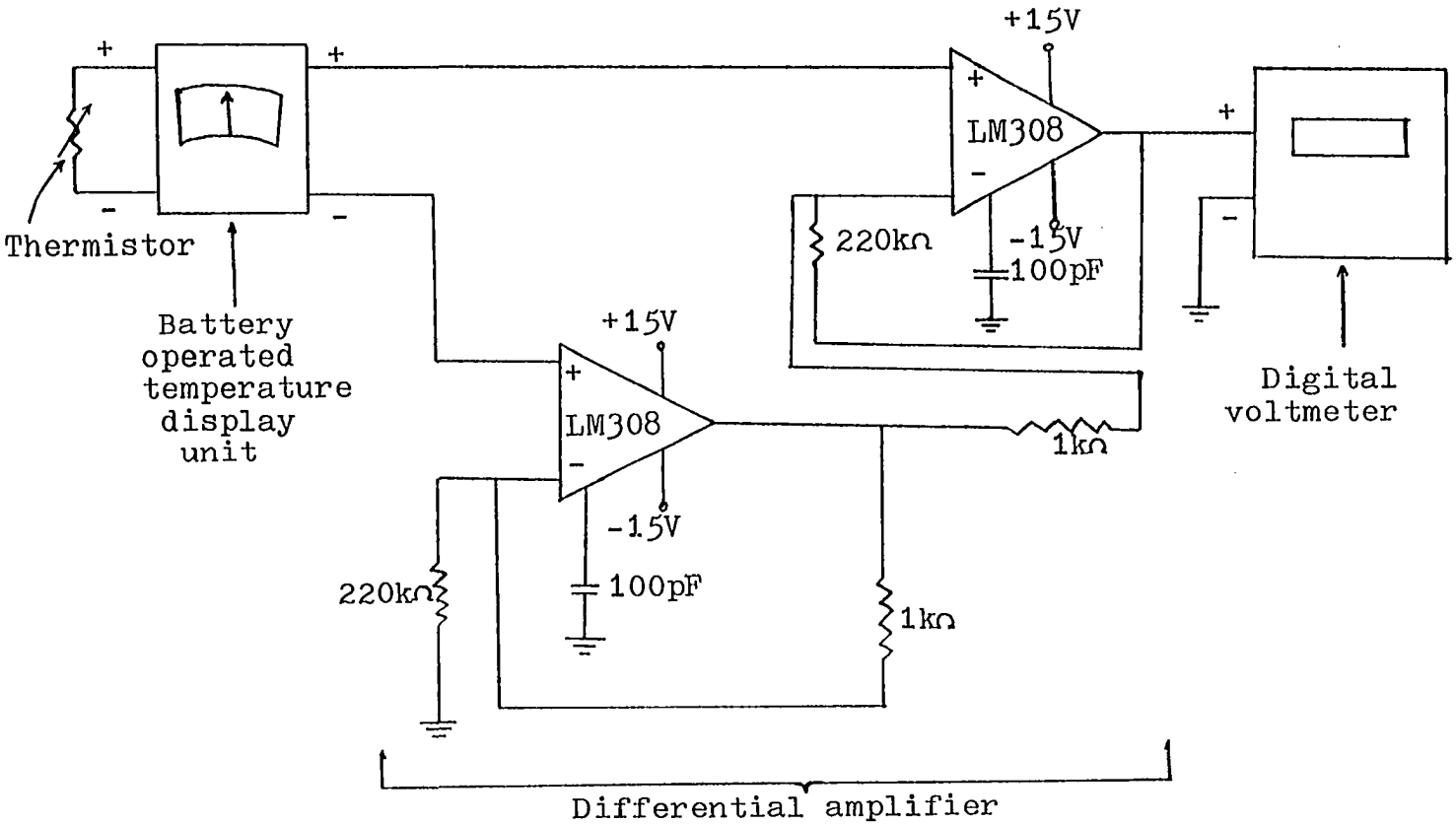

Figure 1. Temperature measurement apparatus

of experiments involving animals.

AGA thermovision[1] infrared thermography equipment was used for obtaining pictorial representations of the skin temperature distribution. The apparatus consisted of an infrared camera, a black and white display unit, and a color display unit. The infrared camera unit scans the subject of interest and measures the intensity of thermal radiation in the near infrared region as a function of position. This quantity is then converted to an electrical signal and displayed as a map on a video output. Using a color monitor, bands of color represent increments of surface temperature, providing that factors such as view angle, surface emissivity, and interfering radiation can be held constant.

Blood flow parameters measuring devices

Catheters were made by joining 30 cm lengths of Teflon® tubing (0.25 cm outside diameter and 0.23 cm inside diameter) with 30 cm lengths of Silastic® tubing (0.32 cm outside diameter and 0.25 cm inside diameter). The catheter was connected to a Statham P23Dc pressure transducer[2].

---

[1]AGA AKTIEDOLAG, Infrared Instruments Department, Lidingö, Sweden.

[2]Statham Medical Instruments, Inc., Hato Rey, Puerto Rico.

The output of the transducer was connected to a Philips modular patient monitoring system[1]. The output from the Philips modular patient monitoring systems was connected to a Hewlett-Packard 7402A[2] dual channel chart recorder with 17402A preamplifiers. The cardiac output module derives an estimate of relative stroke volume by electronically integrating the area under the arterial pressure versus time signal. The cardiac output is obtained by multiplying this quantity by the heart rate. The user supplies an estimate of the impedance of the vascular system, which is usually assumed to be constant during the procedure. The estimated relative cardiac output is is then given by the ratio of the product of the pressure-time integration and heart rate to the impedance.

Simulation device

The IBM 360-65 system in the Iowa State University Computer Center was used.

---

[1]Model XV1513 cardiac output module, Model XV1505 blood pressure module, Model XV1063 numeric display module, Medical System Division, Philips Medical Electronics, Eindhoven, The Netherlands.

[2]Hewlett-Packard Company, San Diego, California.

Experimental Procedures

Animal preparation

Pigs were anesthetized with 2.5% Surital® (Sodium Thiamyl for Injection) solution. After the animal was anesthetized, the femoral artery at the junction of the leg and the trunk was exposed. A catheter was inserted into the artery for a distance of about 27 cm. The Teflon part was advanced to the origin of that artery. The Silastic portion was directed through the subcutaneous fat layer up to the dorsal midline. A puncture wound was made on the back skin of the animal. The Silastic end of the catheter was pushed through the puncture wound and was capped with an injection cap. The animals were allowed to recover post-operatively for at least a week before halothane administration and temperature measurements were done. Animals were kept off feed 12 hours prior to halothane administration.

Data acquisition

One day prior to the halothane administration, the animal was brought into a room adjacent to the laboratory in which the hyperthermia experiment was to be conducted. Both the pens in which the animals were raised and the laboratory were located at the Iowa State University (ISU)

Swine Farm in Madrid, Iowa.

The animal was led into the laboratory, restrained manually, placed in sternal recumbency on a bench and secured in position by rope.

Thermistors were then inserted into various locations of the pig. Thermistor A was inserted into the skin layer of the upper hind leg. Thermistor B was inserted into the skin layer of the abdomen. These two thermistors were placed as close to the skin surface as possible. Thermistor 1 was inserted 6 cm into the rectum. Thermistor 2 was inserted 2.5 cm into the fat layer of the back. Thermistor 3 was inserted 5 cm into the biceps femoris. Thermistor 4 was inserted 5 cm into the triceps brachii. Thermistor 5 was inserted 6 cm into the longissimus.

After the thermistors were in place, the catheter was connected to the blood pressure transducer which had previously been calibrated for pressure measurement using the Philips modular patient monitoring system and a mercury manometer system. The time it took to put the thermistors in place and connect the catheter was five minutes. The animal was allowed two to four minutes of rest to obtain initial temperature readings before gas administration. The animal was held tightly by the head and given an initial 8% halothane gas mixture through a mask fitted tightly over

the snout. Once the animal calmed down, anesthesia was maintained at 3% to keep the animal in a light plane. The concentration was varied from time to time to keep the animal at the desired anesthetic plane. Anesthesia was maintained for one hour or until cessation of cardiac function. Data were recorded every one or two minutes until about two hours after the animal had apparently died, or in the case of a normal non-stress-prone pig, until anesthesia was discontinued.

Infrared thermography measurements were taken during the experiments. Color slides were taken of the pictorial display on the color TV screen showing the temperature profile of the animal. These pictorial data were interpreted by comparing with the temperature recordings from the skin thermistors.

Data manipulation

Data were recorded and plotted. Because the smaller animals tended to have faster temperature changes than larger ones, data from different animals were combined into an average pig by introducing a reduced time variable to stretch the temperature data of smaller animals into longer time periods. This made it possible for both the large and small animals to have similar temperature profiles over time. The reduced time was defined as

$$t_{reduced} = t_{real} \left(1 + 0.25\left(\frac{W_{max} - W}{W_{max} - W_{min}}\right)\right)$$

where t_{real} is the real time, W is the weight of the pig, W_{max} is the weight of the heaviest animal averaged and W_{min} is the weight of the lightest animal averaged.

EXPERIMENTAL RESULTS

Clinical Observations

Temperature changes

Table 1 lists the weights of the animals, the peak rectal temperatures and the fate.

Figure 2 shows the temperature responses with respect to time of one of the six MHS pigs. Figure 3 shows the temperature responses for one of the normal non-stress-prone pigs. Figure 4 depicts the temperature changes of the averaged MHS pigs, which were based on the combined data of pigs 4, 781 and 782. These three animals had similar temperature profiles and relatively close values of temperature which were suitable for producing a meaningful averaged temperature profile to be used as a standard for the mathematical model. Since the numerical results of temperature measurements depended strongly on the location and depth of thermistor insertion, it is conceivable that this could lead to some disagreement among temperature measurements in MHS animals. Graphs of the rest of the temperature information from the MHS animals are in Appendix B.

At the beginning of the experiment, before the administration of halothane, the normal animals showed

Table 1. Experimental subjects

Pig	Type	Weight,kg	Trial	Peak rectal temp.,°C	Ambient temp.,°C	Fate
392	Normal	66.22	1st	42.35	25.	Lived
324	Normal	62.60	1st	42.65	25.	Lived
392	Normal	66.22	2nd	41.55	25.	Lived
321	Normal	61.69	1st	42.0	24	Lived
993	Normal	65.32	1st	40.8	21	Lived
991	Normal	58.97	1st	40.5	21	Lived
321	Normal	61.69	2nd	40.7	24	Lived
991	Normal	58.97	2nd	40.1	24	Lived
993	Normal	65.32	2nd	41.5	25	Lived
324	Normal	62.6	2nd	42.1	25	Lived
120	Normal	54.43	1st	41.35	24	Lived
1	MHS	69.4	1st	43.3	24	Died
2	MHS	79.38	1st	42.8	25	Died
3	MHS	77.11	1st	42.6	24	Died
4	MHS	61.69	1st	43.4	26	Died
782	MHS	52.62	1st	44.35	24	Died
781	MHS	38.1	1st	42.8	24	Died

Figure 2. Temperature variation of MHS pig 781

Legend[a]:

Rc = rectal temperature
Bm = temperature at *longissimus*
Lm = temperature at *biceps femoris*
Am = temperature at *triceps brachii*
Fa = temperature at backfat
Ls = temperature at hind leg skin
As = temperature at abdominal skin

---

[a]The same legend is applicable for all subsequent experimental temperature versus time data plots.

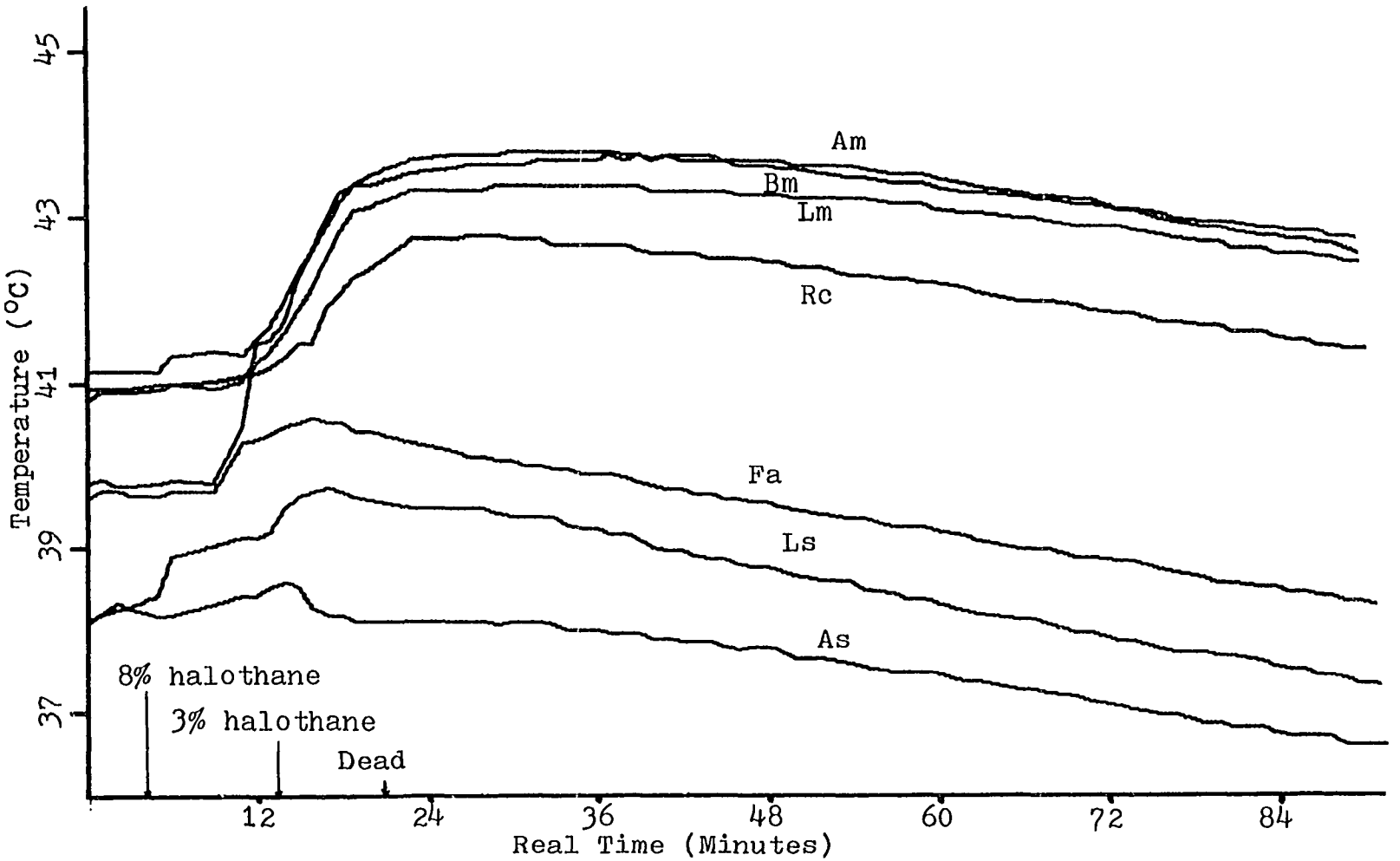
Temperature (°C)
45
43
41
39
37
Am
Bm
Lm
Rc
Fa
Ls
As
8% halothane
3% halothane
Dead
12
24
36
48
60
72
84
Real Time (Minutes)

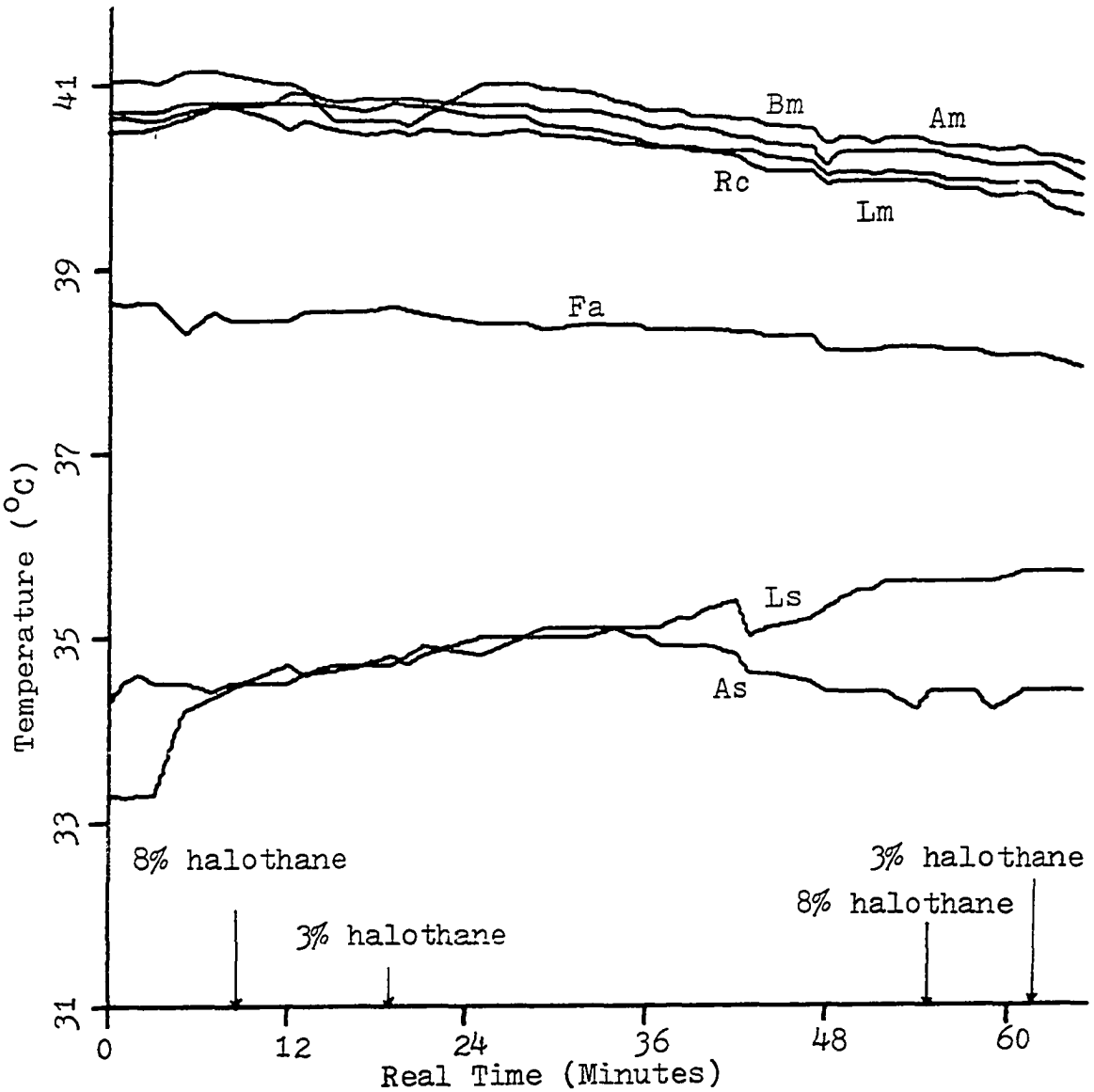

Figure 3. Temperature variation of normal pig 993

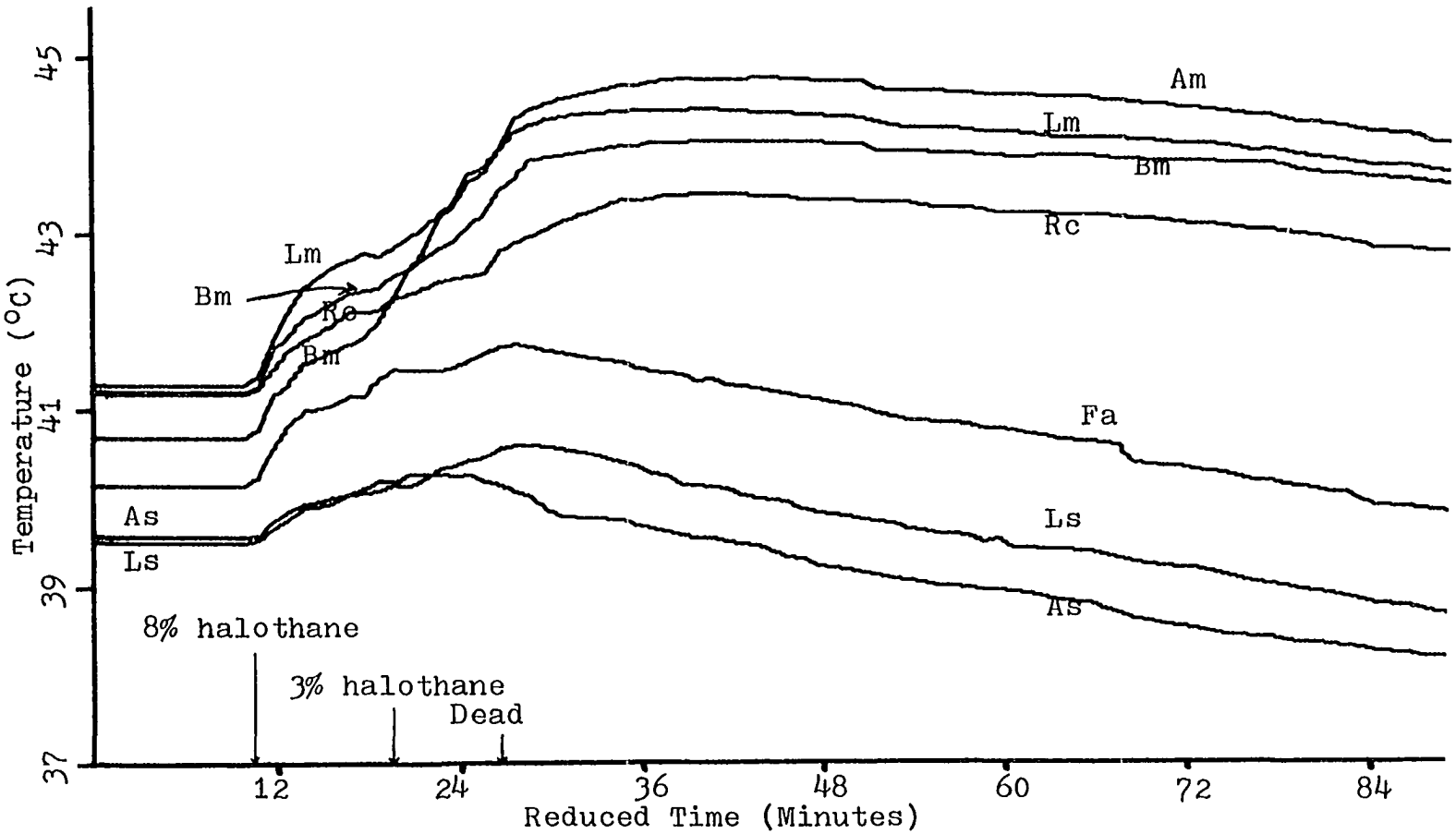

Figure 4. Temperature variation of the average MHS pig

very stable temperature profiles. The muscle temperatures were close to the rectal temperature. The variations among animals were small.

The malignant hyperthermia susceptible animals had higher initial (about 0.5°C) muscle and rectal temperatures than the normal subjects. However, the temperature pattern among the MHS animals were less consistent than those of the normal subjects. In most cases temperatures started to increase even before any anesthetic was administered.

After the administration of halothane, the core, muscle and fat temperature in the normal animals began to decrease. The temperature changes in the muscles of the limbs were most marked. The skin temperatures, on the other hand, tended to rise. There were a few exceptions in which the temperature, instead of decreasing, increased in all of the sites monitored. However, the rates of change were small and decreased with time for all of the non-stress-prone pigs. The average changes were about -1°C per hour in the muscles.

After the withdrawal of anesthetic, the normal subjects recovered within two or three minutes. They showed no apparent signs of rigidity, no temperature rise, no skin vascular reaction and no apparent ill effects.

For the malignant hyperthermia susceptible subjects,

the temperature change patterns were not as uniform as those of the normal subjects. Generally, the temperatures started to increase immediately after the needle thermistors were inserted. When halothane was administered, the temperature increased at a faster rate. However, the rate of increase of temperature varied from animal to animal and from site to site. This rate was affected by the weight of the animal, the anesthetic history of the animal and the level of halothane received. For the skin and back-fat temperatures, both the rate of increase and the magnitude of the increase were smaller than those of the core and the muscle layers. The muscle layers also showed more significant and faster temperature changes than did the rectum. This was probably due to the fact that the thermistor was inserted six to seven cm into the rectum, so the measured value was probably not a true reflection of the core temperature. The longissimus, biceps femoris and the triceps brachii showed similar temperature change patterns. They tended to reach a maximum temperature of 3 to 5°C above the normal temperature in a period of 30 minutes. The maximum rate of rise in temperature reached a value of 0.2°C per minute in pig 782. The muscle temperatures usually increased for a period of 5 to 15 minutes after respiration and cardiac function ceased. The

skin and fat temperatures, on the other hand, usually fell immediately after respiration and cardiac cessation. The rates of decrease were faster than those of the muscles or the rectum. The changes of temperature for the skin and the backfat were not consistent. In some cases changes were marked (pig 4 and 782), but in some cases the changes were hardly noticeable (pig 781).

Statistical analysis of the difference in temperature data between MHS and normal pigs

Table 2. Maximal temperature deviations for the pigs[a]

Pig	ΔTB, °C at biceps f.	ΔTT, °C at triceps b.	Type
781	2.6	4.05	MHS
782	4.5	4.05	MHS
4	3.05	3.7	MHS
1	2.65	3.0	MHS
3	3.1	2.9	MHS
2	3.3	2.95	MHS
392	2.3	1.45	Normal
324	-0.05	0.3	Normal
321	0.0	0.4	Normal
993	-1.0	-0.55	Normal
991	-1.5	-1.25	Normal
120	2.95	1.05	Normal
392A	2.25	1.95	Normal
321A	-0.5	-0.5	Normal
991A	0.0	-1.2	Normal
993A	-0.95	-0.75	Normal
324A	0.45	1.0	Normal

[a]The last five sets of measurements were the results of the second trials on five of the normal animals.

Table 2 lists the maximal temperature deviation (ΔT) within 60 minutes of halothane administration for both the *biceps f.* (B) and the *triceps b.* (T) of the animals.

Table 3 lists the averages and standard deviations (SD) calculated from the data of Table 2.

Table 3. Averages and SD's of maximal temperature deviations

Group	No. of samples	Average ΔTB, °C	SD of ΔTB, °C	Average ΔTT, °C	SD of ΔTT, °C
MHS	6	3.2	0.692	3.442	0.554
Normal[a]	6	-0.158	1.333	0.092	0.917
Normal[b]	12	0.4	1.472	0.173	1.098

[a]Information based on 6 initial measurements, here and in all subsequent tables.

[b]Information based on 11 measurements including repeated trials on 5 animals, here and in all subsequent tables.

The Student's t test is performed on the above data using the equation

$$(\mu_m - \mu_n) = (\overline{X_m} - \overline{X_n}) \pm t_{0.025} \left(\frac{s_m^2}{n_m} + \frac{s_n^2}{n_n}\right)^{\frac{1}{2}}$$

where $(\mu_m - \mu_n)$ is the true mean difference between the MHS and the normal data, $(\overline{X_m} - \overline{X_n})$ is the sample mean difference, s is the standard deviation, n is the sample size, and $t_{0.025}$ is the table value of t at the error probability of

0.05.

Table 4 lists the values of ($\mu_m - \mu_n$) with a 95% confidence interval for the comparison of the maximal temperature deviations for both the triceps b. and the biceps f. between the MHS and the normal animals.

Table 4. ($\mu_m - \mu_n$) for ΔTB and ΔTT

Group	($\mu_m - \mu_n$) for ΔTB at biceps f.	($\mu_m - \mu_n$) for ΔTT at triceps b.
MHS vs. Normal[a]	3.358°C ± 1.366°C	3.35°C ± 0.974°C
MHS vs. Normal[b]	2.80°C ± 1.122°C	3.27°C ± 0.854°C

From the above analysis, every one of the comparisons indicated that there is a significant difference between the MHS and the normal data because the zero points did not lie within the 95% confidence intervals of ($\mu_m - \mu_n$).

Table 5 lists the initial temperatures at the start of halothane administration for both the biceps f. and the triceps b. of the animals.

The averages and the standard deviations for the data of Table 5 were calculated and subsequently used for performing the Student's t test. Table 6 lists the values of ($\mu_m - \mu_n$) obtained by performing the Student's t test with a 95% confidence interval for the comparison

of the initial temperature for both the triceps b. and the biceps f. between the MHS and the normal animals.

Table 5. Initial muscle temperatures of the pigs

Pig	TB, °C at biceps f.	TT, °C at triceps b.	Type
781	41.15	39.75	MHS
782	41.1	41.55	MHS
4	42.0	41.3	MHS
1	41.7	41.85	MHS
3	40.7	40.45	MHS
2	41.65	42.1	MHS
392	40.65	42.1	Normal
324	41.35	41.65	Normal
321	41.85	41.3	Normal
993	40.5	40.65	Normal
991	40.75	40.6	Normal
120	38.5	41.25	Normal
392A	39.85	40.1	Normal
321A	41.05	40.15	Normal
991A	40.6	40.7	Normal
993A	41.45	40.7	Normal
324A	41.35	41.0	Normal

Table 6. $(\mu_m - \mu_n)$ for the initial muscle temperatures

Group	$(\mu_m - \mu_n)$ for initial temp. at biceps f.	$(\mu_m - \mu_n)$ for initial temp. at triceps b.
MHS vs. Normal[a]	0.783°C ± 1.13°C	0.150°C ± 0.91°C
MHS vs. Normal[b]	0.665°C ± 0.722°C	0.370°C ± 0.837°C

From these tests, it can be concluded that even though there are differences in initial muscle temperatures

between the MHS and the normal subjects, the differences are not statistically significant.

Table 7 lists the initial temperatures at the start of halothane administration for the skin layers of both the abdomen and the hind leg.

Table 7. Initial skin temperatures of the pigs

Pig	Temperature, °C at hind leg	Temperature, °C at abdomen	Type
781	38.5	38.25	MHS
782	38.0	38.9	MHS
4	41.57	41.92	MHS
1	37.5	39.1	MHS
3	38.0	39.7	MHS
2	36.45	34.35	MHS
392	40.4	40.45	Normal
324	39.6	40.9	Normal
321	38.25	39.9	Normal
993	34.9	34.9	Normal
991	35.6	36.25	Normal
120	34.5	37.55	Normal
392A	38.8	40.0	Normal
321A	38.0	36.35	Normal
991A	37.5	35.5	Normal
993A	38.0	38.2	Normal
324A	39.7	39.65	Normal

The averages and the standard deviations for the data of Table 7 were calculated and used subsequently for performing the Student's t test with a 95% confidence interval. Table 8 lists the values of $(\mu_m - \mu_n)$ obtained by performing the Student's t test for the comparison of the initial skin temperature for both the hind leg and the

abdomen between the MHS and the normal animals.

Table 8. $(\mu_m - \mu_n)$ for initial skin temperature comparison

Group	$(\mu_m - \mu_n)$ for skin temp. at hind leg	$(\mu_m - \mu_n)$ for skin temp. at abdomen
MHS vs. Normal[a]	1.129°C ± 2.795°C	0.378°C ± 3.176°C
MHS vs. Normal[b]	0.587°C ± 1.969°C	0.553°C ± 2.562°C

The above statistical analysis indicated that even though there are differences in the initial abdominal and hind leg skin temperatures between the MHS and the normal animals, the differences are not statistically significant.

Relation between amount of halothane received and temperature

Table 9 lists the subject numbers, the weights, the amount of halothane received and the peak leg muscle temperature differences.

Animals 1, 2 and 3 received 8% halothane gas mixture for relatively short durations of time before anesthesia was maintained with 3% halothane. They were also the heavier subjects among the MHS pigs. The amount of halothane received per unit weight for these animals was

Table 9. Relation of weight, halothane concentration and peak temperature difference

Pig	Weight,kg	8% halothane given,min	3% halothane given,min	T,°C biceps f.	T,°C triceps b.	Death time,min
781	38.1	8.0	8.0	2.6	4.05	16.0
782	52.62	6.0	9.0	4.5	4.05	15.0
4	61.69	10.0	7.0	3.05	3.7	17.0
1	69.4	2.0	40.0	2.65	3.0	42.0
3	77.11	7.0	24.0	3.1	2.9	31.0
2	78.38	4.0	30.0	3.3	2.95	34.0

therefore relatively small compared with the rest of the pigs. Pig 1 had the slowest rate and the smallest value of temperature increase. It was also the animal which received the shortest period of exposure to 8% halothane. For the smaller animals, pig 782 had the fastest rate and the largest change in temperature, while pig 781 had the slowest and the smallest increase. Pig 781 was the smallest animal and it received the second longest exposure to 8% halothane. As a whole, the animals that were heavier and received the 8% halothane for shorter periods tended to have slower rates and smaller values of temperature increase.

After respiration and cardiac function ceased, the rate of fall in temperature for the various locations for all of the MHS animals was approximately 0.025°C per minute. The skin temperature fell faster than the backfat temperature, which in turn decreased more rapidly than that of the muscles or the core. However, the differences were not very large.

Infrared Thermography Results

Infrared thermography gave an indication of the skin temperature variation during malignant hyperthermia. Different temperatures were represented by different colors in the screen of the infrared thermography display

unit.

The color changes, which corresponded approximately to the temperature changes, were quite consistent as a whole for the MHS animals. At the beginning of the experiment, the head, trunk and legs were quite close in apparent temperature. When hyperthermia was progressing and temperature was increasing, the colors shifted to those which represented higher temperatures. The head and the leg skin showed the highest rates of increase in temperature. At the time cardiac function ceased, these sites had the highest apparent skin temperatures. The decline of post-mortem temperature was slow and was only obvious over a long period of time. The image slowly shifted to the cooler colors.

For the non-stress-prone animals, the colors shifted to a cooler pattern over a long period of time. The changes were very slow and hardly noticeable. In many cases, the colors shifted to the warmer end very slowly. Figure 5 shows the typical thermographic color changes for a pig undergoing malignant hyperthermia.

The thermograph could not be used to determine the skin temperatures quantitatively because the equipment tended to drift to warmer colors with time, and the sensitivity was affected by the amount of liquid nitrogen

Anterior part of animal, 3 minutes after initiation of anesthesia

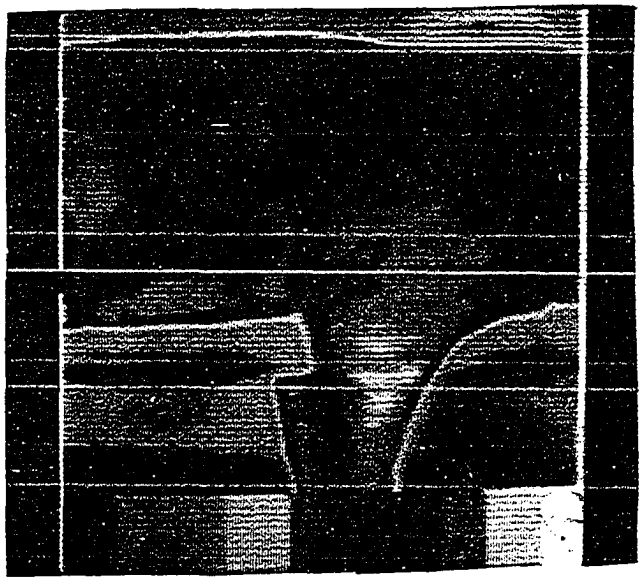

Anterior part of animal, 27 minutes after initiation of anesthesia

Figure 5. Infrared thermographic pictures of MHS pig 3 during malignant hyperthermia

Posterior part of animal, 3 minutes after initiation of anesthesia

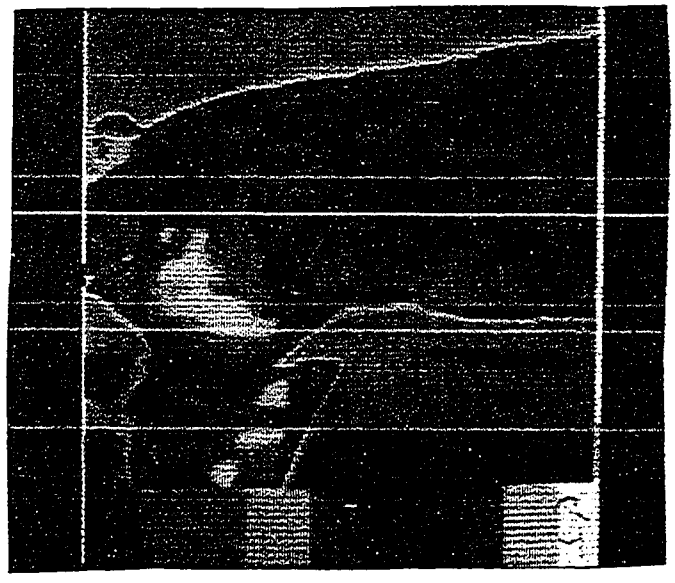

Posterior part of animal, 27 minutes after initiation of anesthesia

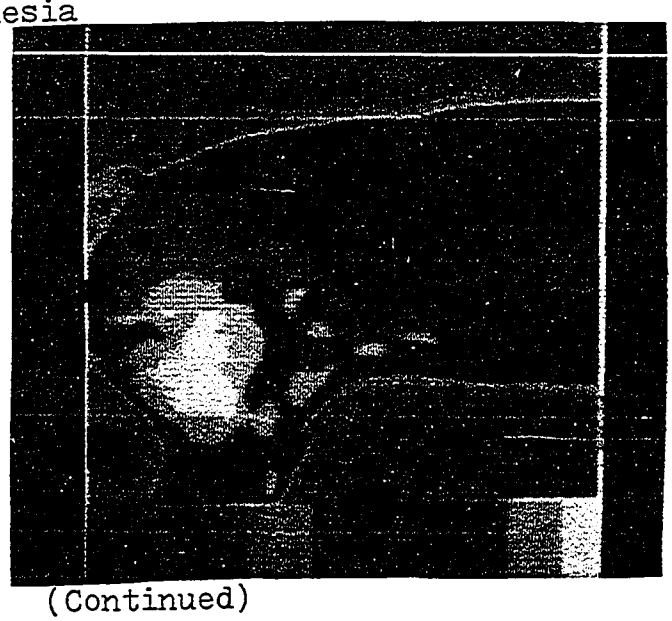

Figure 5. (Continued)

present in the cooling chamber of the camera. Temperatures measured by the infrared equipment could be calibrated by the use of a skin thermistor which was visible in the photographs, as seen in Figure 5. Data from the thermograph were not used directly in this model study.

Circulatory Responses

Figure 6 shows the halothane concentration, heart rate, experimentally derived relative cardiac output, stroke volume and various pressure changes for a typical non-stress-prone pig under halothane anesthesia. All of these parameters tended to decrease in value for the first ten minutes of anesthesia administration before coming to a relatively steady condition. However, the values increased again as the plane of anesthesia became light. To keep the animals sedated, the gas concentration was increased as the anesthetic plane of the animals became light. The changes in pressures, heart rate and cardiac output, while noticeable, were not marked.

Relative measurements of cardiac output using pressure wave integration depend on an assumption that the impedance of the arterial system remains constant. The user must set an initial value of the system impedance,

Figure 6. Blood flow information for normal pig 324A

Units for the variables[a]:

halothane concentration in percent,
pulse pressure in mm Hg,
systolic pressure in mm Hg,
stroke volume in arbitrary units,
heart rate in beats per minute,
cardiac output in arbitrary units

---

[a]The same units for the variables are applicable for all subsequent plots of experimental blood flow information.

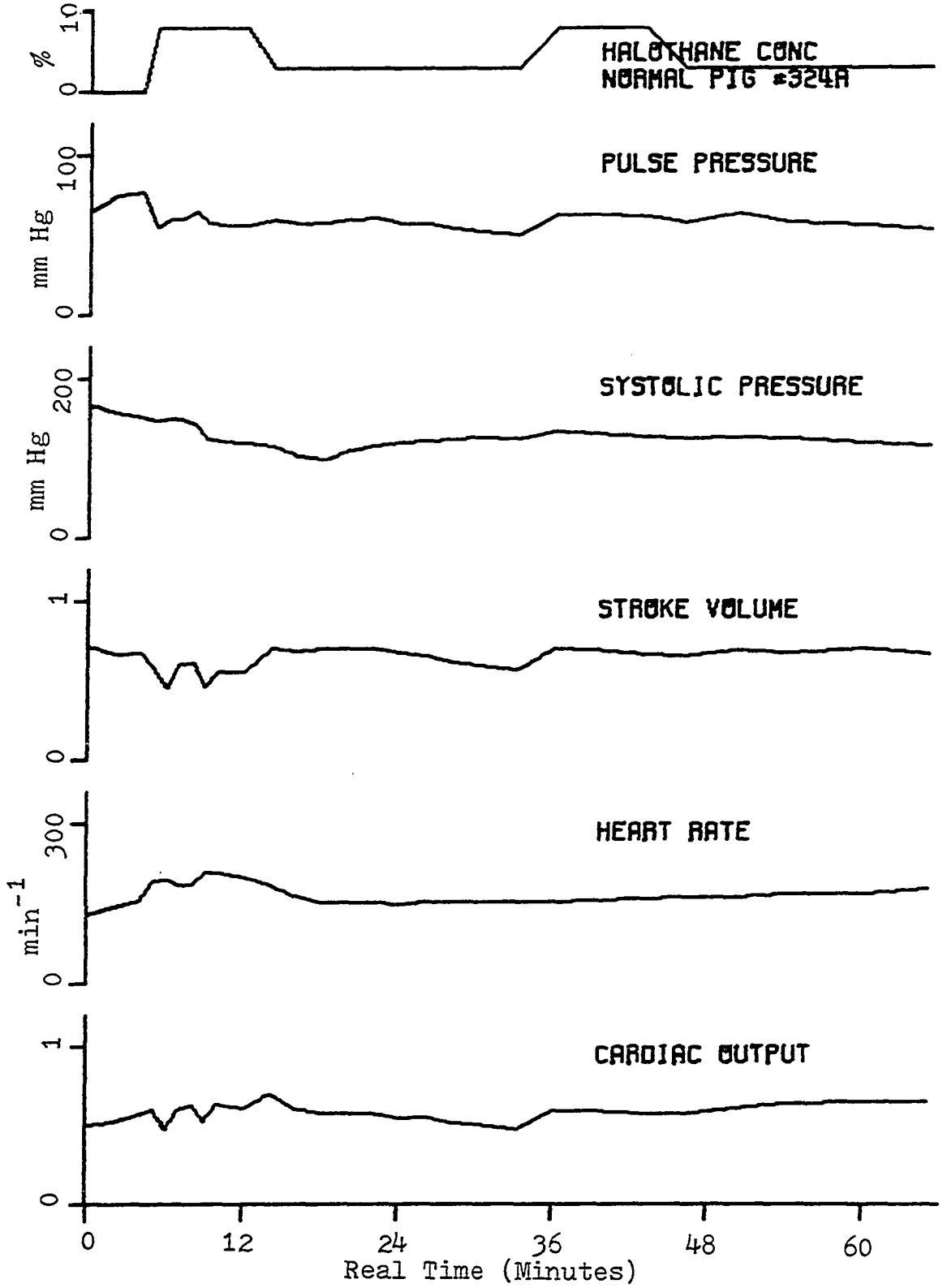
%
10
0
HALOTHANE CONC
NORMAL PIG #324A
PULSE PRESSURE
mm Hg
100
0
SYSTOLIC PRESSURE
mm Hg
200
0
STROKE VOLUME
1
0
HEART RATE
min-1
300
0
CARDIAC OUTPUT
1
0
0
12
24
36
48
60
Real Time (Minutes)

which cannot be determined exactly without a second independent flow measurement method. It is possible that during the last stages of the experiment that some changes in arterial properties occur. Consequently, the error in determining relative stroke volumes can increase in this region. No studies exist on this point. The units shown on Figure 6 for stroke volume and cardiac output therefore represent relative values only.

The instrument used in this research automatically compensates for an irregular pressure waveform by not producing results. Continued output is an indication of the absence of cardiac fibrillation, and of regular beats. The continuous graphical recordings of blood pressure showed the presence of regular beats in the experiments.

Figure 7 shows the heart rate and other circulatory responses for a MHS pig. All of the parameters except the apparent relative cardiac output decreased in value for the first ten minutes after halothane administration. Following this period, the pressures remained relatively constant, whereas the stroke volume and apparent cardiac output continued to decrease. The heart rate increased steadily after the initial administration of 8% halothane. About ten minutes before the time of cardiac cessation, all the measured circulatory parameters increased in value

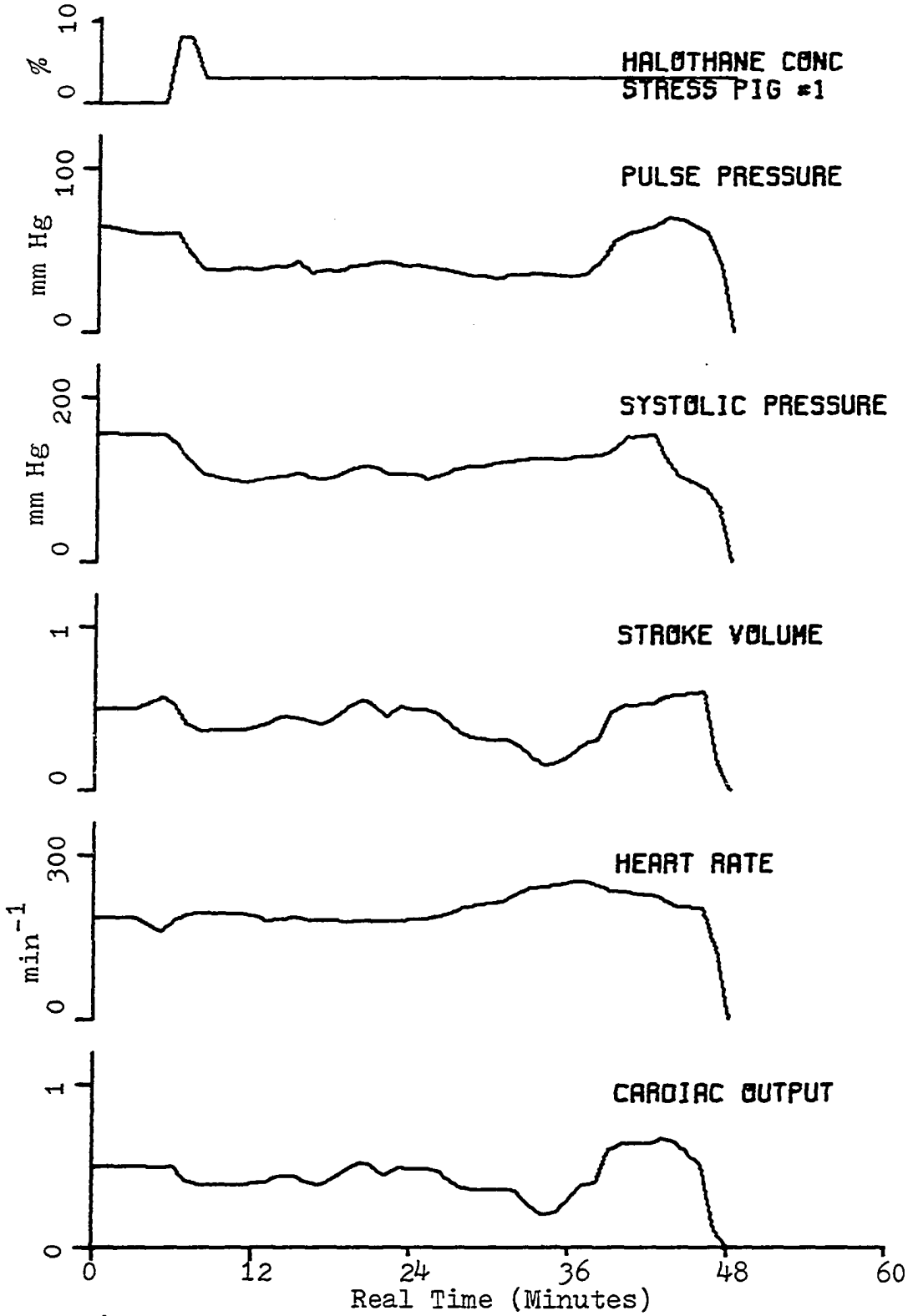

Figure 7. Blood flow information for MHS pig 1

markedly and reached peak values in about five minutes before falling off again, this time terminally.

Other graphs relating information about blood flow for the MHS animals can be found in Appendix C. On the graphs of blood flow information, the units used on the vertical axes are as follows:
The halothane concentration was given in percent. All pressures were given in mm of mercury (Hg). The units for stroke volumes and cardiac outputs were arbitrary. Heart rate was given in beats per minute.

Other Observations

Signs of muscle rigidity were observable within about five minutes after the initial administration of 8% halothane for the MHS animals. Pink blotches were sometimes seen on the skin surface. Heavy panting was also observed.

Overall Body Heat Transfer Coefficient

The heat transfer coefficient is necessary for the determination of the rate at which heat is transferred to the surroundings by conduction, convection and radiation. Other than obtaining the value by correlation as will be done in the later sections, it is also possible to measure

an approximate value experimentally.

If it is assumed that there is negligible heat generation at one hour after cardiac function ceases, and if the heat loss by evaporation of fluid is also negligible, then the overall energy balance equation for the whole body is

$$W_o C_{po} \frac{dT_o}{dt} = -hA\ (T_o - T_a)$$

where T_a = temperature of the ambient air in ^oC,

T_o = temperature of the skin layer in ^oC,

W_o = total body weight in kg,

C_{po} = average heat capacity of the animal in kcal/kg ^oC,

h = overall heat transfer coefficient for the whole body in kcal/m^2 min ^oC.

From Figure 4 which shows the temperature change data for the average pig, h can be calculated. At one hour after cardiac function ceased it was found that the overall rate of fall of temperature was 0.025^oC/min. The skin temperature was about 37.5^oC. Assuming

$T_a = 25^oC$,

$C_{po} = 0.8$ kcal/kg ^oC,

$W_o = 79.4$ kg,

and substituting the values for the variables into the

heat balance equation, the value of hA was found to be

$$hA = 0.159 \text{ kcal/min } ^{o}C.$$

The surface area of the swine, according to Brody's equation (10), is

$$\text{Area} = 0.097 \text{ (Weight in kg)}^{0.633} \text{ m}^2,$$

or, $$A = 0.097 \ (79.4)^{0.633} \text{ m}^2,$$

or, $$A = 1.546 \text{ m}^2.$$

Therefore $h = hA/A$ becomes

$$h = \frac{0.159 \text{ kcal/min } ^{o}C}{1.546 \text{ m}^2},$$

or, $$h = 0.103 \text{ kcal/min m}^2 \ ^{o}C,$$

or, $$h = 6.17 \text{ kcal/hr m}^2 \ ^{o}C.$$

The overall heat transfer coefficient for swine skin is therefore 6.17 kcal/hr m^2 ^{o}C.

If there is continued heat generation at one hour after cardiac cessation, its effect on the estimated value of the heat transfer coefficient may be determined as follows:

$$W_o C_{po} \frac{dT_o}{dt} = -hA \ (T_o - T_a) + \mathbb{M}$$

where $\mathbb{M}$ is the residual heat generation in kcal/min.

Table 10 shows the effect of residual heat generation on the calculated value of the heat transfer coefficient. $\mathbb{M}/\mathbb{M}_o$ is the residual heat generation rate at one hour after

cessation of cardiac function expressed in percentage of the steady-state metabolic rate.

Table 10. Effect of residual heat generation on the calculated value of h

M/M_o, %	0.0	1.0	5.0	10.0	20.0	40.0	60.0	80.0	100.0
h, $\frac{kcal}{hr\ ^oC\ m^2}$	6.17	6.23	6.46	6.75	7.34	8.53	9.70	10.88	12.06

DESCRIPTION OF THE MODEL

Structure of the Model

The model consists of ten segments (head, trunk, two front legs, two front feet, two hind legs and two hind feet). The model is depicted in Figure 8. Each segment is a cylinder of four layers: core, muscle, fat and skin. The core layer represents the internal organs and bones. The fat layer represents the subcutaneous fat layer, and the skin layer represents the skin covering the segment.

Each layer has an assigned basal metabolic rate and blood supply which are functions of the temperatures of the layers around it. The metabolic rate and blood supply are assumed to be large for the muscle layers, and small for the fat layers.

Heat transfer between concentric layers is by conduction and convective blood flow. Heat transfer between segments is by blood flow only, the conductive part is assumed to be negligible. The blood flow scheme is depicted by arrows in Figure 8. The head, front legs and hind legs all receive blood from the core of the trunk. The front feet and hind feet receive blood from the core tissue of the front legs and hind legs respectively. In each segment, blood is assumed to flow from the core to the other three

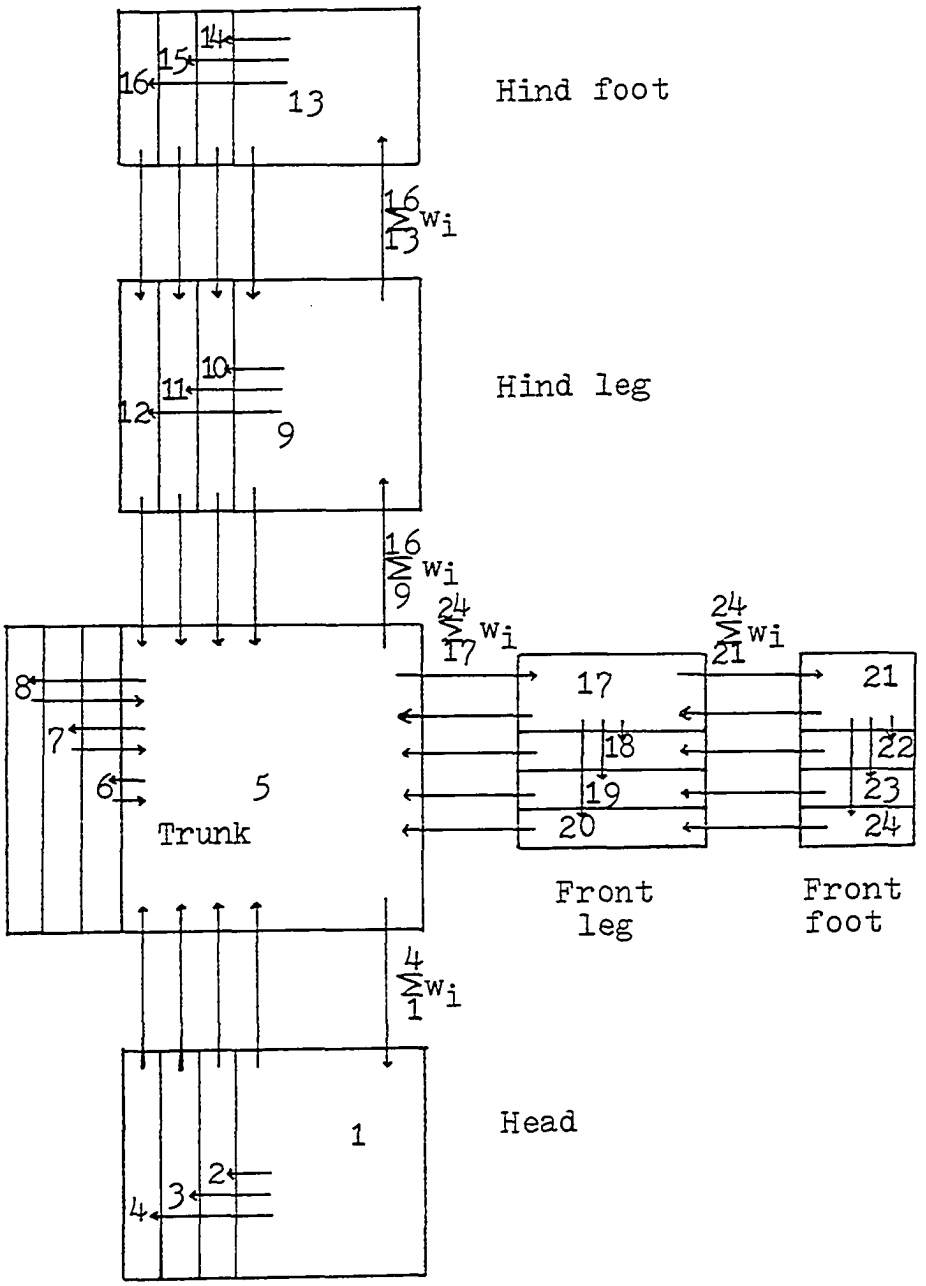

Figure 8. The model

layers directly. Venous return from the different layers in the distal part of the limbs are assumed to go into the same layers of the proximal part. All blood is assumed to return directly to the trunk core from the various layers of the trunk, the head and the front and hind legs. Blood leaving an element is assumed to be at the same temperature as the element.

Heat loss to the surrounding environment is by radiation and convection from the skin. Respiration is also responsible for about 10% of the heat loss before it ceases.

Mathematical description of the model

According to the First Law of Thermodynamics, energy is always conserved. In the absence of external work, the energy accumulation of a system equals the heat input plus the heat generated minus the heat output. Applying this principle to the core layer of a four-layered cylinder as depicted by Figure 9, the applicable equation is

$$V_c \rho C_p \frac{dT_c}{dt} = -Q_c + CB + \mathbb{M}. \qquad (1)$$

For the muscle layer, it is

$$V_m \rho C_p \frac{dT_m}{dt} = Q_c - Q_m + CB + \mathbb{M}. \qquad (2)$$

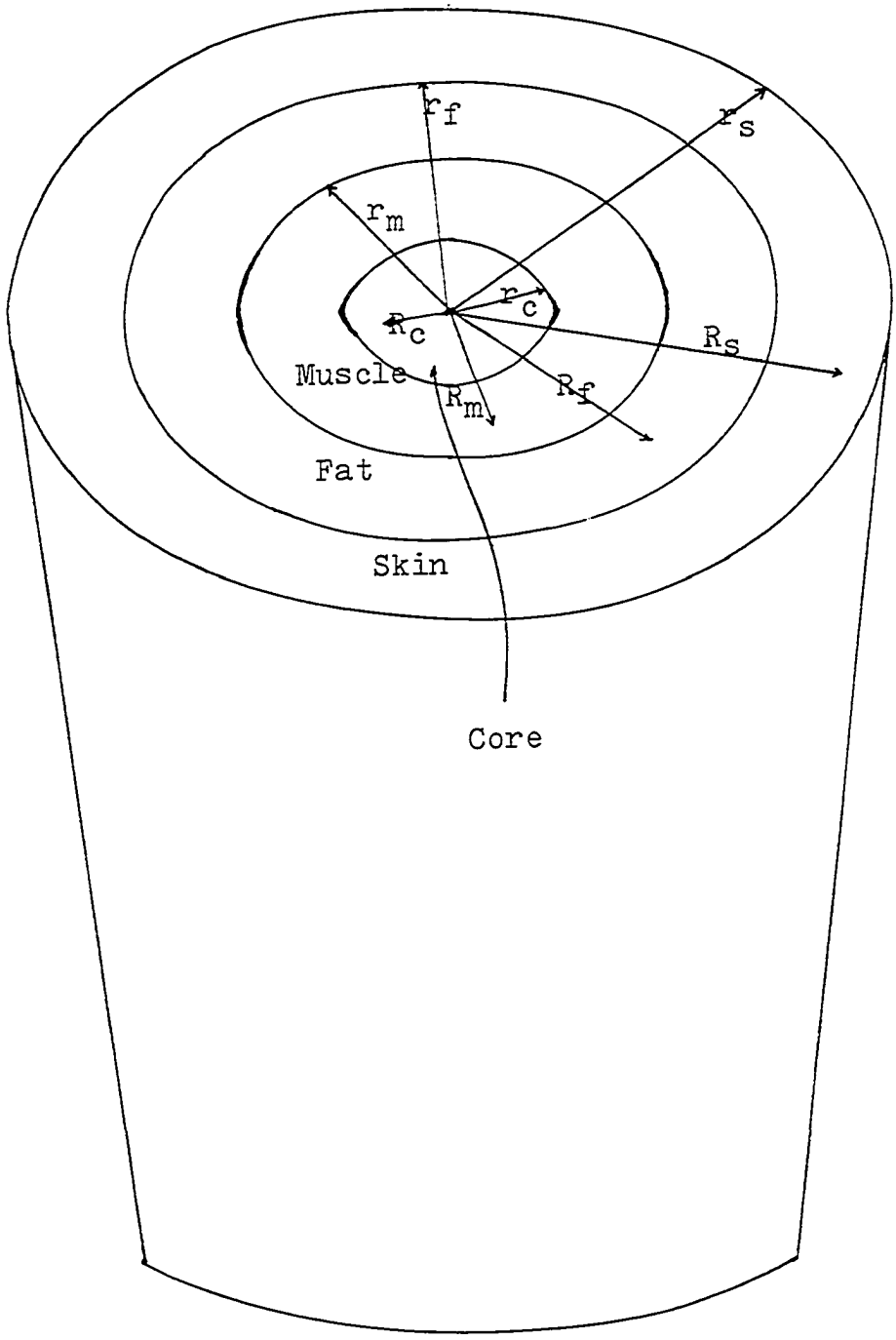

Figure 9. Cyclindrical model of a body segment

For the fat layer, it is

$$V_f \rho C_p \frac{dT_f}{dt} = Q_m - Q_f + CB + \mathbb{M}. \tag{3}$$

For the skin layer, it is

$$V_s \rho C_p \frac{dT_s}{dt} = Q_f + CB + \mathbb{M} - H. \tag{4}$$

In the above equations, CB is the rate of heat energy input into a compartment by convective blood flow, $\mathbb{M}$ is the metabolic heat energy generation rate, H is the rate of surface heat loss by radiation and free convection, and Q is the rate of heat flow through any cylindrical surface of any of the segments of the model. Q_i, the rate heat is conducted from the ith layer to the i+1st layer, can be represented by

$$Q_i = -2\, r_i L k \left(\frac{T_{i+1} - T_i}{R_{i+1} - R_i}\right) \tag{5}$$

where L is the length of the cylinder and k is the average thermal conductivity. R is the geometric averaged radius of the layer (R_i divides the ith layer into two equal volumes). The R's for the various layers are

$$R_c = \left(\frac{r_c^2}{2}\right)^{\frac{1}{2}}, \tag{6}$$

$$R_m = \left(\frac{r_m^2 + r_c^2}{2}\right)^{\frac{1}{2}}, \tag{7}$$

$$R_f = \left(\frac{r_f^2 + r_m^2}{2}\right)^{\frac{1}{2}}, \text{ and} \tag{8}$$

$$R_s = \left(\frac{r_s^2 + r_f^2}{2}\right)^{\frac{1}{2}} \tag{9}$$

where r_c, r_m, r_f, r_s are the outside radius of the core, muscle, fat and skin layers respectively.

If the thermal conductivities of layers i and i+1 in Equation 5 are not equal, the average is used:

$$k = \frac{(\text{Mass of ith layer})\ k_i + (\text{Mass of i+1st layer})\ k_{i+1}}{\text{Mass of ith layer} + \text{Mass of i+1st layer}}$$

Heat loss to the surrounding environment by the skin is assumed to be by conduction, convection and radiation. These three effects are all described using a single heat transfer coefficient, h. The surface heat loss is a function of the skin surface temperature. Since the average temperature of the skin layer, T_s, is not the same as the true surface temperature, T_{ss}, it is necessary to find the relationship between the two. The surface heat loss rate is

$$H = hA\ (T_{ss} - T_a) \tag{10}$$

where A is the surface area of the cylindrical segment. The rate at which heat is conducted to the surface is

$$Q = \frac{k_s A\ (T_s - T_{ss})}{r_s - R_s}, \tag{11}$$

$$\text{or,}\quad Q = \frac{k_s A\,(T_s - T_a - T_{ss} + T_a)}{r_s - R_s}. \tag{12}$$

Since Q equals H, Equation 10 and Equation 12 can be combined. Rearranging the resulting equation, it is found that

$$(T_{ss} - T_a) = (T_s - T_a)\left(h\,\frac{r_s - R_s}{k_s} + 1\right). \tag{13}$$

Defining β as

$$\beta = 1 + \frac{h\,(r_s - R_s)}{k_s}, \tag{14}$$

the surface heat loss rate, H becomes

$$H = Ah\beta\,(T_s - T_a). \tag{15}$$

The heat transfer coefficient used in the above equations is a parameter that combines the effect of heat loss by radiation, conduction and convection.

The heat loss rate by radiation can be represented as

$$Q_{rad} = e\sigma A\,(T_{ss}^{\,4} - T_a^{\,4}) \tag{16}$$

where e is the emissivity and σ is the Stefan-Boltzmann constant. Putting the heat loss rate into a form involving a constant that is similar to the heat transfer coefficient for convective heat transfer, Equation 16 becomes

$$Q_{rad} = h_{rad} A \, (T_{ss} - T_a). \tag{17}$$

Therefore, it is found that

$$h_{rad} = e\sigma \, (T_{ss}^{\,2} - T_a^{\,2})(T_s - T_a). \tag{18}$$

The total combined heat transfer coefficient is

$$h = h_{rad} + h_{con} \tag{19}$$

where h_{con} is the heat transfer coefficient for free convection.

The convective heat transfer by blood into the ith layer of a cylinder may be represented by

$$CB_i = \sum_j w_j \, (\rho C_p)_b \, (T_i - T_b) \tag{20}$$

where w_j represents the different blood flows that go into the ith layer, and T_b represents the temperatures of the blood flows entering the ith layer. The summation is over j flows.

With the above parameters, it is possible to rewrite Equations 1 to 4 in greater detail.

Considering the model of four layers, the heat balance equation for the core layer is

$$V_c \rho C_p \frac{dT_c}{dt} = 2 \, r_c k L \, \frac{(T_m - T_c)}{(R_m - R_c)} + M_c + \sum_j w_j \, (\rho C_p)_b \, (T_b - T_c). \tag{21}$$

In the above equation, the term on the left is the rate of accumulation of heat. On the right, the first term is the conductive heat flux, and the third term is the convective heat flux. $\mathbb{M}$ is the generation of heat by chemical means.

Dividing both sides of Equation 21 by $V_c \rho C_p$, it is found that

$$\frac{dT_c}{dt} = \frac{2k\ (T_m - T_c)}{r_c \rho C_p (R_m - R_c)} + \frac{\sum_j w_j\ (\rho C_p)_b\ (T_b - T_c)}{V_c\ \rho C_p}$$

$$+ \frac{\mathbb{M}_c}{V_c \rho C_p} \cdot \qquad (22)$$

By performing the same kind of analysis on the other layers of a cylindrical segment, it is found that for the muscle layer, the equation is

$$\frac{dT_m}{dt} = \frac{2r_c}{r_m^2 - r_c^2} \frac{k}{\rho C_p} \frac{T_c - T_m}{R_m - R_c} + \frac{2r_m}{r_m^2 - r_c^2} \frac{k}{\rho C_p} \frac{T_f - T_m}{R_f - R_m}$$

$$+ \frac{\sum_j w_j\ (\rho C_p)_b}{V_m\ \rho C_p} (T_b - T_m) + \frac{\mathbb{M}_m}{\rho C_p V_m}, \qquad (23)$$

for the fat layer, the equation is

$$\frac{dT_f}{dt} = \frac{2r_m}{r_f^2-r_m^2}\frac{k}{\rho C_p}\frac{T_m-T_f}{R_f-R_m} + \frac{2r_f}{r_f^2-r_m^2}\frac{k}{\rho C_p}\frac{T_s-T_f}{R_s-R_f}$$

$$+ \frac{\sum_j w_j\,(\rho C_p)_b\,(T_b-T_f)}{V_f\quad \rho C_p} + \frac{M_f}{\rho C_p V_f}\,, \qquad (24)$$

for the surface layer, the equation is

$$\frac{dT_s}{dt} = \frac{2r_f}{r_s^2-r_f^2}\frac{k}{\rho C_p}\frac{T_f-T_s}{R_f-R_s} + \frac{\sum_j w_j\,(\rho C_p)_b\,(T_b-T_s)}{V_s\quad \rho C_p}$$

$$- \frac{2r_s}{r_s^2-r_f^2}\frac{h\beta\quad (T_s-T_a)}{\rho C_p} + \frac{M_s}{\rho C_p V_s}\,. \qquad (25)$$

These are the general equations for the four different layers in each of the cylindrical segments. If the heat loss by respiration is assumed to occur at the core of the head, inserting the details of the proper blood flow terms into the above equations, the equations that describe the the heat transfer in the 24 different parts of the body are obtained. The equation for the head core is

$$\frac{dT_1}{dt} = \frac{2k_1}{r_1\rho C_{p1}}\frac{T_2-T_1}{R_2-R_1} + \frac{w_1+w_2+w_3+w_4}{V_1}\frac{(\rho C_p)_b\,(T_5-T_1)}{\rho C_{p1}}$$

$$+\frac{M_1}{\rho C_{p1}V_1} - \frac{RESP}{\rho C_{p1}V_1}\,. \qquad (26)$$

The rest of the equations that describe the heat transfer in the core, muscle, fat and skin layers of all the segments of the body can be found in Appendix E.

Description of the Assumed Control Mechanisms

At steady-state, where there is no change of body temperature or blood flow rate, the metabolic rates and the blood flow rates at the various sites are assumed to be at the basal level. When an animal undergoes malignant hyperthermia, the metabolic rate at the ith site is assumed to jump to a new value $\mathbb{M}_i$, which is a function of the steady-state basal value $\mathbb{M}_{io}$,

$$\mathbb{M}_i = \mathbb{M}_{io} \ (1. + EXP1_i) \tag{27}$$

where EXP1 is a constant.

The blood flow rates for the different sites are assumed to be functions of the basal rates and the temperatures. For the core layers of the head, front legs and hind legs, the flow rate equation is

$$w_c = w_{co} \ (1. + ALFA(\frac{T_c - T_{co}}{T_{5o} - T_{co}})) \tag{28}$$

where ALFA is a constant, T_{co} is the basal temperature, T_{5o} is the basal trunk core temperature, and w_{co} is the basal

blood flow rate in the core.

For the front and hind feet, the equation for the blood flow rate in the core is

$$w_c = w_{co} \left(1. + ALFA\left(\frac{T_c - T_{co}}{T_{bo} - T_{co}}\right)\right) \tag{29}$$

where T_{bo} is the basal temperature of the blood entering the layer.

For the muscle layer, the blood flow rate equation is

$$w_m = w_{mo} \left(1. + ALFA\left(\frac{T_m - T_{mo}}{T_{co} - T_{mo}}\right)\right). \tag{30}$$

For the fat layer, the blood flow rate equation is

$$w_f = w_{fo} \left(1. + ALFA\left(\left(\frac{T_m - T_f}{T_{mo} - T_{fo}}\right) - 1.\right)\right). \tag{31}$$

For the skin layer, the flow rate equation is

$$w_s = w_{so} \left(1. + ALFA\left(\left(\frac{T_m - T_s}{T_{mo} - T_{so}}\right) - 1.\right)\right). \tag{32}$$

The respiratory heat loss is assumed to be a function of the body core temperature and the basal respiratory loss,

$$RESP = RESP_o(1. + DETA(T_c - T_{co})) \tag{33}$$

where $RESP_o$ is the basal loss, and DETA is a constant.

When the body core temperature rises to a certain temperature, the heat generation term $\mathbb{M}$ is assumed to switch to a lower value in all of the 24 parts,

$$\mathbb{M}_i = \mathbb{M}_{io} \, (1. + EXP2_i) \tag{34}$$

where EXP2 is a constant.

The model animal is assumed to "die" when the body core temperature rises to a certain value, DTEMP. At this point, the respiratory heat loss and the blood flow rates are all set equal to zero. The metabolic rates are assumed to fall exponentially with time constants of EXP3's,

$$M_i = M_{io} \, e^{-EXP3_i(t-t_o)} \tag{35}$$

where t is the independent variable, time, and t_o is the time of "death".

COMPUTATIONAL METHODS

All computations were done on the IBM 360-65 using the Fortran IV language.

The 24 first-order differential equations were solved numerically by the Modified Euler's Method to obtain the various temperatures at the different sites as a function of time. A subroutine TRAP was written to handle this computation. The method is described in the following:

Let $\dot{y}$ be defined as $\frac{dy}{dx}$, and

$$\frac{dy}{dx} = f(x,y). \tag{36}$$

The predicted value of y at the ith position of x is y_i. The predicted value of y at the i+1st position for an increment in x of Δx is y_{i+1}, and the value of $\dot{y}$ at the i+1st position is $\dot{y}_{i+1}$,

$$\dot{y}_i = f(x_i,y_i) \tag{37}$$

The first predicted value of y_{i+1} is $\overline{y_{i+1}}$, and by Euler's Method

$$\overline{y_{i+1}} = y_i + f(x_i,y_i)\Delta x. \tag{38}$$

The first predicted value of $\dot{y}_{i+1}$ is $\overline{\dot{y}_{i+1}}$ or

$$\overline{\dot{y}_{i+1}} = f(x_{i+1},\overline{y_{i+1}}). \tag{39}$$

The repredicted value of y_{i+1} is

$$y_{i+1} = y_i + \tfrac{1}{2}(\dot{y}_i + \overline{\dot{y}_{i+1}})\Delta x. \tag{40}$$

Substituting in the values of $\dot{y}_i$ and $\overline{\dot{y}_{i+1}}$, the above equation becomes

$$y_{i+1} = y_i + \tfrac{1}{2}(f(x_i,y_i) + f(x_{i+1},\overline{y_{i+1}}))\Delta x. \tag{41}$$

Here, y_{i+1} is the final corrected value of the i+1st value of y computed from the value of y at the ith position with a time increment of Δx.

PARAMETERS USED IN THE MODEL

The physiological parameters necessary for building a mathematical model for heat transfer in swine are numerous. Values of many of these parameters are not readily available. For this reason, some of the values used in this study were obtained by direct measurement on animals, and some were obtained by assuming that values for the parameters in swine were the same as their counterparts in other animals.

For simplicity and flexibility of the model, empirical methods were used for obtaining many of the physiological parameters, such as blood flow rate, body surface area, and metabolic rate.

Because each segment of the body is represented by a cylinder in the model, careful consideration had to be used in obtaining reasonable values of length, surface area and radius of every segment. The mathematical relationship between the area, length and radius must always hold. The sizes and surface areas of the segments must also agree with the actual animal parts. The shapes of the model segments should also conform to the respective experimental animal parts. Sometimes not all of the above constraints could be met and compromises had to be made in the form of changing the numerical values of some of the parameters.

For a cylinder, the volume is

$$V = \pi r^2 L, \tag{42}$$

and the surface area is

$$A = 2\pi r L \tag{43}$$

where L is the length and r is the radius of the cylinder. From these two equations, it is found that

$$r = \frac{2V}{A} \tag{44}$$

and

$$L = \frac{A^2}{4\pi V}. \tag{45}$$

According to Brody (10), the surface area of a pig is

$$\text{Area} = 0.097\ (\text{Weight in kg})^{0.633}\ m^2. \tag{46}$$

This gives results that agree quite closely with measurements made on pigs by Deighton (18).

Gnaedinger et al. (30) reported that in pigs weighing around 100 kg, the weight of the head as a percentage of the body weight was 6%, the internal organs combined were 15%, and the rest of the body was 79%. Heap and Lodge (46) investigated the body composition of swine that weighed around 200 kg. They reported that the head and backbone weights combined were about 9% of the total body weight. The internal organs comprised 20% of the total weight, and the rest of the body comprised 71%. The shoulder took 26%,

the back 19%, the belly 12%, and the hams represented 17% of the weight of the animal. They also reported the weights of different kinds of tissue in various segments of the body. The ratio of skin, bone, muscle and fat was 4.5:12:57:24 for the shoulders, 5.7:8.3:55:32 for the back, 9:5:48:37 for the belly and 5.3:11:63:21 for the hams.

Deighton (18) reported that for pigs of around 90 kg the trunk had about 76% of the total body surface area. He also reported values of 5.3%, 7.5% and 11% for the surface areas of the front legs, hind legs and the head, respectively, as percentages of the total body surface area.

Since many of the values of parameters obtainable from the literature were for animals larger in size than those used in these experiments, it was necessary to make measurements of the surface area and weight distribution for the different parts of the body. The final values used in the model were based on these measured values, but efforts were made to minimize the discrepancies between the measured values and the values found in the literature.

The total surface area of the animal was obtained with Brody's equation.

The surface area of every segment of two pigs was measured by covering the segments with flexible sheets of

plastic, then cutting and weighing the appropriate pieces. The plastic sheets were assumed to have a constant weight per unit area. The percentage of surface area for the different segments assumed in the model are shown in Table 11.

Table 11. Surface area of body segments in percentage of total

Segment	Head	Trunk	Front legs	Hind legs	Front feet	Hind feet
Area %	16.3	44.9	13.0	16.0	3.5	5.4

Three of the MHS pigs that died in the experiments were dissected and the different segments weighed. Then the gastrointestinal tract, bone, muscle, fat and skin were all separated and weighed. The detailed weight distribution for different parts of the body are listed in the Appendix. The volumes of the segments were obtained by dividing the weights of these segments by the appropriate densities. Table 12 shows the volume percentage of the different segments of the pig.

Table 12. Volume of body segments in percentage of total

Segment	Head	Trunk	Front legs	Hind legs	Front feet	Hind feet
Volume %	9.5	49.9	17.5	20.2	1.2	1.7

Table 13 shows the percentage of different kinds of tissue in each segment of the body. These are given in percentage of weight.

Table 13. Weight of tissue type given in percentage

Tissue / Segment	Core	Muscle	Fat	Skin	Total
Head	40.0	10.0	20.0	30.0	100.0
Trunk	39.5	38.5	16.0	6.0	100.0
Front legs	16.0	65.0	10.0	9.0	100.0
Hind legs	12.5	66.5	9.0	12.0	100.0
Front feet	42.0	25.0	5.0	28.0	100.0
Hind feet	42.0	25.0	5.0	28.0	100.0

To obtain the volume of the different segments and layers, it was necessary to divide the weights of the different parts by their appropriate densities. In the model, the densities for all the different tissues were assumed to be 1 gm/cm^3. Therefore, the volumes of the various parts were numerically equal to weights.

Poppendiek (73) measured the thermal conductivities for a variety of biological tissues such as lung tissue, kidney tissue, muscle, fat, skin and bone marrow for a few different animals. By assuming that the values given for tissues of other animals were also valid for swine, the thermal conductivities for bone, internal organs, muscle, fat, and skin in units of cal/min cm ^{o}C are 0.033, 0.078,

0.085, 0.033 and 0.055, respectively. The values of thermal conductivities used in the final model are listed in Table 14. The variations in thermal conductivities for muscle tissues were within the limit of values reported by Poppendiek. The value of 0.025 cal/min°C cm for the thermal conductivity of fat was also reasonable when comparison was made with some of the values reported by Poppendiek.

Table 14. Thermal conductivities for tissues in units of cal/min°C cm

Tissue / Segment	Core	Muscle	Fat	Skin
Head	0.071	0.076	0.025	0.051
Trunk	0.071	0.076	0.025	0.051
Front legs	0.071	0.071	0.025	0.051
Hind legs	0.071	0.071	0.025	0.051
Front feet	0.071	0.076	0.025	0.051
Hind feet	0.071	0.076	0.025	0.051

The specific heats for different tissues have been reported by Burton and Edholm (12). Considering this information and the assumptions of the values of the densities of the tissues, the values used for the product of density and heat capacity were 0.74 for the head core, 0.82 for the body core, 0.6 for the limb cores, 0.9 for the muscle layer, 0.6 for the fat layer, 0.9 for the skin layer and 0.9 for the blood. These values have the units

of cal/ml °C.

Because of the assumed size of the head core, and the fact that air entering the trachea is saturated with water vapor and nearly at body temperature, the heat loss by respiration was assumed to take place mainly in the core of the head. The loss is usually about 10% of the total heat loss in humans (40). The same was assumed to be true in pigs.

Table 15 shows the basal temperatures of the different parts of the body. The values for the temperatures were estimated from the temperature data obtained from the experiments. Since the measured temperatures depended on the location of the needle and the depth of insertion, the values used in the model were set to agree with the data.

Table 15. Basal temperature of different parts of the body in °C

Tissue / Segment	Core	Muscle	Fat	Skin
Head	41.0	40.4	39.45	37.9
Trunk	41.01	40.85	39.35	37.65
Front legs	41.0	40.8	39.1	37.85
Hind legs	41.0	40.8	39.1	37.85
Front feet	40.35	39.12	38.5	37.6
Hind feet	40.35	39.12	38.5	37.6

The model blood flow rates and basal metabolic rates

were determined by solving the 24 differential equations under steady-state conditions. With the assumption of steady-state, the temperatures all would remain unchanged at certain values. By first putting in the basal temperatures, values for blood flow rates and metabolic rates were determined by iteration until the equations balanced. Peterson (72) listed the blood flow rates and metabolic rates of different tissues. He reported that the viscera had a blood flow rate of about 0.6 ml per gm per minute. The values for muscle and skin were both about 4 ml/gm min. Guyton (38) reported higher flow rates of up to 7 ml/gm min for muscle tissue. Values for the blood rates used in the models were selected to approximate these values. The values for basal metabolic rates are listed in Table 16.

Table 16. Metabolic rates of different tissues in cal/min

Tissue / Segment	Core	Muscle	Fat	Skin
Head	165.013	7.425	5.494	3.543
Trunk	1026.771	85.238	9.892	30.773
One front leg	4.987	19.712	2.784	4.618
One hind leg	9.900	33.430	3.022	4.375
One front foot	1.817	1.445	0.173	0.298
One hind foot	3.220	2.916	0.146	0.236

The blood flow rates are listed in Table 17. The total overall blood flow rate was obtained by the equation

$$w = 3085.5 \text{ (Weight in kg)}^{0.17} \text{ ml/min.}$$

Table 17. Blood flow rate to various body parts (ml/min)

Tissue / Segment	Core	Muscle	Fat	Skin
Head	216.54	37.0	16.0	30.165
Trunk	4068.27	229.98	40.0	85.45
One front leg	43.30	185.0	23.0	15.141
One hind leg	70.678	200.0	27.0	18.169
One front foot	10.808	8.0	0.9	1.292
One hind foot	19.533	13.0	1.6	0.867

Heat loss by the skin was assumed to be lumped into a single term in each of the equations. This term combined the effect of radiation and free convection. The heat transfer coefficient was determined by engineering correlations for both radiation and free convection.

The emissivity for skin was assumed to be 0.87 in the laboratory environment under normal conditions (74). The radiation heat transfer coefficient is

$$h_{rad} = e\sigma (T^2+T_a^2)(T+T_a).$$

Substituting in the values for emissivity and Stefan-Boltzmann constant, the equation becomes

$$h_{rad} = 0.87 (1.355 e^{-12} (T^2+T_a^2)(T+T_a)) \text{ cal/sec}^{\circ}\text{C cm}^2.$$

The conductive-convective heat transfer coefficient for natural convection of cylinders (both horizontal or vertical), according to the equation published by McAdams (63), is

$$h_{con} = 0.27 \left(\Delta T/D \right)^{0.25} \text{ BTU/hr } {}^{o}\text{F ft}^2$$

where ΔT is the temperature difference in ^{o}F between the surface of the body and the environment and D is the diameter of the cylinder in feet. Transforming the equation into the metric system, it becomes

$$h_{con} = 1.0 \left(\Delta T/D \right)^{0.25} (10^{-4}) \text{ cal/sec } {}^{o}\text{C cm}^2$$

where ΔT is in ^{o}C and D is in cm. Putting D in terms of A, the surface area and V, the volume of the cylinder, the above equation becomes

$$h_{con} = 1.0 \, (10^{-4}) \left(\frac{\Delta T \, A}{4V} \right)^{0.25} \text{ cal/sec } {}^{o}\text{C cm}^2.$$

Because of the odd shapes of the limbs and head, and also of the closeness of the segments to each other, the convective-conductive heat transfer coefficient was assigned a value of 0.75 times that value being obtained from the above equation.

The overall heat transfer coefficient is

$$h = h_{rad} + h_{con}.$$

Assuming a cylinder of radius 15 cm, a room temperature of 26°C and an overall surface temperature of 38°C, h_{rad} is

$$h_{rad} = 1.34 \times 10^{-4} \text{ cal/sec } ^{\circ}\text{C cm}^2,$$

and h_{con} is

$$h_{con} = 0.75 \times 0.8 \times 10^{-4} \text{ cal/sec } ^{\circ}\text{C cm}^2.$$

The overall heat transfer coefficient is therefore

$$h = 1.94 \times 10^{-4} \text{ cal/sec } ^{\circ}\text{C cm}^2,$$

or $h = 6.98 \text{ kcal/hr } ^{\circ}\text{C m}^2.$

Since the animals were positioned upright on a wooden bench with the legs hanging over the edges, the heat transfer from the trunk would be less than if the animals were standing on the ground. For this reason, the heat transfer coefficient for the trunk was assigned a value of 90% of $h = h_{rad} + h_{con}$,

$$h_{trunk} = 0.9 \times 6.98 \text{ kcal/hr } ^{\circ}\text{C m}^2,$$

or $h_{trunk} = 6.28 \text{ kcal/hr } ^{\circ}\text{C m}^2.$

The value of either 6.98 kcal/hr °C m^2 or 6.28 kcal/hr °C m^2 agrees quite well with the experimentally determined value of 6.17 kcal/hr °C m^2. For comparison,

the values reported for humans in room temperature is around 9 kcal/hr ^{o}C m^2 (5).

EFFECTS OF CHANGES IN PARAMETERS

To test the performance of the model, many of the parameters used in the description of the model were changed for observance of the effect on the result of the simulation.

Figure 10 depicts the temperature changes for a model in which the thermal conductivities for the muscle layers were assumed to be 0.076 cal/min ^{o}C cm. The blood flow rates to all the layers were assumed to increase with temperature. The convective-conductive heat transfer coefficient was assumed to be $1.0 \times 10^{-4}(\Delta T/D)^{0.25}$ cal/cm^2 sec ^{o}C, and the overall heat transfer coefficient was assumed to be 100% of $h_{rad} + h_{con}$. The metabolic rates were assumed to change to a different set of values when the body core temperature rose to 43.2^{o}C. The "death" temperature was taken to be 44.6^{o}C. The hump at the peak of the trunk core temperature was due to the fact that at death, the flow of blood was stopped, but the heat generation term did not become zero immediately. Without the help of convective blood flow, heat was not conducted away from the trunk core fast enough, so in this simulation, the core temperature rose at a faster rate than usual at the time of "death".

Figure 11 depicts the changes for a model with the following alteration made on the values of the parameters.

Figure 10. Simulated temperature changes

Legend[a]:

Rc = temperature at trunk core
Lc = temperature at hind leg core
Bm = temperature at trunk muscle
Lm = temperature at hind leg muscle
Am = temperature at front leg muscle
Fa = temperature at trunk fat
Ls = temperature at hind leg skin
As = temperature at trunk skin

---

[a]The same legend is applicable for all subsequent simulated temperature change plots.

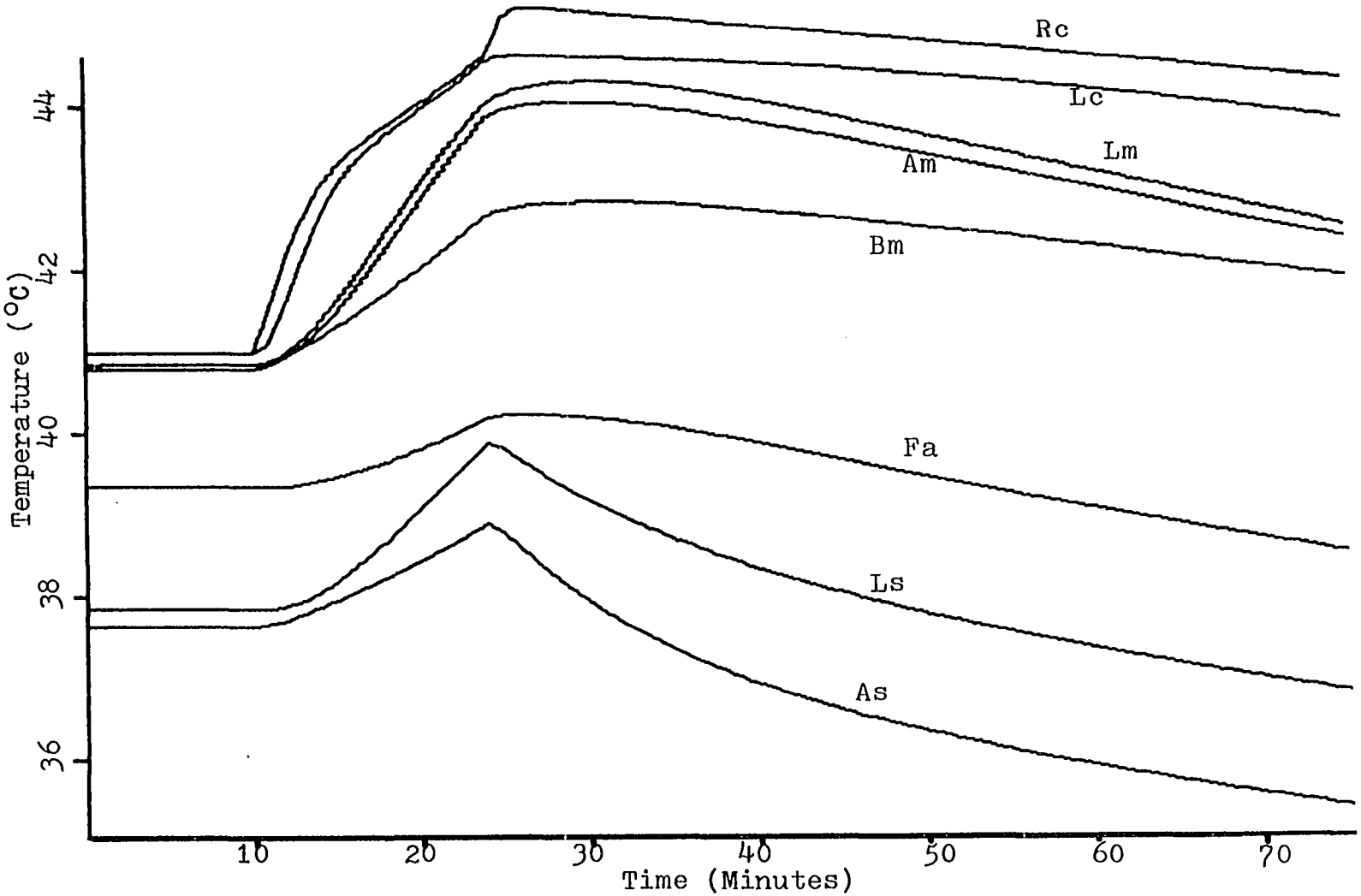
Rc
Lc
Lm
Am
Bm
Fa
Ls
As
Temperature (°C)
44
42
40
38
36
10
20
30
40
50
60
70
Time (Minutes)

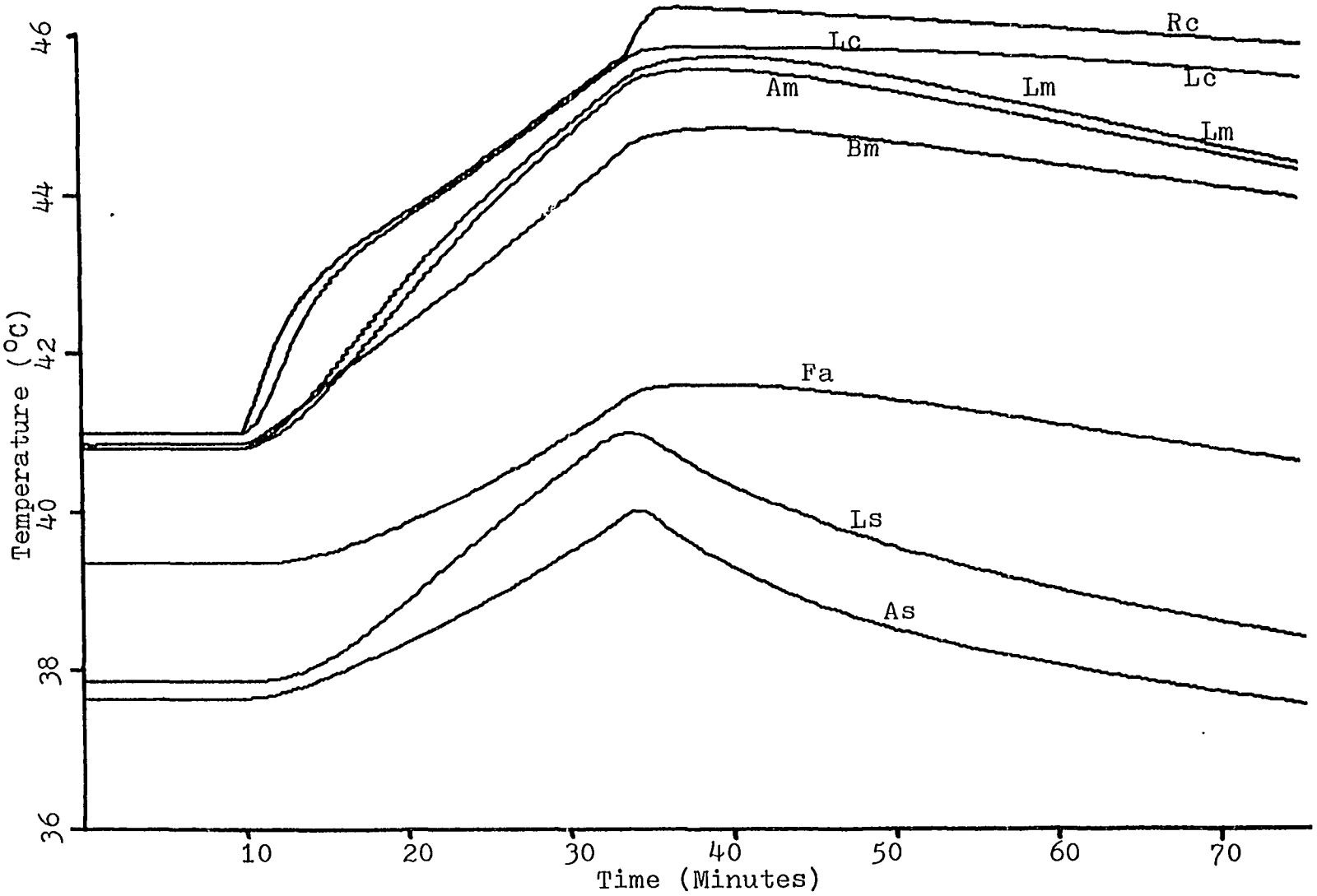

Figure 11. Simulated temperature changes

The thermal conductivities for the muscle layers in the legs were assumed to decrease to a value of 0.071 cal/min^{o}Ccm. The convective-conductive heat transfer coefficient was assumed to be 75% of the previous value. The overall heat transfer coefficient was assumed to be 0.9 that of the $h_{rad} + h_{con}$ for the trunk. The death temperature was assumed to be 45.8^{o}C. The heat generation term for the muscle layers were increased. With these changes, higher values for the peak temperatures in the muscle layers were found. Because of the decrease in conductivities in the muscle layers, the rates of decrease of temperature after death for the muscle layers were less than in the previous simulation. The slower rates of decrease in skin temperatures after death were due to the decrease in the heat transfer coefficients. The model was tested with the same parameters with a death temperature of 44.6^{o}C. The same qualitative results were obtained except that the peak temperatures were lower and the time it took to change was less.

Figure 12 shows the results of further changes in the values of some of the parameters. The rates of increase of blood flow with temperature to the skin layers and the heat generation rates to the skin layers were decreased. The rate of increase of blood flow rate with temperature to

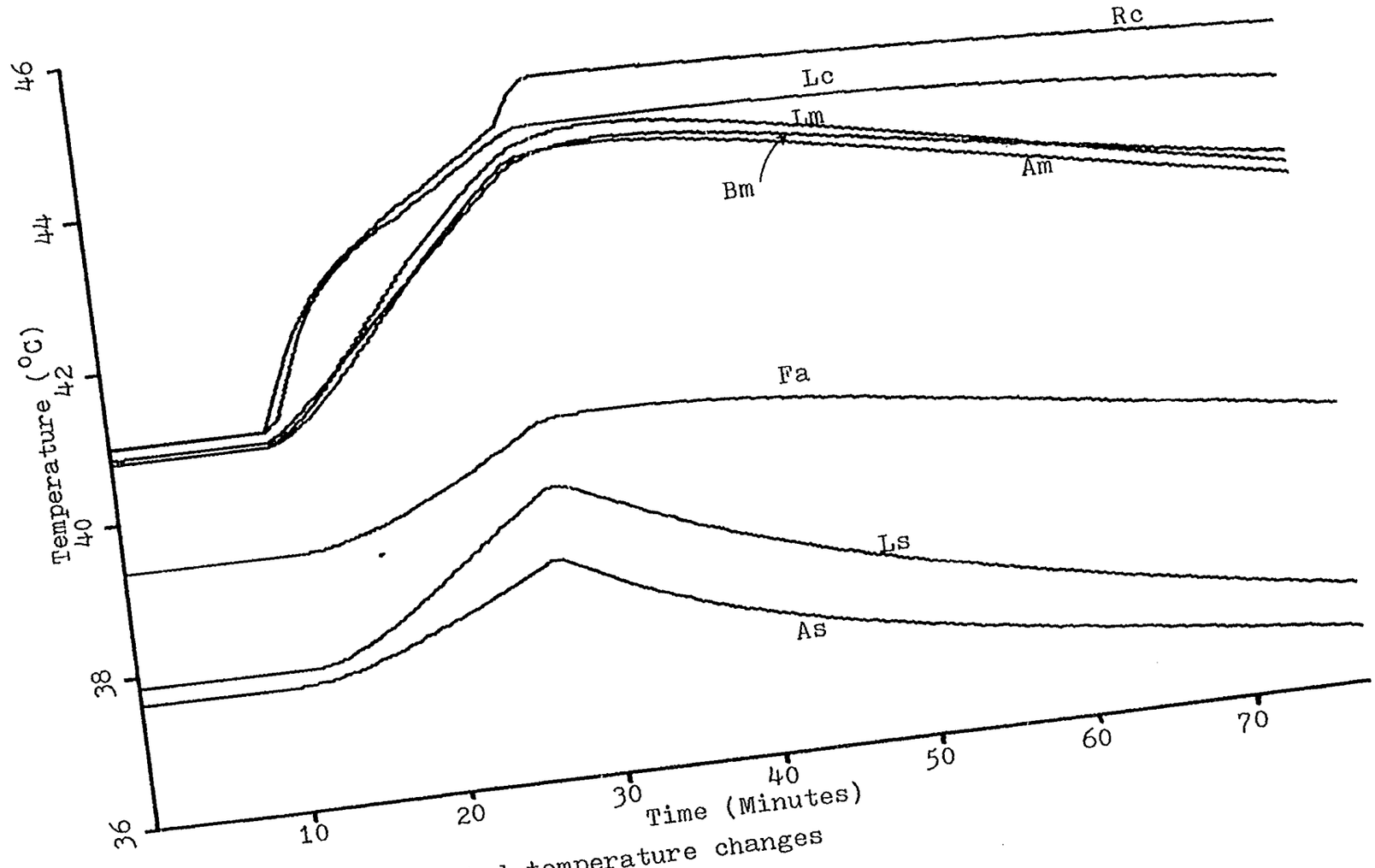

Figure 12. Simulated temperature changes

the back muscle and the heat generation rate were both increased. The death temperature was set at 44.6°C. When compared with the previous simulation with the same death temperature, these changes produced higher peak temperatures for the back muscle and the backfat, whereas the peak temperatures for the skin layers were lower. Because of the higher temperatures of the back muscle and backfat at the time of "death", the rate of the post-mortem fall of trunk skin temperature was slower than that shown in the previous figure. The falls in temperature at the back muscle and the backfat, however, were faster than before. Figure 13 shows the blood flow rate pattern for this simulation. The blood flows to all the parts were assumed to increase with the increase in temperature.

Figure 14 shows the result of further changes made in the values of the parameters. The rates of increase in blood flow rate with temperature to the core and muscle were decreased. For all layers of the limbs as well as all the fat and skin layers of all the segments, the blood flow rates were assumed to decrease with the progress of hyperthermia. These assumptions were consistent with the measurements made by Williams *et al.* (84). They were also consistent with the data from the experiments in this work. To compensate for the loss of energy due to the reduced

Figure 13. Simulated blood flow rate changes

Legend[a]:

Tr = total blood flow rate
Hc = head core blood flow rate
Tm = trunk muscle blood flow rate
Lc = hind leg core blood flow rate
Ac = front leg core blood flow rate
Lm = hind leg muscle blood flow rate
Am = front leg muscle blood flow rate

---

[a]The same legend is applicable for all subsequent simulated blood flow rate change plots.

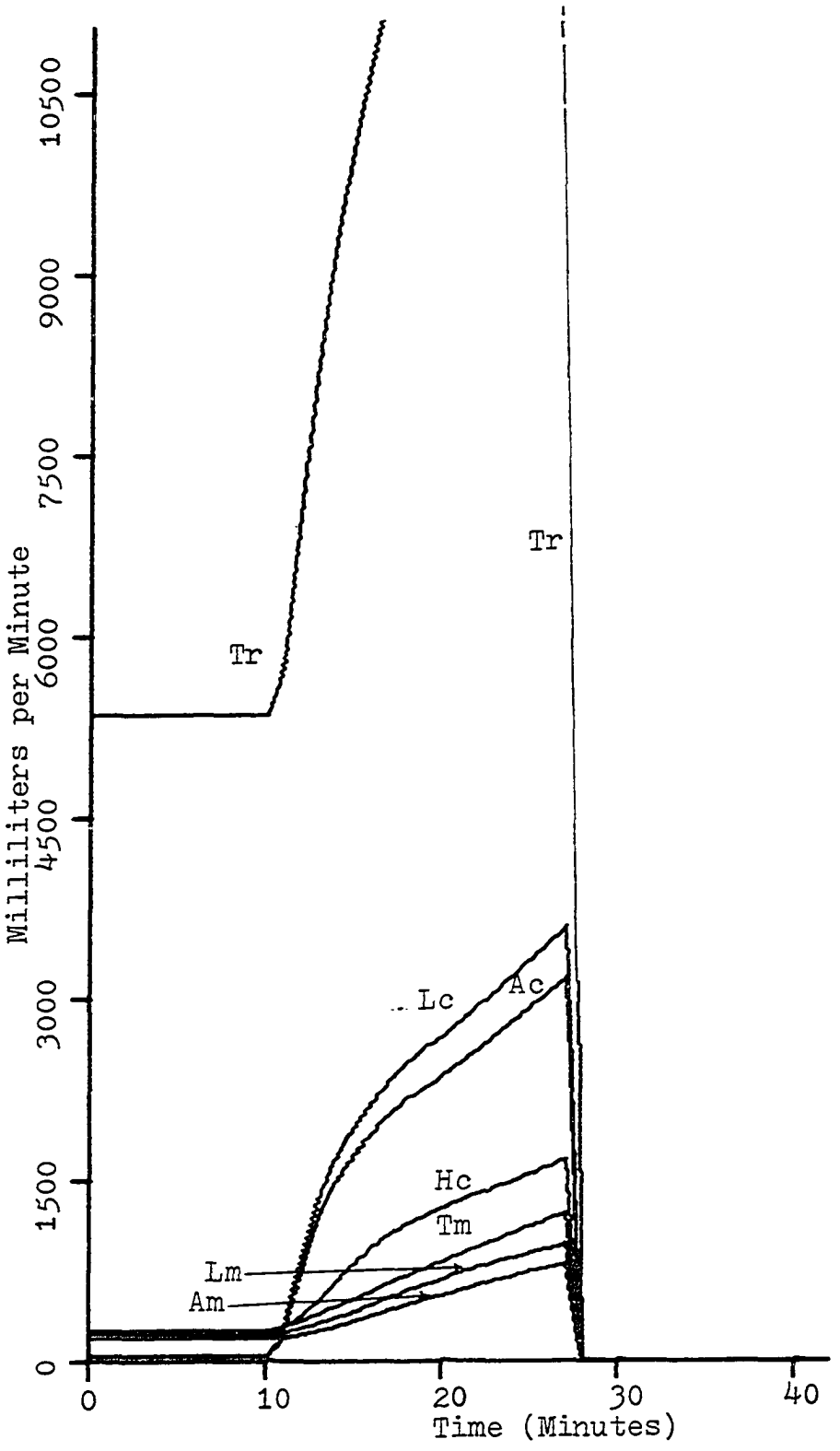
Milliliters per Minute
0
1500
3000
4500
6000
7500
9000
10500
Tr
Tr
Tr
Lc
Ac
Hc
Tm
Lm
Am
0
10
20
30
40
Time (Minutes)

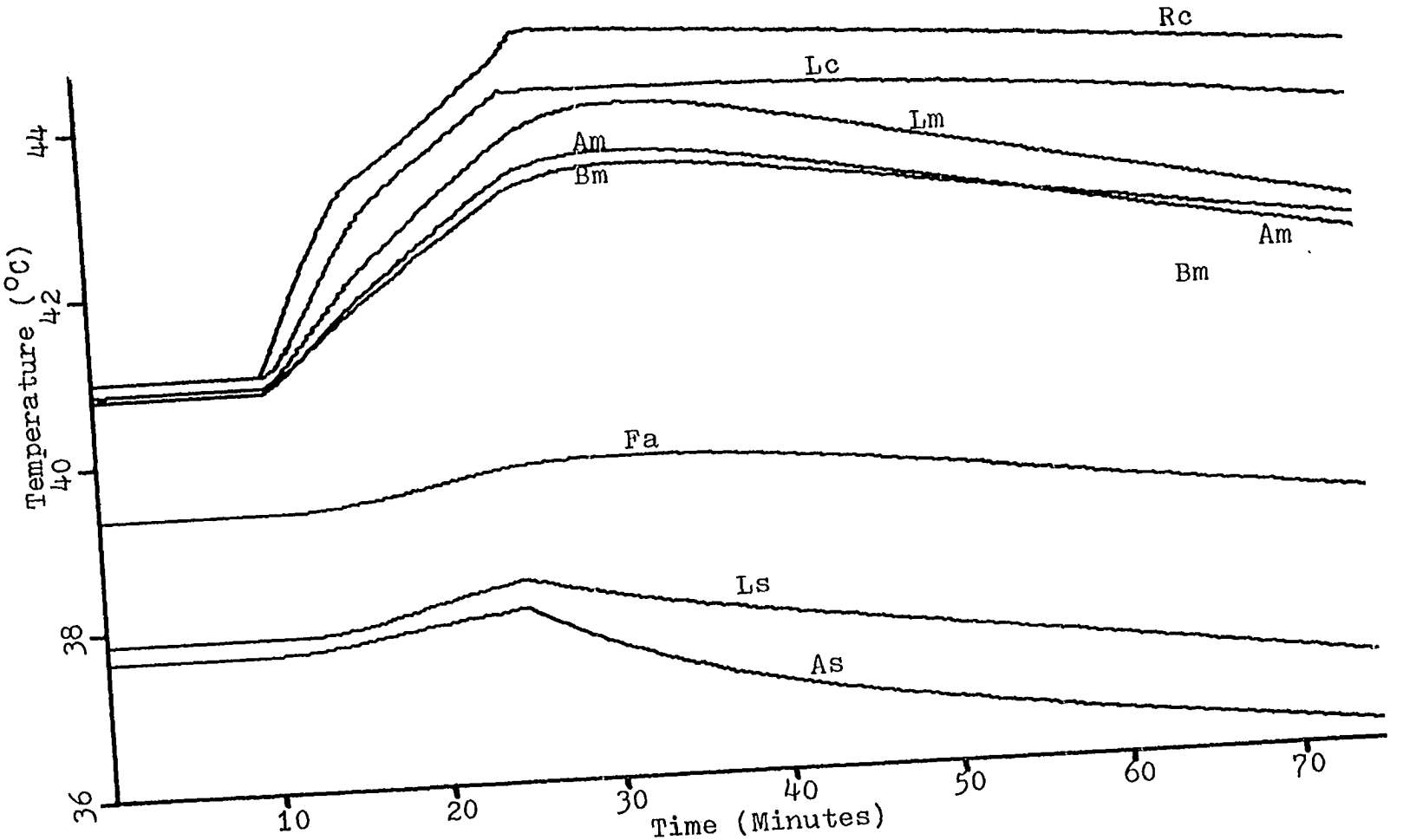

Figure 14. Simulated temperature changes

blood flow rates, the heat generation rates for the muscle layers of the legs were increased. The heat generation rates for the cores of the trunk and the legs were decreased. These changes produced lower peak temperatures for the muscle, fat and skin layers of the trunk. Because of this lowering of peak temperatures, the rates of decrease of post-mortem temperatures at these sites were also decreased. Figure 15 shows the changes of the blood flow rates associated with the temperature changes of Figure 14.

The thermal conductivities for all the fat layers were then assumed to decrease to a value of 0.025 cal/cm ^{o}C min. The death temperature was assumed to be 45.2^{o}C, and the trunk core temperature at which the metabolic rates changed values was set at 43.6^{o}C. The overall heat generation rate for the body was also decreased. These changes produced the results shown in Figure 16. The rates of increase in temperatures for both the fat layers and the skin layers during hyperthermia declined, as did the rates of post-mortem fall of core and muscle temperatures. The peak temperatures reached by all the layers were increased due to the increase in death temperature. This also led to the longer time for "death" to occur.

Figure 17 gives the results of increased heat generation rates for the trunk muscle, the front leg muscle and the

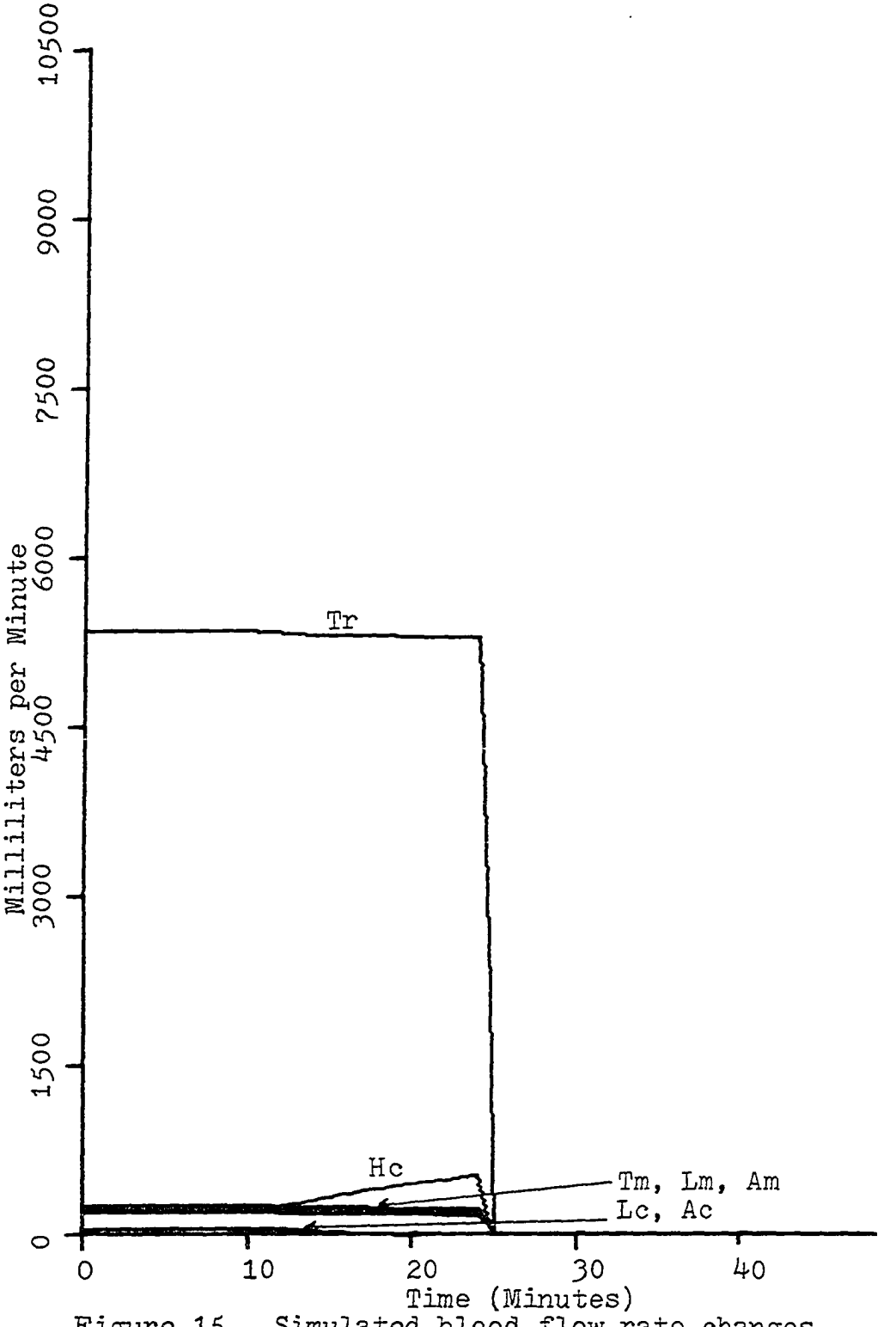

Figure 15. Simulated blood flow rate changes

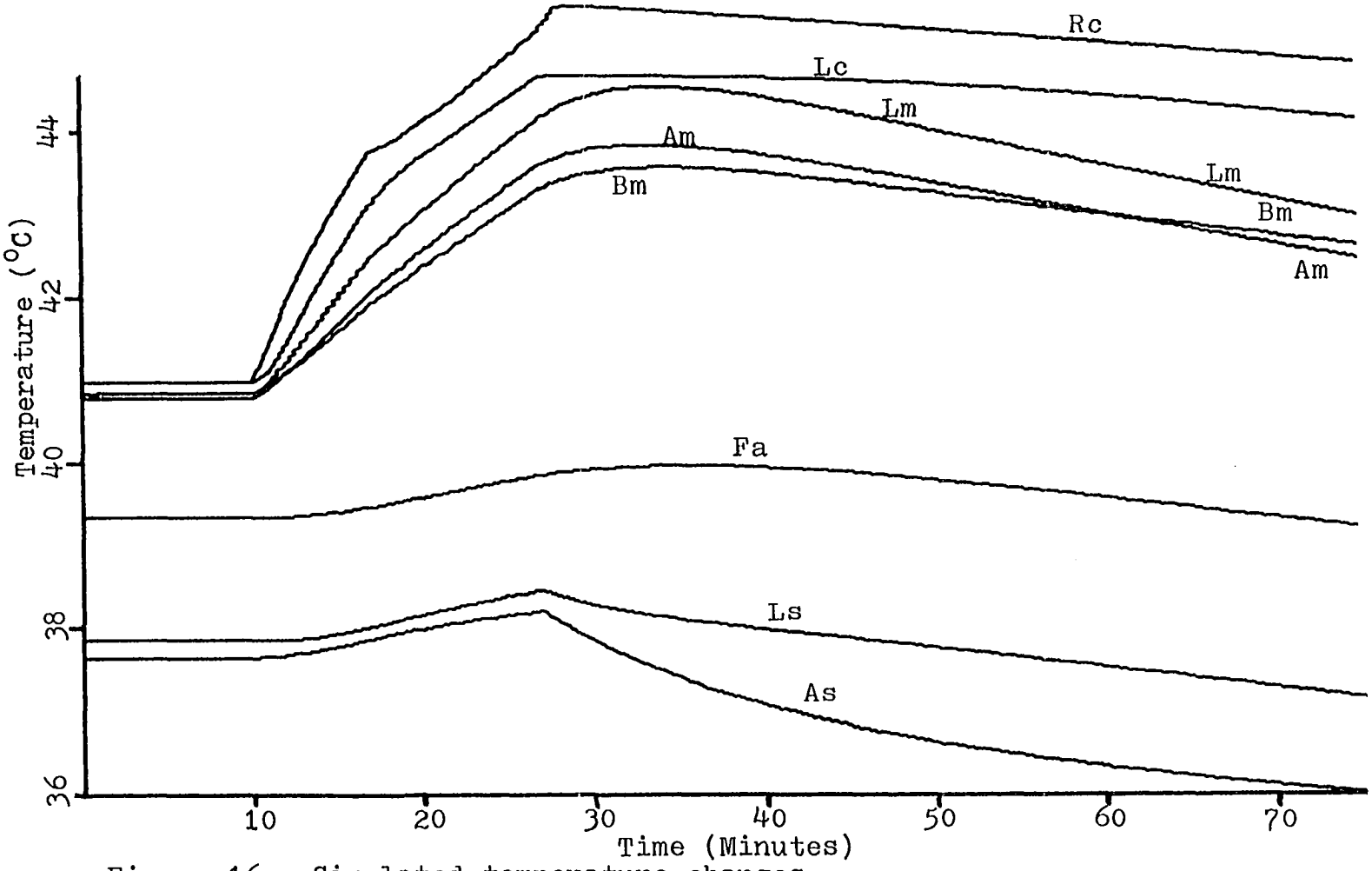

Figure 16. Simulated temperature changes

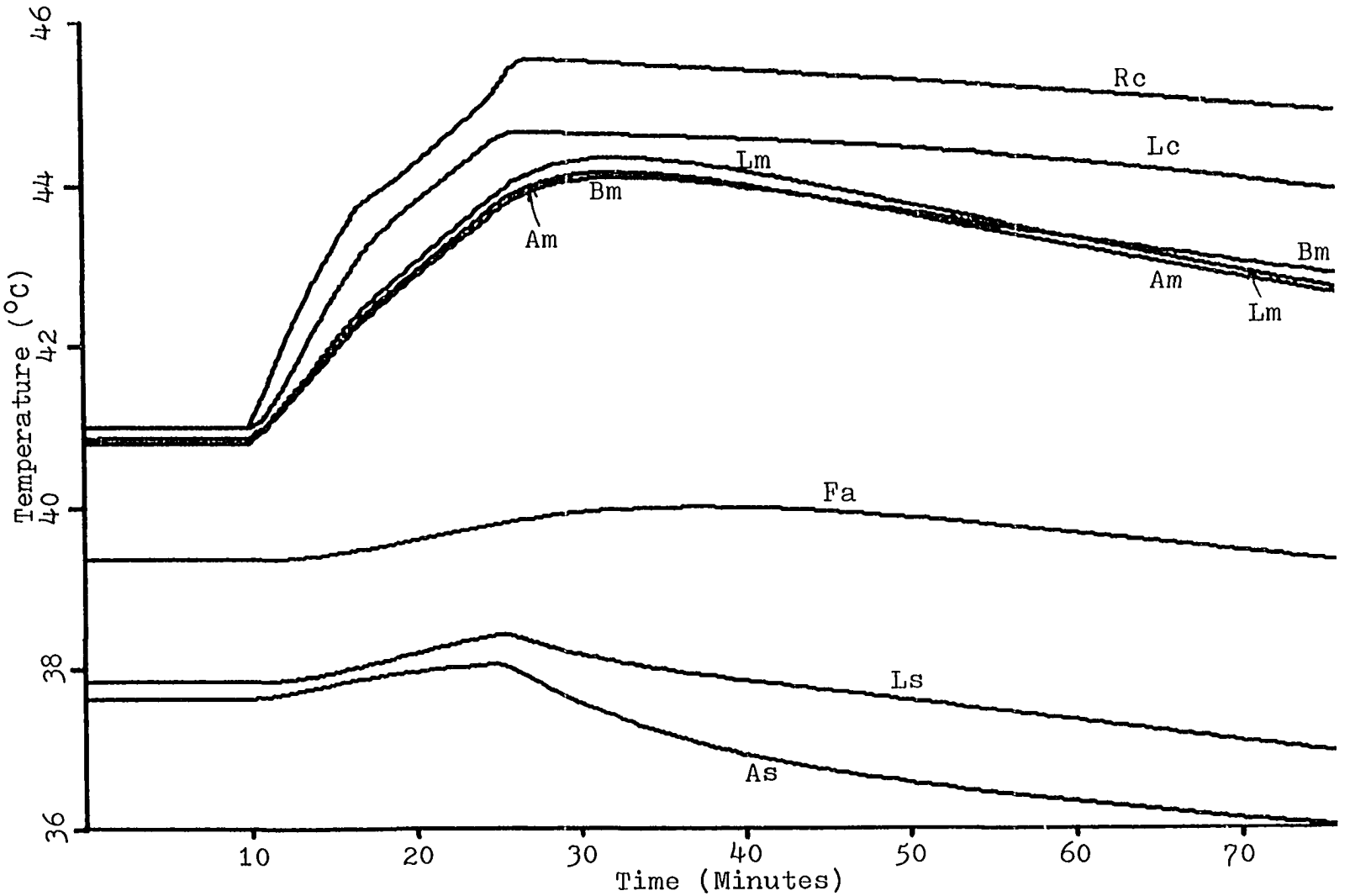

Figure 17. Simulated temperature changes

skin layers of all the segments except the feet. These changes increased the peak temperatures for the muscle layers of the front legs and the trunk. Because of the increased values of heat generation rates, the trunk core temperature rose faster, and the time it took to reach the death temperature was shorter than that of the simulation associated with Figure 15. Due to the shorter period of hyperthermia, the peak temperatures for the skin layers were less than before.

The values of the parameters used to produce the temperature profile of Figure 17 are listed in the following tables. Table 18, 19, 20 and 21 show the values of ALFA, EXP1, EXP2 and EXP3 respectively.

Table 18. Values of the constant ALFA

Tissue / Segment	Core	Muscle	Fat	Skin
Head	0.005	-0.01	-0.6	-0.6
Trunk	0.0001	-0.01	-0.6	-0.6
Front legs	-0.005	-0.01	-0.6	-0.6
Hind legs	-0.005	-0.01	-0.6	-0.6
Front feet	-0.01	-0.01	-0.6	-0.6
Hind feet	-0.01	-0.01	-0.6	-0.6

Table 19. Values of EXP1

Segment \ Tissue	Core	Muscle	Fat	Skin
Head	1.0	20.0	0.0	1.0
Trunk	4.0	17.0	0.0	1.0
Front legs	1.0	30.0	0.0	1.0
Hind legs	1.0	22.0	0.0	1.0
Front feet	1.0	3.0	0.0	0.0
Hind feet	1.0	3.0	0.0	0.0

Table 20. Values of EXP2

Segment \ Tissue	Core	Muscle	Fat	Skin
Head	0.5	15.0	0.0	0.0
Trunk	2.5	13.0	0.0	0.0
Front legs	0.6	20.0	0.0	0.0
Hind legs	0.6	15.0	0.0	0.0
Front feet	1.0	3.0	0.0	0.0
Hind feet	1.0	3.0	0.0	0.0

Table 21. Values of EXP3

Segment \ Tissue	Core	Muscle	Fat	Skin
Head	0.9	0.5	0.5	0.5
Trunk	1.9	0.2	0.5	0.5
Front legs	0.9	0.2	0.5	0.5
Hind legs	0.9	0.2	0.5	0.5
Front feet	0.9	0.5	0.5	0.5
Hind feet	0.9	0.5	0.5	0.5

COMPARISON OF PREDICTED AND EXPERIMENTAL RESULTS

The comparison of the experimental temperature data with the simulated temperature results are shown in Figure 18. The temperatures shown are the reduced temperatures, which are the differences in ^{o}C between the transient and basal values. The time shown is the reduced time, which was defined earlier in the section on experimental procedures. In the figure, the trunk core temperatures gave the worst fit. This is understandable because the experimental values which were assumed to be the body core temperature were obtained from the rectal region. Since the organs that produce the largest quantity of heat energy are located in the thorax and upper abdomen, and because the blood supply to the lower viscera is not as good as that to the upper region, the rectal temperature would be expected to be quite a bit lower than the true core temperature, especially under the fulminant hyperthermia condition. The relative lack of smoothness of the modeled trunk core temperature was due to the sudden change in heat generation rate assumed in the model. The rates of decrease of post-mortem muscle temperatures in the model were faster than that of the experimental results. This could be due to the assumed sizes and shapes of the segments. During the course of this study, it was found

Figure 18. Comparison of simulated and experimental temperature variation data

Legend:

Elm = experimental hind leg muscle temperature
Eam = experimental front leg muscle temperature
Ebm = experimental body trunk muscle temperature
Erc = experimental rectal temperatrue
Efa = experimental body trunk fat temperature
Els = experimental hind leg skin temperature
Eas = experimental body trunk skin temperature
Mlm = simulated hind leg muscle temperature
Mam = simulated front leg muscle temperature
Mbm = simulated body trunk muscle temperature
Mrc = simulated trunk core temperature
Mfa = simulated body trunk fat temperature
Mls = simulated hind leg skin temperature
Mas = simulated body trunk skin temperature

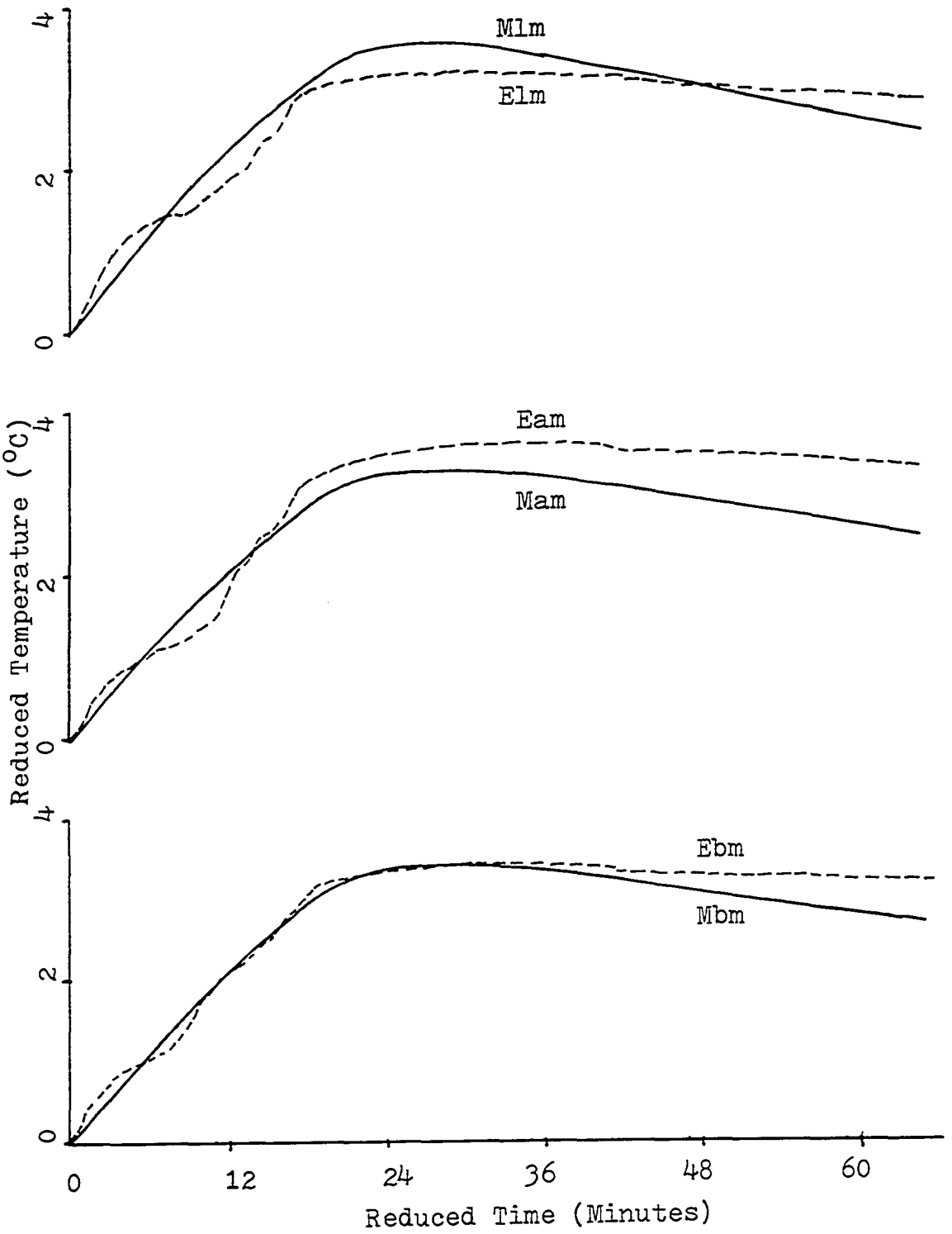
Mlm
Elm
Eam
Mam
Ebm
Mbm
Reduced Temperature (°C)
0
2
4
0
12
24
36
48
60
Reduced Time (Minutes)

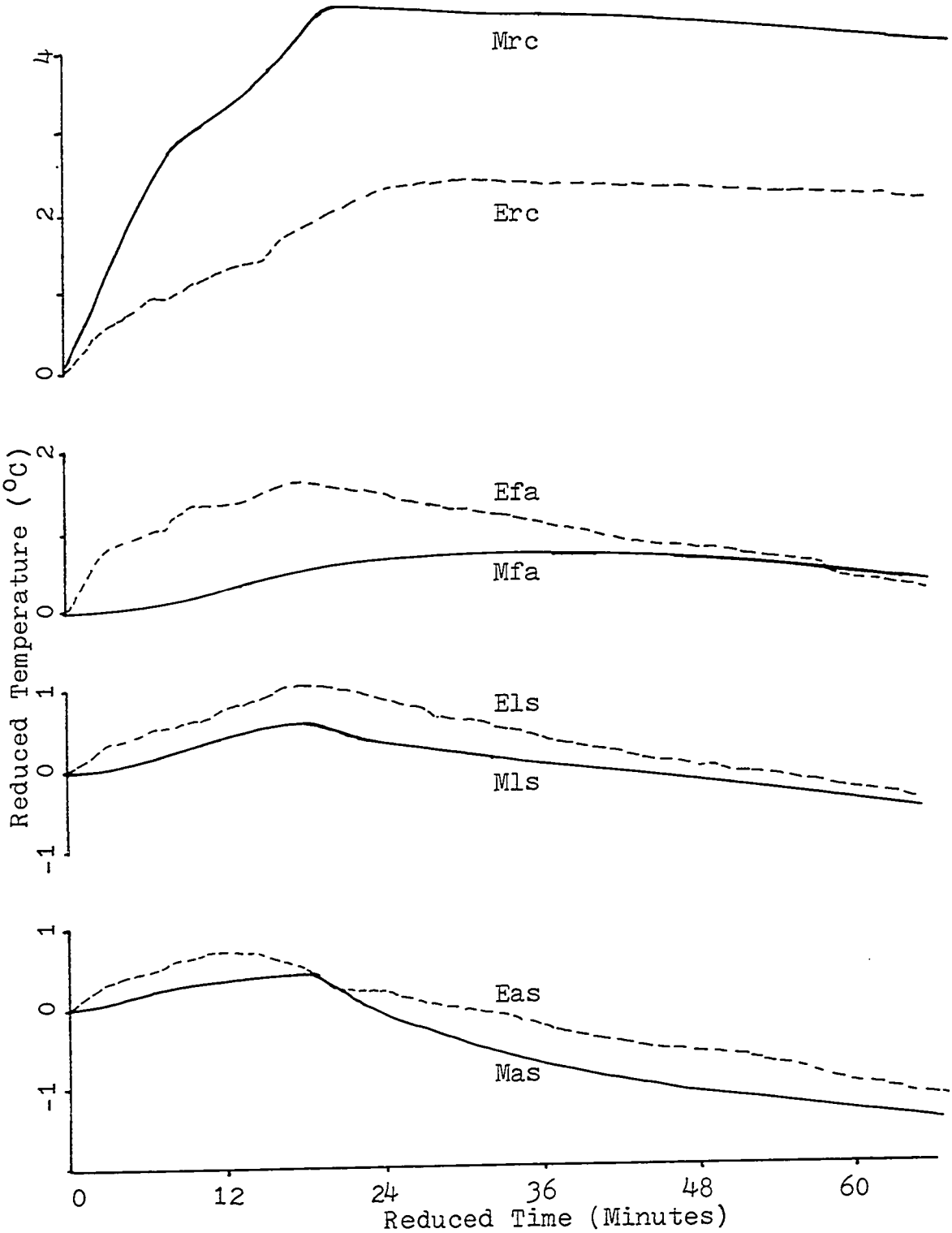

Figure 18. (Continued)

that the shape and size of a segment, which were determined by the volume and surface area values, had very significant influence on the rates of decline of post-mortem temperatures for all the layers in the model. The trunk fat shows a very poor matching in Figure 18. This is due to the fact that this layer is almost entirely passive in its temperature control in the model. The skin temperatures of the model corresponded to the experimental results quite well.

With Figure 10 to 17 in mind, it can be seen that the model responded to changes in values of parameters in a manner that is consistent with the understanding of the effects these parameters have on the physical system. However, because many of these changes are interrelated in this model, to produce the desired simulated results, the values of many of the parameters had to be determined by iteration.

CONCLUSION AND RECOMMENDATIONS

These experiments showed that for swine under the stress of malignant hyperthermia, the experimental temperature changes varied significantly among individuals while the apparent blood flow patterns were quite consistent. Temperatures generally started increasing within a few minutes after the initiation of anesthesia by halothane administration. Although the rates of increase differed from animal to animal, the overall patterns of temperature changes were quite similar. The biceps femoris and the triceps brachii usually showed the highest rate of increase and had the highest peak temperatures. After cardiac and respiratory cessation, the skin temperatures fell rapidly whereas the muscle temperatures continued to increase.

The experimentally derived relative blood flow rates and pressure data were erratic around the first moments of halothane administration. Generally the values fell after this period, only to rise again just before cardiac and respiratory cessation.

It was also found that the temperature measured in a particular layer depended on how deep the thermistor probe had been inserted into the layer. The difference could be as much as 2°C to 3°C. The measurements

of the rates of decrease of post-mortem temperatures were also dependent on the depth of insertion of the thermistors. However, this effect was not very significant.

The results of this study demonstrated that it is possible to simulate the fulminant hyperthermia temperature changes as well as the post-mortem temperature decline with a mathematical model involving a set of differential equations, even though the correspondences may not be exact.

Because of the lack of data on blood flow rates, metabolic rates, thermal conductivities, weights, volumes, thickness, surface areas, and other physiological and physical properties of many of the different parts of the swine, many estimates of the parameter values used in the model were not very accurate. This could have very significant effects on the performance of the model. For a better model to be derived, accurate values of the parameters would be necessary. Careful experimental measurements might be needed.

It has been observed that the recorded temperatures depended very much on the depth of insertion of the thermistor probes. For this reason, each of the thick layers in the present model could be divided into two or more compartments.

It is obvious that the dorsal part of the trunk is anatomically very different from the abdominal part because of the difference in thickness of muscle and fat layers between the two. The difference between the anterior and the posterior ends of the trunk is also large because of the differences in metabolic rate and blood supply. It might be appropriate to model the trunk with four half-cylinders, each having its own layers with separate heat generation terms and blood flow terms.

The feet could probably be left out of the model because of their small size. This would not have much effect on the performance of the rest of the model, and would make the mathematical simulation slightly simpler.

Experimentally, temperature measurements could be obtained from more locations on the animal. This would give a better picture of the temperature profile of the animal. If the infrared thermography system could be stabilized so that the sensitivity would not drift with time or vary with the amount of liquid nitrogen present in the cooling chamber, a more accurate measurement of skin temperatures could possibly be obtained.

BIBLIOGRAPHY

1. Allen, W. M., S. Berrett, J. D. J. Harding, and D. S. P. Patterson. 1970. Experimentally induced acute stress syndrome in Pietrain pigs. Vet. Rec. 87:64.

2. Anderson, I. L., and E. W. Jones. 1976. Porcine malignant hyperthermia: Effect of Dantrolene Sodium on in vitro halothane-induced contraction of susceptible muscle. Anesthesiology 44(1):57.

3. Barnes, S. 1932. A myopathic family: With hypertrophic, pseudotrophic, atrophic and terminal (distal in upper extremities) stages. Brain 55:1.

4. Berman, M. C., G. G. Harrison, A. B. Bull, and J. E. Kench. 1970. Changes underlying halothane-induced malignant hyperthermia in Landrace pigs. Nature 225:633.

5. Bioastronautics Data Book. 1973. 2nd ed. National Aeronautics and Space Administration, Washington D.C.

6. Britt, B. A., L. Endrenyl, and D. L. Cadman. 1975. Calcium uptake into muscle of pigs susceptible to malignant hyperthermia: in vitro and in vivo studies with and without halothane. Brit. J. Anaesth. 47:650.

7. Britt, B. A., and W. Kalow. 1970. Malignant hyperthermia: A statistical review. Can. Anaesth. Soc. J. 17(4):293.

8. Britt, B. A., and W. Kalow. 1970. Malignant hyperthermia: Aetiology unknown! Can. Anaesth. Soc. J. 17(4):316.

9. Britt, B. A., W. Kalow, A. Gordon, J. G. Humphrey, and N. B. Rewcastle. 1973. Malignant hyperthermia: An investigation of five patients. Can. Anaesth. Soc. J. 20(4):431.

10. Brody, S. 1945. Bioenergetics and growth. Reinhold, New York.

11. Brown, R. C. 1954. Hyperpyrexia and anaesthesia. Brit. Med. J. 2:1526.

12. Burton, A. C., and O. G. Edholm. 1955. Man in a cold environment. Edward Arnold Ltd., London.

13. Chan, A. K., R. A. Sigelmann, A. W. Guy, and J. F. Lehmann. 1973. Calculation by the method of finite difference of the temperature distribution in layered tissue. IEEE Trans. Bio-med. Eng. 20:86.

14. Clark, M. G., C. H. Williams, W. F. Pfeifer, D. P. Bloxham, C. A. Taylor, and H. A. Lardy. 1973. Accelerated substrate cycling of Fructose-6-phosphate in the muscle of malignant hyperthermia pigs. Nature 245:99.

15. Cody, J. R. 1968. Muscle rigidity following administration of succinylcholine. Anesthesiology 29:159.

16. Crosbie, R. J., J. D. Hardy, and E. Fessenden. 1963. Electrical analog simulation of temperature regulation in man. In Herzfeld, Charles M., ed. Temperature--its measurement and control in science and industry. Vol. 3. Reinhold Publishing Corporation, New York.

17. Davies, R. M., K. J. Packer, and V. Whitmarsh. 1969. Malignant hyperpyrexia: Two case reports. Brit. J. Anaesth. 41:703.

18. Deighton, Thomas. 1932. The determination of the surface area of swine and other animals. J. Agri. Sci. 22:418.

19. Denborough, M. A. 1975. Serum creatine phosphokinase and malignant hyperpyrexia. Brit. Med. J. 4:408.

20. Denborough, M. A. 1977. Current concepts of the etiology and treatment of malignant hyperthermia. 2nd International Symposium on malignant hyperthermia, Denver.

21. Denborough, M. A., P. Ebeling, J. O. King, and P. Zapf. 1970. Myopathy and malignant hyperpyrexia. Lancet 1:1138.

22. Denborough, M. A., J. F. A. Foster, M. C. Hudson, and N. G. Carter. 1970. Biochemical changes in malignant hyperpyrexia. Lancet 1:1137.

23. Denborough, M. A., R. J. R. Hird, and J. O. King. 1971. Malignant hyperpyrexia. Brit. Med. J. 3:636.

24. Denborough, M. A., and R. R. H. Lovell. 1960. Anaesthetic deaths in a family. Lancet 2:45.

25. Ellis, F. R., I. M. C. Clarke, T. N. Appleyard, and R. C. W. Dinsdale. 1974. Malignant hyperpyrexia induced by nitrous oxide and treated with dexamethasone. Brit. Med. J. 4:270.

26. Ellis, F. R., I. M. C. Clarke, M. Modgill, S. Currie, and D. G. F. Harriman. 1975. Evaluation of creatine phosphokinase in screening patients for malignant hyperthermia. Brit. Med. J. 3:511.

27. Ellis, F. R., N. P. Keaney, D. G. F. Harriman, D. W. Sumner, E. Kyei-Mensah, J. H. Tyrrell, J. B. Hargreafes, J. H. Parikh, and P. L. Malrooney. 1972. Screening for malignant hyperpyrexia. Brit. Med. J. 3:559.

28. Fan, L. T., F. T. Hsu, and C. L. Hwang. 1971. A review on mathematical models of the human thermal system. IEEE Trans. Bio-med. Eng. 18.218.

29. Gjessing, J., J. Barsa, and P. J. Tomlin. 1976. A possible means of rapid cooling in the emergency treatment of malignant hyperthermia. Brit. J. Anaesth. 48(5):469.

30. Gnaedinger, R. H., A. M. Pearson, E. P. Reineke, and V. M. Hix. 1963. Body composition of market weight pigs. J. Anim. Sci. 22:495.

31. Gordon, R. G., and R. B. Roemer. 1975. The effect of radial node spacing on finite difference calculations of temperatures in living tissues. IEEE Trans. Bio-med. Eng. 22:77.

32. Gordon, R. G., and R. B. Roemer. 1975. The effect of radial nodal spacing on the performance of a mathematical model of the human temperature regulatory system. IEEE Trans. Bio-med. Eng. 22:80.

33. Gordon, R. G., R. B. Roemer, and S. M. Horvath. 1976. A mathematical model of the human temperature regulatory system--transient cold exposure response. IEEE Trans. Bio-med. Eng. 23:434.

34. Gronert, G. A., J. H. Milde, and R. A. Theye. 1976. Porcine malignant hyperthermia induced by halothane and succinylcholine. Anesthesiology 44(2):125.

35. Gronert, G. A., J. H. Milde, and R. A. Theye. 1976. Dantrolene in porcine malignant hyperthermia. Anesthesiology 44(6):489.

36. Gronert, G. A., and R. A. Theye. 1976. Halothane-induced porcine malignant hyperthermia: Metabolic and hemodynamic changes. Anesthesiology 44(1):37.

37. Guedel, A. E. 1952. Inhalation Anaesthesia. 2nd ed. Macmillan, New York.

38. Guyton, A. C. 1966. Textbook of medical physiology. 3rd ed. W. B. Saunders Company, Philadelphia.

39. Hall, L. W., C. M. Trim, and N. Woolf. 1972. Further studies of porcine malignant hyperthermia. Brit. Med. J. 2:145.

40. Handbook of Physiology. 1964. Respiration exchange of heat and water. In Respiration. Vol. 1. American Physiology Society, Washington D.C.

41. Harrison, G. G. 1971. Anaesthetic induced malignant hyperpyrexia: A suggested method of treatment. Brit. Med. J. 3:454.

42. Harrison, G. G. 1973. Althesin and malignant hyperpyrexia. Brit. J. Anaesth. 45:1019.

43. Harrison, G. G. 1975. Control of the malignant hyperthermia syndrome in MHS swine by dantrolene sodium. Brit. J. Anaesth. 47:62.

44. Harrison, G. G., J. G. Biebyck, J. Terblanche, D. M. Dent, R. Hickman, and S. J. Saunders. 1968. Hyperpyrexia during anesthesia. Brit. Med. J. 3:594.

45. Harrison, G. G., S. J. Saunder, J. F. Biebyck, R. Hickman, D. M. Dent, V. Weaver, and J. Terblanche. 1969. Anaethetic-induced malignant hyperpyrexia and a method for its prediction. Brit. J. Anaesth. 41:844.

46. Heap, F. C., and G. A. Lodge. 1966. Changes in body composition of the sow during pregnancy. Anim. Prod. 9:237.

47. Heffron, J. J. A., R. A. Theye, and G. A. Gronert. 1977. Porcine malignant hyperthermia: Calcium binding and release by isolated sarcoplasmic reticulum. 2nd International Symposium on Malignant Hyperthermia, Denver.

48. Huckaba, C. E., H. S. Tam, R. C. Darling, and J. A. Downey. 1975. Prediction of dynamic temperature distributions in the human body. AIChE J. 21(5):1006.

49. Iberall, A. S. 1972. Comments on 'A review on mathematical models of the human thermal system'. IEEE Trans. Bio-med. Eng. 19:67.

50. Isaacs, S. H., and M. B. Barlow. 1970. The genetic background to malignant hyperpyrexia revealed by serum creatine phosphokinase estimations in asymptomatic relatives. Brit. J. Anaesth. 42:1077.

51. Isaacs, H., and M. B. Barlow. 1970. Malignant hyperpyrexia during anaesthesia: Possible association with subclinical myopathy. Brit. Med. J. 1:275.

52. Isaacs, H., G. Frere, and J. Mitchell. 1973. Histological, histochemical and ultramicroscopic findings in muscle biosies from carriers of the trait for malignant hyperpyrexia. Brit. J. Anaesth. 45:860.

53. Isaacs, H., and J. J. A. Heffron. 1975. Morphological and biochemical defects in muscles of human carriers of malignant hyperthermia syndrome. Brit. J. Anaesth. 47:475.

54. Jones, E. W., D. D. Kerr, and T. E. Nelson. 1971. Malignant hyperthermia--observations in Poland China pigs. 1st International Symposium on Malignant Hyperthermia, Toronto.

55. Jones, E. W., T. E. Nelson, I. L. Anderson, D. D. Kerr, and T. K. Burnap. 1972. Malignant hyperthermia of swine. Anesthesiology 36(1):42.

56. Kalow, W., B. A. Britt, M. E. Tureau, and C. Haist. 1970. Metabolic error of muscle metabolism after recovery from malignant hyperthermia. Lancet 4:895.

57. King, J. O., M. A. Denborough, and P. W. Zapf. 1972. Inheritance of malignant hyperpyrexia. Lancet 1:365.

58. la Cour, D., P. Juul-Jensen, and E. Reske-Nielsen. 1971. Central and peripheral mechanism in malignant hyperthermia. 1st International Symposium on Malignant Hyperthermia, Toronto.

59. Leading Article. 1968. Malignant hyperpyrexia. Brit. Med. J. 3:69.

60. Leading Article. 1971. Malignant hyperpyrexia. Brit. Med. J. 3:441.

61. Leading Article. 1974. New causes of malignant hyperpyrexia. Brit. Med. J. 4:488.

62. Lucke, J. N., G. M. Hall, and D. Lister. 1976. Porcine malignant hyperthermia I: Metabolic and physiological changes. Brit. J. Anaesth. 48:297.

63. McAdams, W. H. 1942. Heat transmission. 2nd ed. McGraw-Hill Book Company, Inc, New York.

64. Miller, N. C., and R. C. Seagrave. 1974. A model of human thermoregulation during water immersion. Comp. in Bio. and Med. 4(2):165.

65. Moulds, R. F. W., and M. A. Denborough. 1974. Identification of susceptibility to malignant hyperpyrexia. Brit. Med. J. 2:245.

66. Mount, L. E., and D. L. Ingram. 1971. The pig as a laboratory animal. Academic Press, London.

67. Nelson, T. E. 1977. Excitation-contraction coupling: A common etiologic pathway for malignant hyperthermia susceptible muscle. 2nd International Symposium on Malignant Hyperthermia, Denver.

68. Nelson, T. E., K. L. Austin, and M. A. Denborough. 1977. Screening for malignant hyperthermia. Brit. J. Anaesth. 49:169.

69. Nelson, T. E., D. M. Bedell, and E. W. Jones. 1975. Porcine malignant hyperthermia: Effects of temperature and extracellular calcium concentration on halothane-induced contracture of susceptible skeletal muscle. Anesthesiology 42(3):301.

70. Nelson, T. E., E. W. Jones, J. H. Venable, and D. D. Kerr. 1972. Malignant hyperthermia of Poland China swine: Study of a myogenic etiology. Anesthesiology 36(1):52.

71. Parikh, R. K., and W. H. S. Thomson. 1972. Malignant hyperthermia: A fatal case and his family. Brit. J. Anaesth. 44:742.

72. Peterson, L. H. 1965. Control and regulation of the cardiovascular system. In Yamamoto, W. S. and J. R. Brobeck. Physiological controls and regulations. W. B. Saunders Company, Philadelphia.

73. Poppendiek, H. F., R. Randall, J. A. Breeden, J. E. Chambers, and J. R. Murphy. 1966. Thermal conductivity measurements and predictions for biological fluids and tissues. Cryobiology 3(4):318.

74. Seagrave, R. C. 1971. Biomedical applications of heat and mass transfer. I. S. U. Press, Ames, Iowa.

75. Shitzer, A. 1973. Addendum to 'A review on mathematical models of the human thermal system'. IEEE Trans. Bio-med. Eng. 20:65.

76. Steers, A. J. W., J. A. Tallack, and D. E. A. Thompson. 1970. Fulminating hyperpyrexia during anesthesia in a member of a myopathic family. Brit. Med. J. 2:341.

77. Stolwijk, J. A. J., and J. D. Hardy. 1965. Skin and subcutaneous temperature changes during exposure to intense thermal radiation. J. Appl. Physiol. 20:1006.

78. Stolwijk, J. A. J., and J. D. Hardy. 1966. Temperature regulation in man--a theoretical study. Pfluegers Archiv. 291:129.

79. Sybesma, W., and G. Eikelenboom. 1969. Malignant hyperthermia syndrome in pigs. Neth. J. Vet. Sci. 2(2):155.

80. Tobey, G. E., J. G. Graeme, and L. P. Huelsman. 1971. Operational Amplifiers--Design and Application. McGraw-Hill, Kogakusha, Japan.

81. Topel, D. G., E. I. Bicknell, K. S. Preston, L. L. Christian, and C. Y. Matsushima. 1968. Porcine stress syndrome. Mod. Vet. Prac. 49(5):40.

82. Wang, J. K., E. A. Moffitt, and J. W. Rosevear. 1969. Oxidative phosphorylation in acute hyperthermia. Anesthesiology 30(4):439.

83. Williams, C. H., C. Houchins, M. D. Shanklin. 1975. Pigs susceptible to energy metabolism in the fulminant hyperthermia stress syndrome. Brit. Med. J. 3:411.

84. Williams, C. H., D. H. Stubbs, C. G. Payne, and J. D. Benedict. 1976. Role of hypertension in fulminant hyperthermia stress syndrome. Brit. Med. J. 1:628.

85. Wilson, R. D., R. J. Nichols, T. E. Dent, and C. R. Allen. 1966. Disturbances of the oxidative phosphorylation mechanism of a possible etiological factor in sudden malignant hyperthermia. Anesthesiology 27(2):231.

86. Wissler, E. H. 1963. An analysis of factors affecting temperature levels in the nude human. In Herzfeld, Charles M., ed. Temperature--its measurement and control in science and industry. Vol. 3. Reinhold Publishing Corporation, New York.

87. Wissler, E. H. 1964. A mathematical model of the human thermal system. Bulletin of Mathematical Biophysics 26:147.

88. Woolf, N., L. Hall, C. Thorne, M. Down, and R. Walker. 1970. Serum creatine phosphokinase levels in pigs reacting abnormally to halogenated anaesthetics. Brit. Med. J. 3:386.

89. Wyndham, C. H., and A. R. Atkins. 1960. An approach to the solution of the human biothermal problem with the aid of an analog computer. Proc. 3rd International Conf. Med. Electronics 3:32.

ACKNOWLEDGMENTS

I am greatly indebted to Dr. Richard Seagrave for his patient guidance and enthusiastic encouragement during the years of my graduate study.

Thanks are extended to the committee members (Drs. Neal Cholvin, Lauren Christian, Curran Swift, and David Topel) for their valuable suggestions and interest in the project. A special thank you is due Dr. Topel and Dr. Christian who literally got their hands dirty when participating in some of the experimental work.

My appreciation goes to Mr. Joseph Morrisey and Miss Margaret Cooper, whose skillful help and humor made my monstrous task of working with struggling pigs easier and sometimes, even enjoyable.

APPENDIX A. USE OF THE COMPUTER PROGRAM

In the main program, MAIN, the ambient temperature, the death temperature, the length of the time of simulation and the step size of the independent variable have to be specified. The body core temperature at which the metabolic rates change is specified in CMET.

Normally, the subroutine CBFLO is called instead of CBFLOW for estimating the steady-state blood flow rates. Even though values of R11(6), R22(6), R33(6) and R4X(6) are read into the program, usually the calculated values of R1(6), R2(6), R3(6) and R4(6) are used for the values of radii bounding the tissue layers in the segments of the body.

The metabolic rates of the 24 parts of the body are the last physical parameters determined. After all the steady-state values of the other information have been specified, the exact power for the equation, TMAT=(186000*WEIT**POWER)/(24*60) in subroutine CPARAM is found. It is to be determined only after the steady-state equations have been solved by hand so that the body metabolic rate is known.

The other data that are needed for the simulation are read in by the program with READ statements. The following is a list of data read in at the end of the

program:

```
Trial number
SEG(6)
TCOND1(6), TCOND2(6), TCOND3(6), TCOND4(6)
ROCOR(6), ROMUS(6), ROFAT(6), ROSKN(6)
ROBLD
BTEM(24)
DA(6)
DC(6)
DD(6)
BETA(6)
ALFA(24)
EXP1(24)
EXP2(24)
EXP3(24)
DETA
WEIT
COR(6), XMUS(6), FAT(6), SKN(6)
PCWT(6)
PCAT(6)
PCMT(24)
XLL(6), R11(6), R33(6), R4X(6)
PCBL(24)
```

Discussion of the Program and the Subroutines

MAIN-----This starts the operation of the program and controls the progress of the simulation. The length of time of simulation, the death temperature, the ambient temperature and the time increment size are stated in this part. Initial conditions are obtained by calling STRTUP. The transient state simulation is carried out by calling TRAP.

STRTUP---This subroutine collects all the input characteristics of the animal and tabulates them. It reads in the thermal conductivities, the products of

density and heat capacities, and the constants involved in blood flow and metabolic rates. This subroutine also calls the subroutines CPARAM, CLCOEF, HTCOEF, FILCOD, and CBFLO for obtaining the physical parameters such as blood flow rates, metabolic rates, heat transfer coefficients, body surface area, and other constants of the differential equations.

TRAP-----This subroutine uses the numerical integration method, the "Modified Euler's Method", to solve the differential equations. Every value of each of the dependent variables is obtained by multiplying the size of the independent variable by the value of the slope at the previous position of the independent variable. The subroutine FCT is called to calculate the first derivative of the dependent variable with respect to the independent variable. The subroutines CRESP, CMET and CFLOW are called for every increment of the independent variable to readjust the respiratory heat loss, the metabolic rates and the blood flow rates.

FCT------This subroutine calculates the first derivatives of the dependent variables with respect to time in the differential equations. The subroutine FILCOV is

called to calculate the coefficients of the convective heat exchange.

FILCOD---This subroutine calculates the unvarying coefficients describing the conductive heat transfer and arrange them in the matrix form of COND(24,24) for use in FCT.

FILCOV---This subroutine calculates the coefficients for the convective heat transfer and arrange them in the matrix form of CONV(24,25). Interaction with the environment and metabolic rate terms are also included.

OUTP-----This subroutine arranges the simulated data in forms suitable for numerical and graphical outputs. It also specifies the form of output desired, whether it be in printouts, cards or graphical forms. Subroutine PRNT is called to plot out data in graphical form.

CLCOEF---This subroutine calculates the radii, volumes, and average thermal conductivies of the segments, and uses this information to find the unvarying coefficients of the terms in the differential equations. These coefficients COEF(24,3) are later used by subroutines FILCOD and FILCOV to find the coefficients for the conductive and

convective terms in the differential equations.

CPARAM---Based on body weight, this subroutine uses empirical equations to calculate physical parameters such as body surface areas, metabolic rates and volumes of the segments.

CBFLO----This subroutine estimates the steady-state values of blood flow rates in different parts of the body. This is done by reading in the blood flow rates in different parts of the body as a percentage of the total flow rate and multiplying by the total flow rate. The read-in estimates are compared with the estimates made by solving the differential equations at steady-state. If the difference is large, the metabolic rates are changed to decrease the difference within a certain range. The empirical equation for WTO was obtained by plotting the logarithmic values of cardiac outputs versus body weights.

HTCOEF---This subroutine calculates the heat transfer coefficients for all the segments by calling the function HTX.

HTX------This function uses an empirical formula to calculate the convective and radiative heat transfer coefficients of a segment basing on the information

of volume, area and temperature.

CMET-----This subroutine calculates the metabolic rates for all the parts of the body as the temperatures and time change. At the start of hyperthermia, the metabolic rates are assumed to take on a specific set of values. When the body core temperature rises to a specified value, the metabolic rates are assumed to take on a different set of values. When the body core temperature reaches DTEMP, all the metabolic rates are assumed to fall exponentially to zero.

CBFLOW---This subroutine estimates the steady-state values of blood flow rates in different parts of the body. This is done by reading in the blood flow rates in different parts of the body as a percentage of the total flow rate and multiplying by the total flow rate. Either CBFLO or CBFLOW is used in the program.

CRESP----This subroutine calculates the heat loss due to respiration by gas exchange and evaporation as a function of the body core temperature.

CFLOW----This subroutine calculates the blood flow rates to different parts of the body as functions of the temperature distribution during the transient conditions. When the body core temperature reaches

DTEMP, all the flows are assumed to fall to zero.

PRNT-----This subroutine plots out the variables specified in graphical form.

Glossary

Variables and terms used in the program are listed below. The numbers shown in the subscripts are the maximal values used for the variables.

ALFA(24) In CFLOW, a set of constants that change the flows with temperature

ABFLO In OUTP, the total cardiac output

AUX(4,24) Storage array used in TRAP

BETA(6) The term for correcting the difference between the skin temperature and the true surface temperature

BFLO(24) Blood flow rate to each of the layers in all the segments

BT Skin temperature, used in function HTX

BTEM(24) The temperature of each of the parts

COEF(24,3) The matrix of coefficients of the terms in the 24 differential equations

COND(24,24) Matrix of constants of terms describing the conductive heat transfer in the differential equations

CONV(24,25) Matrix of constants of terms describing the convective heat transfer in the differential equations

COR(6) The percentage of the segment that is the core tissue, used in CPARAM and CLCOEF

DA(6)	Steady-state temperature difference between muscle layer and core layer, used in STRTUP for calculation of steady-state temperatures
DC(6)	The temperature difference between the fat and skin layers, used in STRTUP for steady-state temperature determination
DD(6)	The temperature difference between the core and skin layers used in STRTUP for steady-state temperature determination
DETA	A constant used to vary RESP with the change of the body core temperature, used in CRESP
DERT(24)	The first derivative of temperature with respect to time for each layer, used in FCT
DERY(24)	The first derivative of temperature with respect to time for each layer, used in TRAP
DTEMP	The body core temperature at which the model animal "dies"
EXP1(24)	The number of times the heat generation terms are increased over the steady-state metabolic rates at the start of hyperthermia, used in CMET
EXP2(24)	The number of times the heat generation terms are increased over the steady-state metabolic rates at the later part of hyperthermia, used in CMET
EXP3(24)	The time constants for the decay of heat generation rates after death, used in CMET
FAT(6)	For all of the segments, the percentage of a segment that is fat tissue, used in CPARAM and CLCOEF
H	The step size of the increment of the independent variable, time in minutes, used in TRAP
HCOV	The convective heat transfer coefficient for free convection, used in HTX
HRAD	The radiative heat transfer coefficient, used in HTX

HT(6)	The heat transfer coefficients for the different segments, used in HTCOEF
ISKIN(6)	A vector that stores the numbers 4, 8, 12, 20 and 24 that represent the skin layers of the body
IVEC(92)	A vector that stores the locations of the non-zero terms of the CONV(24, 25), used in FCT to facilitate matrix multiplication
IX	The same as (x-10.0), a way of counting time, used in OUTP to get the 10 minutes of steady-state output before hyperthermia begins
L	A term used in FCT to help fill the matrix IVEC(92) once only
LCOL	Used in FCT as part of the subscripts of CONV(24,25), it indicates the part from which blood flows
LL	A term used in FCT to help fill the matrix IVEC(92) once only
LROW	Used in FCT as part of the subscripts of CONV(24,25), it indicates the part to which blood flows
MET(24)	The metabolic rates for each of the layers
NDIM	The number of differential equations that have to be solved, used in TRAP
NTERM	The number of points to be plotted in each curve in the graphs plotted, used in PRNT
OBFLO(24)	The steady-state blood flow rates
OBTEM(24)	The steady-state temperatures of the various parts of the body
OMET(24)	The steady-state metabolic rates of the various parts of the body
OOMET(24)	The metabolic rates of the various parts of the body at the moment of death, used in CMET

ORESP	The steady-state respiratory heat loss, used in CRESP
PCAT(6)	The surface area of each of the segments as a percentage of the total body area, used in CPARAM
PCBL(24)	The steady-state blood flow rates of the parts of the body as percentages of the total cardiac output, used in CPARAM and CBFLO
PCMT(24)	The steady-state metabolic rates of the parts of the body as percentages of the total metabolic rate, used in CPARAM
PCWT(24)	The weight of the parts of the body as percentages of the total body weight, used in CPARAM
R1(6)	The radius bounding the core layer of each of the segments, used in CLCOEF
R2(6)	The radius bounding the muscle layer of each of the segments, used in CLCOEF
R3(6)	The radius bounding the the fat layer of each of the segments, used in CLCOEF
R4(6)	The radius of each of the segments, used in CLCOEF
R11(6)	Same as R1(6), except that these are read in instead of calculated, used in CLCOEF
R22(6)	Same as R2(6), except that these are read in instead of calculated, used in CLCOEF
R33(6)	Same as R3(6), except that these are read in instead of calculated, used in CLCOEF
R4X(6)	Same as R4(6), except that these are read in instead of calculated, used in CLCOEF
RESP	The respiratory heat loss rate
ROBLD	The product of density and heat capacity of blood, used in CLCOEF
ROCOR(6)	The product of density and heat capacity for the core tissue for every segment, used in CLCOEF

ROFAT(6)	The product of density and heat capacity for the fat tissue for every segment
ROMUS(6)	The product of density and heat capacity for the muscle tissue for every segment
ROSKN(6)	The product of density and heat capacity for the skin tissue for every segment
RR1(6)	The geometric radius of the core layer, used in CLCOEF
RR2(6)	The geometric radius of the muscle layer
RR3(6)	The geometric radius of the fat layer
RR4(6)	The geometric radius of the skin layer
SA(6)	The surface area for each of the segments, used in CLCOEF and CPARAM
SEG(6)	A vector that stores the numbers that represents the segments, i.e., 1, 2, 3, 4, 5, and 6
SKN(6)	For each segment, the percentage of each of the segment that is skin tissue, used in CLCOEF
SL	A term used in MAIN and FCT to help fill the matrix IVEC(92) once only
SUMARA	A variable that is used in STRTUP to help add up the body surface area
SUMVOL	A variable that is used in STRTUP to help add up the body volume
TA	Ambient temperature, used in HTX
TAMB	Ambient temperature, used in MAIN and other parts of the program except HTX
TAREA	The body surface area obtained by empirical formula in CPARAM
TCON1	The average thermal conductivity of the core and muscle tissues, used in CLCOEF

TCON2	The average thermal conductivity of the muscle and fat layers
TCON3	The average thermal conductivity of the fat and skin layers
TCOND1(6)	The thermal conductivity of the core tissue for each segment, used in CLCOEF
TCOND2(6)	The thermal conductivity of the muscle tissue for each segment
TCOND3(6)	The thermal conductivity of the fat tissue for each segment
TCOND4(6)	The thermal conductivity of the skin tissue for each segment
TIME	The length of time for which the simulation is specified to last, it is specified in MAIN
TMAT	The total body metabolic rate, calculated from the body weight in CPARAM
VOL(6)	The volume of each of the segments, used in CLCOEF
VOLUME(24)	The volume of each of the parts of the body, used in CLCOEF
WEIT	The body weight of the animal
WTO	The total blood flow rate calculated by empirical formula in CPARAM
WTPT(6)	For each of the segments, the percentage of the total body weight that is a certain segment, used in CPARAM
X	The independent variable, time in minutes, used in TRAP, and OUTP
XEND	The specified time at which the simulation stops, used in TRAP
XL(6)	The length of each segment, used in CLCOEF
XLL(6)	Same as XL(6), except that these are read in instead of calculated, used in CLCOEF

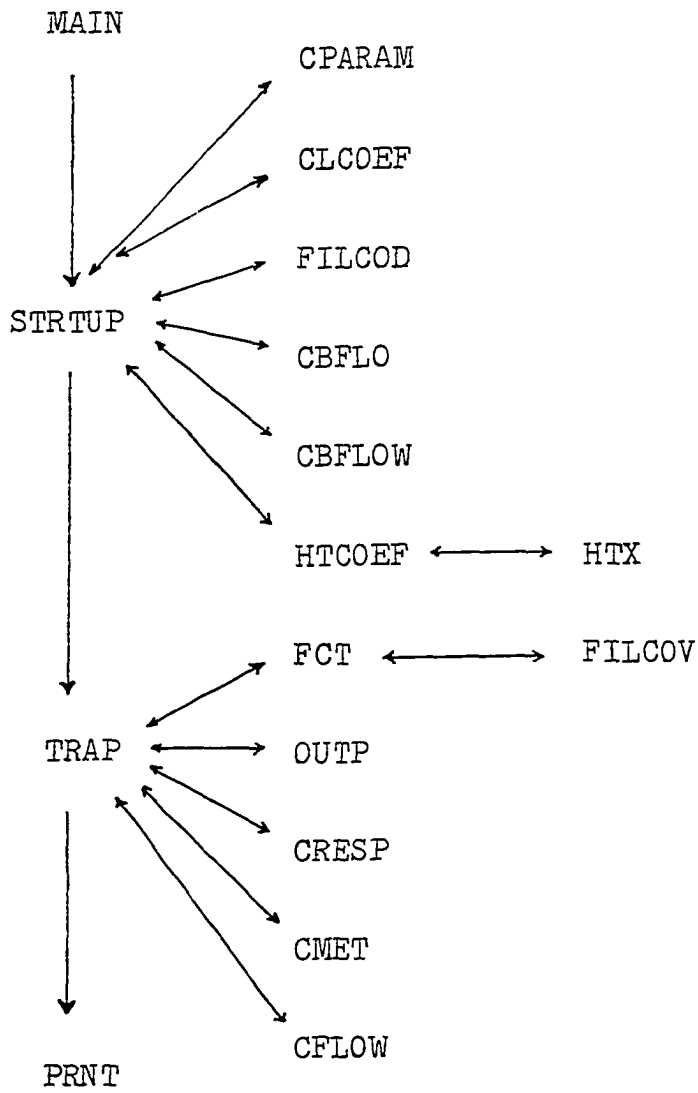

Figure 19. Flow chart of computer program

```
C      THIS PROGRAM CALCULATES THE TRANSIENT TEMPERATURES OF
C      THE ANIMAL.  IT REQUIRES SUBROUTINES FCT,OUTP,FILCOV,
C      FILCOD,STRTUP,CRESP,CFLOW,CMET,TRAP,CPARAM,CBFLOW,
C      CLCOEF,HTCOEF, AND PRNT IF WE WANT TO INPUT AND
C      LAY OUT EXPERIMENTAL DATA.
       EXTERNAL FCT,OUTP
       COMMON BETA(6),COEF(24,3),BFLO(24),ISKIN(6),MET(24),
      1COND(24,24),TAMB,SA(6),RESP,R4(6),RR4(6),
      2OMET(24),OBFLO(24),ABFLO,VOLUME(24),SL,DTEMP
      3,OBTEM(24),WEIT,TMAT,ORESP,TIME
       DIMENSION PRMT(5),AUX(24,24),BTEM(24),DERT(24),
      1ALFA(24),EXP1(24),EXP2(24),EXP3(24)
       SL=0.
       TAMB=26.
       TIME=90.
       DTEMP=45.2
       PRMT(1)=0.
       PRMT(2)=TIME+0.009
       PRMT(3)=0.04
       PRMT(4)=0.05
       CALL STRTUP(BTEM,ALFA,EXP1,EXP2,EXP3,DETA)
C      CALCULATE UNSTEADY STATE TEMPERATURE CHANGES
       CALL TRAP(PRMT,BTEM,DERT,24,IHLF,FCT,OUTP,AUX,
      1ALFA,EXP1,EXP2,EXP3,DETA)
       STOP
       END


       SUBROUTINE STRTUP(BTEM,ALFA,EXP1,EXP2,EXP3,DETA)
C      THIS SUBROUTINE COLLECTS ALL THE INPUT CHARACTERISTICS
C      OF THE ANIMAL AND TABULATE IT.
       COMMON BETA(6),COEF(24,3),BFLO(24),ISKIN(6),MET(24),
      1COND(24,24),TAMB,SA(6),RESP,R4(6),RR4(6),
      2OMET(24),OBFLO(24),ABFLO,VOLUME(24),SL,DTEMP
      3,OBTEM(24),WEIT,TMAT,ORESP,TIME
       DIMENSION TCOND1(24),TCOND2(24),TCOND3(24),TCOND4(24)
       DIMENSION ROCOR(24),ROMUS(24),ROFAT(24),ROSKN(24),
      1ALFA(24)
       DIMENSION COR(6),XMUS(6),FAT(6),SKN(6),VOL(6),XL(6),
      1R1(6),R2(6),R3(6),SEG(6),BTEM(24),HT(6)
      2,EXP1(24),EXP2(24),EXP3(24),PCMT(24),PCBL(24)
       DIMENSION DA(6),DC(6),DD(6),XLL(6),R11(6),R22(6),
      1F33(6),R4Y(6)
       REAL MET
C      TITLE THE OUTPUT TRIAL NUMBER
       READ(5,991) TRIAL
 991   FORMAT(F10.5)
       WRITE (6,992) TRIAL
 992   FORMAT(10X,'TRIAL RUN # ',F10.5)
C      READ IN CONDUCTIVITIES OF VARIOUS PARTS OF THE BODY.
```

```
C      IF WE WANT TO READ IN 24 DIFFERENT VALUES OF THERMAL
C      CONDUCTIVITIES AND 24 VALUES OF PRODUCTS OF DENSITY
C      AND HEAT CAPACITY, THEN USE THE FOLLOWING READ AND
C      WRITE STATEMENTS.
       READ(5,993) (SEG(I),I=1,6)
  993  FORMAT(6F10.2)
       READ(5,994) (TCOND1(I),TCOND2(I),TCOND3(I),TCOND4(I),
      1I=1,6)
  994  FORMAT(4F20.8)
C      READ IN PRODUCTS OF DENSITY AND HEAT CAPACITY
       READ(5,994) (ROCOR(I),ROMUS(I),ROFAT(I),ROSKN(I),
      1I=1,6),ROBLD
       WRITE(6,1000)
 1000  FORMAT(///25X,'PARAMETERS USED TO DESCRIBE THE PIG')
       WRITE(6,1004)
       WRITE(6,1005)
 1004  FORMAT(//20X,'THERMAL CONDUCTIVITIES')
 1005  FORMAT(/2X,'SEGMENT',6X,'CORE',11X,'MUSCLE',9X,'FAT',
      112X,'SKIN')
       WRITE(6,1010) (SEG(I),TCOND1(I),TCOND2(I),
      1TCOND3(I),TCOND4(I),I=1,6)
 1010  FORMAT(F10.0,5X,F10.6,5X,F10.6,5X,F10.6,5X,F10.6)
       WRITE(6,1015)
 1015  FORMAT(//10X,'PRODUCTS OF DENSITY AND HEAT CAPACITY')
       WRITE(6,1005)
       WRITE(6,1010) (SEG(I),ROCOR(I),ROMUS(I),
      1ROFAT(I),ROSKN(I),I=1,6)
       WRITE(6,1025) ROBLD
 1025  FORMAT(5X,'ROBLD=',5X,F10.6)
C      READ IN STEADY STATE TEMPERATURES
       READ(5,3090) BTEM(4),BTEM(6),BTEM(7),BTEM(8),BTEM(10)
       READ(5,3090) BTEM(12),BTEM(16),BTEM(18),BTEM(20),
      1BTEM(24)
 3090  FORMAT(5F10.6)
       READ(5,3092) (DA(I),DC(I),DD(I),I=1,6)
 3092  FORMAT(3F10.6)
       DO 3095 I=9,17,8
       J=(3+I)/4
       D=BTEM(I+1)-BTEM(I+3)
       BTEM(I+2)=BTEM(I+3)+D*DC(J)/DD(J)
 3095  BTEM(I)=BTEM(I+1)+D*DA(J)/DD(J)
       BTEM(5)=BTEM(9)+0.01
       DO 3096 I=13,21,8
       J=(3+I)/4
       BTEM(I)=BTEM(I-4)-0.65
       D=BTEM(I)-BTEM(I+3)
       BTEM(I+2)=BTEM(I+3)+D*DC(J)/DD(J)
 3096  BTEM(I+1)=BTEM(I)-D*DA(J)/DD(J)
       BTEM(1)=BTEM(5)-0.01
       D=BTEM(1)-BTEM(4)
```

```
      BTEM(2)=BTEM(1)-D*DA(1)/DD(1)
      BTEM(3)=BTEM(4)+D*DC(1)/DD(1)
      WRITE(6,3101)
 3101 FORMAT(/5X,'BTEM(I)S READ IN')
      WRITE(6,3120) (BTEM(I),I=1,24)
 3120 FORMAT(8F10.4)
      COUN=0.
C     IDENTIFY THE SKIN LAYERS
C     THESE ARE FOR THE CONVENIENCE OF CALCULATION FOR
C     SUBROUTINE FCT, CALCULATION OF METABOLIC RATE, HEAT
C     LOSS THROUGH SKIN LAYER ...ETC.
      DO 10 I=1,6
 10   ISKIN(I)=4*I
C     CALCULATE THE PHYSICAL PARAMETERS OF THE ANIMAL.
C     THE FOLLOWING FEW DATA INPUT CARDS ARE TO BE USED IF
C     WE WANT TO READ IN (INSTEAD OF CALCULATING) PARAMETERS
C     THAT ARE CHARACTERISTIC OF THE BODY, SUCH AS WEIGHT
C     OF SECTION, BLOOD FLOWS...ETC.
C     READ(5,5997) (VOL(J),MET(J),J=1,4)
C     READ(5,5997) (VOL(J),MET(J),J=5,8)
C     READ(5,5997) (VOL(J),MET(J),J=9,12)
C     READ(5,5997) (VOL(J),MET(J),J=13,16)
C     READ(5,5997) (VOL(J),MET(J),J=17,20)
C     READ(5,5997) (VOL(J),MET(J),J=21,24)
C     READ(5,5998) (BFLO(I),I=1,4)
C     READ(5,5998) (BFLO(I),I=5,8)
C     READ(5,5998) (BFLO(I),I=9,12)
C     READ(5,5998) (BFLO(I),I=13,16)
C     READ(5,5998) (BFLO(I),I=17,20)
C     READ(5,5998) (BFLO(I),I=21,24)
C     READ(5,5999) (SA(I),I=1,6)
C5997 FORMAT(8E10.5)
C5998 FORMAT(4E15.5)
C5999 FORMAT(6F12.4)
C     CALL CLCOEF(TCOND1,TCOND2,TCOND3,TCOND4,ROCOR,ROMUS,
C    1ROFAT,ROSKN,ROBLD,VOL,COR,XMUS,SKN,FAT,XL,R1,R2,R3,
C    2XLL,R11,R22,R33,R4X)
C     CALL HTCOEF(HT,VOL,BTEM)
C     CALL FILCOD
      READ(5,700) (BETA(I),I=1,6)
 700  FORMAT(6F12.5)
      READ(5,800) (ALFA(I),I=1,24)
      READ(5,800) (EXP1(I),I=1,24)
      READ(5,800) (EXP2(I),I=1,24)
      READ(5,800) (EXP3(I),I=1,24)
      READ(5,801) DETA
 800  FORMAT(8F10.5)
 801  FORMAT(F20.5)
      WRITE(6,802)
 802  FORMAT('VALUES OF ALFA FOR 24 DIFFERENT PARTS:')
```

```
      WRITE(6,800) (ALFA(I),I=1,24)
      WRITE(6,804)
  804 FORMAT('VALUES OF EXP1 FOR 24 DIFFERENT PARTS:')
      WRITE(6,800) (EXP1(I),I=1,24)
      WRITE(6,806)
  806 FORMAT('VALUES OF EXP2 FOR 24 DIFFERENT PARTS:')
      WRITE(6,800) (EXP2(I),I=1,24)
      WRITE(6,807)
  807 FORMAT('VALUES OF EXP3 FOR 24 DIFFERENT PARTS:')
      WRITE(6,800) (EXP3(I),I=1,24)
      WRITE(6,808) DETA
  808 FORMAT('VALUE OF DETA:',F20.5)
      CALL CPARAM(VOL,COR,XMUS,FAT,SKN,RCMT)
      CALL CLCOEF(TCOND1,TCOND2,TCOND3,TCOND4,ROCOR,ROMUS,
     1ROFAT,ROSKN,ROBID,VOL,COR,XMUS,SKN,FAT,XL,R1,R2,R3,
     2XLL,R11,R22,R33,R4X)
      CALL HTCOEF(HT,VOL,BTEM)
      CALL FILCOD
      WRITE(6,1030)
 1030 FORMAT(///35X,'VOLUME AND AREA OF THE SEGMENTS'//5X,
     1'SEGMENT',6X,' COR',6X,' XMUS ',4X,'FAT',7X,' SKN',
     26X,'AREA',6X,'VOLUME',4X,'LENGTH',4X,'RCORE',5X,
     3'RMUSCLE',3X,'RFAT',6X,'RSKIN'/)
      WRITE(6,1040) (SEG(I),COR(I),XMUS(I),FAT(I),SKN(I),
     1SA(I),VOL(I),XL(I),R1(I),R2(I),R3(I),R4(I),I=1,6)
 1040 FORMAT(2X,F10.0,3X,11E10.3)
      SUMARA=SA(1)+SA(2)
      SUMVOL=VOL(1)+VOL(2)
      DO 1045 I=3,6
      SUMARA=SUMARA+2.*SA(I)
 1045 SUMVOL=SUMVOL+2.*VOL(I)
      WRITE(6,1050) SUMVOL,SUMARA
 1050 FORMAT(///20X,'THE TOTAL VOLUME IS',E15.5,'AND THE
     1TOTAL SURFACE AREA IS',E15.5)
      WRITE(6,1060) ((COEF(I,J),J=1,3),I=1,24)
 1060 FORMAT('1',5X,'THE VALUES OF THE CONSTANTS CALLED
     1COEF(I,J)'//(3E20.5))
      WRITE(6,1070) (BETA(I),I=1,6)
 1070 FORMAT(/2X,'BETA VALUES FOR VARIOUS SKIN SEGMENTS'/
     110X,6F10.3)
      WRITE(6,2000) HT
 2000 FORMAT(20X,'THE HEAT TRANSFER COEFFICIENTS ARE'/(30X,
     1F12.3))
C     IF STEADY STATE BLOOD FLOW RATES CALCULATED FROM
C     TEMPERATURE AND METABOLIC RATE INFORMATION ARE DESIRED
C     ,CALL  SUBROUTINE CBFLO INSTEAD OF SUBROUTINE CBFLOW.
C     CALL CBFLOW(PCBL)
      CALL CBFLO(BTEM,ROBLD,PCBL)
      DO 2005 I=1,24
      OBTEM(I)=BTEM(I)
```

```
      OMET(I)=MET(I)
 2005 OBFLO(I)=BFLO(I)
      WRITE(6,2010) (I,I=1,8),(BFLO(I),I=1,8),(MET(I),
     1I=1,8)
 2010 FORMAT(12X,'PART #  ',8I10/12X,'BLODFLOD',8F10.3/12X,
     1'METAB   ',8F10.3)
      WRITE(6,2010) (I,I=9,16),(BFLO(I),I=9,16),(MET(I),
     1I=9,16)
      WRITE(6,2010) (I,I=17,24),(BFLO(I),I=17,24),(MET(I),
     1I=17,24)
      RETURN
      END


      SUBROUTINE TRAP(PRMT,Y,DERY,NDIM,IHLF,FCT,OUTP,AUX,
     1ALFA,EXP1,EXP2,EXP3,DETA)
C          PURPOSE
C             TO SOLVE A SYSTEM OF FIRST ORDER ORDINARY GENERAL
C             DIFFERENTIAL EQUATIONS WITH GIVEN INITIAL VALUES.
C
C          USAGE
C             CALL TRAP(PRMT,Y,DERY,NDIM,IHLF,FCT,OUTP,AUX,
C             ALFA,EXP1,EXP2,EXP3,DETA)
C             PARAMETERS FCT AND OUTP REQUIRE AN EXTERNAL
C             STATEMENT.
C
C          DESCRIPTION OF PARAMETERS
C             PRMT   - AN INPUT AND OUTPUT VECTOR WITH DIMEN-
C             SION GREATER OR EQUAL TO 5, WHICH SPECIFIES
C             THE PARAMETERS OF THE INTERVAL AND OF ACCURACY
C             AND WHICH SERVES FOR COMMUNICATION BETWEEN OUT-
C             PUT SUBROUTINE (FURNISHED BY THE USER) AND SUB-
C             ROUTINE TRAP.  EXCEPT PRMT(5) THE COMPONENTS
C             ARE NOT DESTROYED BY SUBROUTINE TRAP, THEY ARE
C             PRMT(1)- LOWER BOUND OF THE INTERVAL (INPUT).
C             PRMT(2)- UPPER BOUND OF THE INTERVAL (INPUT).
C             PRMT(3)- INITIAL INCREMENT OF THE INDEPENDENT
C             VARIABLE (INPUT).
C             PRMT(4)- UPPER ERROR BOUND (INPUT). SUCCESSIVE
C             ITERATIONS AT EACH STEP MUST BE WITHIN THIS VALUE.
C             PRMT(5)- NO INPUT PARAMETER. SUBROUTINE TRAP
C             INITIALIZES PRMT(5)=0. IF THE USER WANTS TO TER-
C             MINATE SUBROUTINE TRAP AT ANY OUTPUT POINT, HE
C             HAS TO CHANGE PRMT(5) TO NON-ZERO BY MEANS OF
C             SUBROUTINE OUTP.
C             Y      - INPUT VECTOR OF INITIAL VALUES.  (DES-
C             TROYED) LATER ON Y IS THE RESULTING VECTOR OF
C             DEPENDENT VARIABLES COMPUTED AT INTERMEDIATE
C             POINTS X.
C             DERY   - THE VECTOR OF DERIVATIVES, WHICH BELONG
```

```
C            TO FUNCTION VALUES Y AT A POINT X.
C            NDIM   - AN INPUT VALUE, WHICH SPECIFIES THE
C            NUMBER OF EQUATIONS IN THE SYSTEM.
C            IHLF   - THE NUMBER OF TIMES THE TIME INCREMENT
C            H IS REDUCED BY HALVES SO AS TO OBTAIN
C            REASONABLE VALUES OF DERY(I)S.
C            FCT    - THE NAME OF AN EXTERNAL SUBROUTINE USED.
C            IT COMPUTES THE RIGHT HAND SIDES DERY OF THE
C            SYSTEM TO GIVEN VALUES OF X AND Y.  ITS PARAME-
C            TER LIST MUST BE X,Y,DERY.  THE SUBROUTINE
C            SHOULD NOT DESTROY X AND Y.
C            OUTP   - THE NAME OF AN EXTERNAL OUTPUT SUB-
C            ROUTINE USED.  ITS PARAMETER LIST MUST BE X,Y,
C            DERY,IHLF,NDIM,PRMT.  NONE OF THESE PARAMETERS
C            (EXCEPT, IF NECESSARY, PRMT(4),PRMT(5)) SHOULD
C            BE CHANGED BY SUBROUTINE OUTP.  IF PRMT(5) IS
C            CHANGED TO NON-ZERO, SUBROUTINE TRAP IS TERMIN-
C            ATED.
C            AUX    - AN AUXILIARY STORAGE ARRAY WITH 4 ROWS
C            AND NDIM COLUMNS.
C
C        REMARKS
C            THE PROCEDURE TERMINATES AND RETURNS TO CALLING
C            PROGRAM, IF
C            (1) THE WHOLE INTEGRATION INTERVAL IS WORKED
C            THROUGH.
C            (2) SUBROUTINE OUTP HAS CHANGED PRMT(5) TO NON-
C            ZERO.
C
C        SUBROUTINES AND FUNCTION SUBPROGRAMS REQUIRED
C            THE EXTERNAL SUBROUTINES FCT(X,Y,DERY) AND
C            OUTP(X,Y,DERY,IHLF,NDIM,PRMT) MUST BE FURNISHED
C            BY THE USER.
C
C        METHOD
C            EVALUATION IS BY MEANS OF THE MODIFIED EULER'S
C            METHOD.
      COMMON BETA(6),COEF(24,3),BFLO(24),ISKIN(6),MET(24),
     1COND(24,24),TAMB,SA(6),RESP,R4(6),RR4(6),
     2OMET(24),OBFLO(24),ABFLO,VOLUME(24),SL,DTEMP
     3,OBTEM(24),WEIT,TMAT,ORESP,TIME
      DIMENSION Y(24),DERY(24),AUX(4,24),PRMT(5)
      DIMENSION ALFA(24),EXP1(24),EXP2(24),EXP3(24)
      X=PRMT(1)
      XEND=PRMT(2)
      PRMT(5)=0.
      IHLF=0
      CALL FCT(X,Y,DERY)
      CALL OUTP(X,Y,DERY,IHLF,NDIM,PRMT)
      IF (PRMT(5).NE.0.) RETURN
```

```
C       IF IT IS DESIRED TO USE A LARGER H TO BEGIN WITH,
C       THEN  IF DEEMED NECESSARY TO REDUCE H BECAUSE
C       DERY(I)S PRODUCED ARE NOT CLOSE ENOUGH IN VALUE,
C       DELETE STATEMENTS 13 AND 33, AND DELETE THE C FROM
C       THE C13 STATMENT.
 5      DO 10 I=1,NDIM
 10     AUX(4,I)=0.
        H=PRMT(3)
 13     H=0.25
C13     H=H/8.
        IHLF=0
        CALL FCT(X,Y,DERY)
        DO 15 I=1,NDIM
        IF (DERY(I).GE.0.7) GOTO 150
        IF (DERY(I).LE.(-0.7)) GOTO 151
        GOTO 14
 150    DERY(I)=0.7
        GOTO 14
 151    DERY(I)=-0.7
 14     AUX(2,I)=Y(I)
 15     AUX(1,I)=DERY(I)
 16     DO 20 I=1,NDIM
 20     Y(I)=Y(I)+H*DERY(I)
        YI=1.
 21     DO 22 J=1,6
        I=4*J-3
        IF (ABFLC.NE.0.) GOTO 220
        YY=Y(I+3)-TAMB
        IF (YY.GT.0.) GOTO 230
        Y(I+3)=TAMB
        GOTO 230
 220    YY=Y(I+3)-32.
        IF (YY.GT.0.) GOTO 230
        Y(I+3)=32.
 230    YY=Y(I+2)-Y(I+3)
        IF (YY.GT.0.) GOTO 231
        Y(I+2)=Y(I+3)
 231    YY=Y(I+1)-Y(I+2)
        IF (YY.GT.0.) GOTO 232
        Y(I+1)=Y(I+2)
 232    YY=Y(I)-Y(I+2)
        IF (YY.GT.0.) GOTO 233
        Y(I)=Y(I+2)
 233    YY=41.-Y(I+3)
        IF (YY.GT.0.) GOTO 234
        Y(I+3)=41.
 234    YY=42.5-Y(I+2)
        IF (YY.GT.0.) GOTO 235
        Y(I+2)=42.5
 235    YY=46.-Y(I+1)
```

```
      IF (YY.GT.0.) GOTO 236
      Y(I+1)=46.
 236  YY=46.-Y(I)
      IF (YY.GT.0.) GOTO 22
      IF (I.EQ.5) GOTO 22
      Y(I)=46.
 22   CONTINUE
      IF (YI.EQ.2.) GOTO 46
 25   CALL FCT(X+H,Y,DERY)
      DO 30 I=1,NDIM
      IF (DERY(I).GE.0.7) GOTO 250
      IF (DERY(I).LE.(-0.7)) GOTO 251
      GOTO 30
 250  DERY(I)=0.7
      GOTO 30
 251  DERY(I)=-0.7
 30   AUX(3,I)=AUX(2,I)+H/2.*(AUX(1,I)+DERY(I))
      DO 31 I=1,NDIM
 31   AUX(4,I)=DERY(I)
 33   IF (PRMT(5).EQ.0.) GOTO 43
      CONTINUE
 35   DO 40 I=1,NDIM
C     SLOPE SHOULD NOT CHANGE FASTER THAN 0.05 DEGREE C/MIN.
      IF (ABS(AUX(4,I)-AUX(1,I)).GT.PRMT(4)) GOTO 50
 40   CONTINUE
 43   DO 45 I=1,NDIM
 45   Y(I)=AUX(3,I)
      YI=2.
      GOTO 21
 46   X=X+H
      CALL CPESP(Y,DETA)
      CALL CMET(X,Y,EXP1,EXP2,EXP3)
      CALL CFLOW(Y,ALFA)
      CALL OUTP(X,Y,DERY,IHLF,NDIM,PRMT)
      IF (PRMT(5).NE.0.) RETURN
      IF (X.LT.XEND) GOTO 5
      RETURN
 50   IF (IHLF-2) 55,46,46
 55   IHLF=IHLF+1
      H=0.5*H
      DO 60 I=1,NDIM
      Y(I)=AUX(2,I)
 60   DERY(I)=AUX(1,I)
      GOTO 16
      END
```

```
      SUBROUTINE FCT(X,BTEM,DERT)
C     THIS SUBROUTINE CALCULATES THE VALUES OF DERIVATIVES
      COMMON BETA(6),COEF(24,3),BFLO(24),ISKIN(6),MET(24),
     1COND(24,24),TAMB,SA(6),RESP,R4(6),R34(6),
     2OMET(24),OBFLO(24),ABFLO,VOLUME(24),SL,DTEMP
     3,OBTEM(24),WEIT,TMAT,ORESP,TIME
      DIMENSION BTEM(24),DERT(24),CONV(24,25)
      DIMENSION IVEC(94),TEMP(6)
C     IVEC(94) ONLY NEEDS 94 UNITS BECAUSE SOME CONV(I,J)=0.
      CALL FILCOV(CONV)
      IF (SL) 25,25,30
 25   L=0
      DO 27 I=1,24
      DO 27 J=1,24
      IF (CONV(I,J).LE.0.0) GOTO 27
C     WE DO NOT USE (CONV(I,J).EQ.0.0) GOTO 27 BECAUSE
C     THERE ARE SOME NEGATIVE CONV TERMS PRESENT WHOSE
C     SIGNS HAD BEEN CHANGED, AND PUT INTO NEW CONV TERMS
C     SO THAT ALL THE BLOOD FLOW TERMS ARE ASSOCIATED WITH
C     POSITIVE CONV TERMS
C     SOME CONV(I,J) ARE  NEGATIVE BECAUSE OF W(T1-T2) TERM
C     HAS -WT2,E.G. CONV(1,1),THEY WILL NOT BE COUNTED INTO
C     IVEC.
      L=L+1
      IVEC(2*L-1)=I
      IVEC(2*L)=J
 27   CONTINUE
      SL=L
      LL=2*L-1
      WRITE(6,100) LL
C     DEFINE CONDUCTIVE PORTION OF DERT
 30   DO 15 I=1,21,4
      DERT(I)=COND(I,I+1)*(BTEM(I+1)-BTEM(I))
      DERT(I+1)=COND(I+1,I)*(BTEM(I)-BTEM(I+1))
     1+COND(I+1,I+2)*(BTEM(I+2)-BTEM(I+1))
      DERT(I+2)=COND(I+2,I+1)*(BTEM(I+1)-BTEM(I+2))
     1+COND(I+2,I+3)*(BTEM(I+3)-BTEM(I+2))
 15   DERT(I+3)=COND(I+3,I+2)*(BTEM(I+2)-BTEM(I+3))
C     IF IT IS DESIRED TO TO ADJUST THE SKIN TEMPERATURES
C     BECAUSE OF POSITION(INVOLVING BETA), THE FOLLOWING
C     CARDS ARE TO BE USED, AND METABOLIC RATES OF SKIN
C     LAYERS ARE TO BE ADJUSTED ACCORDINGLY.
CC    ADJUST SKIN TEMPERATURE FOR POSTULATED POSITION OF
CC    BLOOD FLOW
C     DO 40 I=1,6
C     J=ISKIN(I)
C     TEMP(I)=BTEM(J)
C40   BTEM(J)=BTEM(J)+(1.-BETA(I))*(TAMB-BTEM(J))
C     USE IVEC,OBTAIN CONVECTION PORTION OF DERT , AND ADD
C     INTO DERT
```

```
C      IVEC HAS 2*46=92 UNITS BECAUSE THERE ARE 46
C      POSITIVE CONV TERMS IN THE 24 DIFFERENTIAL EQUATIONS,
C      AND 46 MORE LOCATIONS IS NEEDED TO SHOW WHICH SEGMENT
C      EACH CONV BELONGS TO
C      WHEN 2=91,I+1=92, SO LL=91
       DO 50 I=1,LL,2
C      DO 50 I=1,91,2
       LROW=IVEC(I)
       LCOL=IVEC(I+1)
C      LROW SHOWS THE PART CONCERNED, IE. THE PART TO
C      WHICH BLOOD FLOWS
C      LCOL SHOWS THE PART FROM WHICH BLOOD FLOWS INTO
C      PART LROW.
C      THE NUMBER INDICATED IS THE NUMBER OF THE TEMPERATURE
C      TERM ASSOCIATED WITH IT.
 50    DERT(LROW)=DERT(LROW)+CONV(LROW,LCOL)*(BTEM(LCOL)-BTEM
      1(LROW))
CC     RETURN SKIN TEMPERATURE TO MASS AVERAGE VALUES
       DO 60 I=1,6
       J=ISKIN(I)
C      BTEM(J)=TEMP(I)
 60    DERT(J)=DERT(J)+COEF(J,3)*BTEM(J)
C      STATEMENT 60 INCLUDED COEF(J,3) WHICH IS THE H*BETA
C      TERM FOR SKIN LAYER
C      ADD GENERATION AND ENVIRONMENT INTERACTION
       DO 70 I=1,24
 70    DERT(I)=DERT(I)+CONV(I,25)
C      CONV(I,25) IS THE METABOLIC RATE TERM
       XXJ=Y+0.005
       JX=XXJ
       XJ=JX
       IF ((XXJ-XJ).GE.0.009) RETURN
       IF (JX.EQ.17) GOTO 180
       TX=XXJ/5.
       ITX=TX
       TIX=ITX
       IF ((TX-TIX).GT.0.009) RETURN
 100   FORMAT(/5X,'LL IN FCT IS',I4)
 180   CONTINUE
       WRITE(6,300)
       WRITE(6,200) (BTEM(I),I=1,24)
       WRITE(6,190)
 190   FORMAT(//5X,'DERT(I)S IN FCT ARE')
       WRITE(6,200) (DERT(I),I=1,24)
 200   FORMAT(5X,8E12.4)
 300   FORMAT(//5X,'BTEM(I)S CALCULATED BY FCT')
       RETURN
       END
```

```
      SUBROUTINE FILCOD
C     THIS SUBROUTINE CALCULATES UNVARYING COEFFICIENTS
C     DESCRIBING CONDUCTIVE HEAT TRANSFER FOR USE IN
C     SUBROUTINE FCT.
      COMMON BETA(6),COEF(24,3),BFLO(24),ISKIN(6),MET(24),
     1COND(24,24),TAMB,SA(6),RESP,R4(6),RR4(6),
     2OMET(24),OBFLO(24),ABFLO,VOLUME(24),SL,DTEMP
     3,OBTEM(24),WEIT,TMAT,ORESP,TIME
C     THERE ARE 6*4=24 DIFFERENTIAL EQUATIONS
C     COND(I,J), WHERE 2 IS THE NUMBER OF THE EQUATION
C     CONCERNED, AND J IS THE NUMBER OF THE PARTICULAR TERM
C     IN THE EQUATION.
      DO 100 I=1,24
      DO 100 J=1,24
  100 COND(I,J)=0.
      DO 110 I=1,21,4
      COND(I,I+1)=COEF(I,1)
      COND(I,1)=-COEF(I,1)
C     COND(I,1)=-COEF(I,1) IS USED TO TAKE UP THE SPARE ROOM
C     FOR COND(I,J), WANT J TO BE I+1 WHEN I IS 1,5,9,.....
C     ETC.
      COND(I+1,I)=COEF(I+1,1)
      COND(I+1,I+2)=COEF(I+1,2)
      COND(I+1,I+1)=-COEF(I+1,1)-COEF(I+1,2)
C     COND(I+1,I+1) WILL NOT BE USED IN CALCULATION, JUST
C     IS USED TO TAKE UP SPARE ROOM.
      COND(I+2,I+1)=COEF(I+2,1)
      COND(I+2,I+3)=COEF(I+2,2)
      COND(I+2,I+2)=-COEF(I+2,1)-COEF(I+2,2)
      COND(I+3,I+2)=COEF(I+3,1)
  110 COND(I+3,I+3)=-COEF(I+3,1)
      RETURN
      END


      SUBROUTINE FILCOV(CONV)
C     THIS SUBROUTINE CALCULATES COEFFICIENTS FOR CONVECTIVE
C     HEAT TRANSFER AND INTERACTION WITH THE ENVIRONMENT.
      COMMON BETA(6),COEF(24,3),BFLO(24),ISKIN(6),MET(24),
     1COND(24,24),TAMB,SA(6),RESP,R4(6),RR4(6),
     2OMET(24),OBFLO(24),ABFLO,VOLUME(24),SL,DTEMP
     3,OBTEM(24),WEIT,TMAT,ORESP,TIME
      DIMENSION CONV(24,25)
      REAL MET
      DATA ROBLD/0.9/
      DO 100 I=1,24
      DO 100 J=1,25
  100 CONV(I,J)=0.
C     I IS THE SEGMENT TO WHICH , AND J IS THE SEGMENT FROM
C     WHICH BLOOD FLOWS, IN THE ABOVE CONV STATEMENT.
```

```
C     IN COEF(I,J), I IS THE NUMBER OF THE EQUATION
C     CONCERNED, J IS THE NUMBER ASSOCIATES WITH THE
C     POSITIVE TEMPERATURE TERM.
      DO 110 I=1,5,4
      CONV(I+1,I)=BFLO(I+1)/COEF(I+1,3)
      CONV(I+2,I)=BFLO(I+2)/COEF(I+2,3)
  110 CONV(I+3,I)=BFLO(I+3)/COEF(I+3,2)
      CONV(1,5)=(BFLO(1)+BFLO(2)+BFLO(3)+BFLO(4))/COEF(1,2)
      DO 120 I=1,8
  120 CONV(5,I)=BFLO(I)/COEF(5,2)
      CONV(5,9)=2.*(BFLO(9)+BFLO(13))/COEF(5,2)
      CONV(5,10)=2.*(BFLO(10)+BFLO(14))/COEF(5,2)
      CONV(5,11)=2.*(BFLO(11)+BFLO(15))/COEF(5,2)
      CONV(5,12)=2.*(BFLO(12)+BFLO(16))/COEF(5,2)
      CONV(5,17)=2.*(BFLO(17)+BFLO(21))/COEF(5,2)
      CONV(5,18)=2.*(BFLO(18)+BFLO(22))/COEF(5,2)
      CONV(5,19)=2.*(BFLO(19)+BFLO(23))/COEF(5,2)
      CONV(5,20)=2.*(BFLO(20)+BFLO(24))/COEF(5,2)
C     THE COEFFICIENT OF 2. FOR CONV(5,9 TO 20) IS BECAUSE
C     OF THE PRESENCE OF THE LEFT AND RIGHT SIMITRY OF THE
C     ANIMAL.
      DO 200 I=9,17,8
      SUM=0.
      NUM=I+7
      DO 130 J=I,NUM
  130 SUM=SUM+BFLO(J)
      CONV(I,5)=SUM/COEF(I,2)
      CONV(I,I+4)=(BFLO(I+4)/COEF(I,2))
      CONV(I+1,I)=BFLO(I+1)/COEF(I+1,3)
      CONV(I+1,I+5)=BFLO(I+5)/COEF(I+1,3)
      CONV(I+2,I)=BFLO(I+2)/COEF(I+2,3)
      CONV(I+2,I+6)=BFLO(I+6)/COEF(I+2,3)
      CONV(I+3,I)=BFLO(I+3)/COEF(I+3,2)
  200 CONV(I+3,I+7)=BFLO(I+7)/COEF(I+3,2)
      DO 201 I=13,21,8
      CONV(I,I-4)=(BFLO(I)+BFLO(I+1)+BFLO(I+2)+BFLO(I+3))
     1/COEF(I,2)
      CONV(I+1,I)=BFLO(I+1)/COEF(I+1,3)
      CONV(I+2,I)=BFLO(I+2)/COEF(I+2,3)
  201 CONV(I+3,I)=BFLO(I+3)/COEF(I+3,2)
C     CHANGE THE SIGN OF THE CONV TERM SO THAT THE
C     TEMPERATURE TERM, WHICH HAS THE SAME NUMBER AS THE
C     DIFFERENTIAL EQUATION IS POSITIVE.
      CONV(1,1)=-CONV(1,5)
C     DERT IS CALCULATED AS DERT=AT2-AT1+BT3-BT1+CT4-CT1....
C     ETC., SO WE NEED TO CHANGE A WHICH IS FOR T2 INTO -A,
C     WHICH MULTIPLIES T1, ETC.
      DO 203 I=2,4
  203 CONV(I,I)=-CONV(I,1)
      DO 205 I=6,8
```

```
 205  CONV(I,I)=-CONV(I,5)
C     CALCULATE CONV(5,5) BY ADDING ALL THE FLOW TERMS ASSO-
C     CIATED WITH T5 TOGETHER.
      CONV(5,5)=0.
      DO 206 I=1,4
 206  CONV(5,5)=CONV(5,5)-CONV(5,I)
      DO 207 I=6,24
 207  CONV(5,5)=CONV(5,5)-CONV(5,I)
      DO 208 I=13,21,8
      CONV(I,I)=-CONV(I,I-4)
      CONV(I+1,I+1)=-CONV(I+1,I)
      CONV(I+2,I+2)=-CONV(I+2,I)
 208  CONV(I+3,I+3)=-CONV(I+3,I)
      DO 210 I=9,17,8
      CONV(I,I)=-CONV(I,5)-CONV(I,I+4)
      CONV(I+1,I+1)=-CONV(I+1,I)-CONV(I+1,I+5)
      CONV(I+2,I+2)=-CONV(I+2,I)-CONV(I+2,I+6)
 210  CONV(I+3,I+3)=-CONV(I+3,I)-CONV(I+3,I+7)
C     THE SIGNS ARE NEGATIVE BECAUSE FLOWS GOING INTO THE
C     SAME SEGMENT ARE ADDED TOGETHER.
C     THE FOLLOWING CONV STATEMENTS ARE USED TO CALCULATE
C     THE EFFECT OF METABOLIC RATE AND RESPIRATION ON BODY
C     HEAT TRANSFER.
      DO 220 M=1,6
      I=ISKIN(M)
C     ISKIN(1)=4,  (2)=8, (3)=12, (4)=16, (5)=20, (6)=24
C     ADD THE HEAT TRANSFER COEF TERM INTO CONV TERM FOR
C     SKIN LAYERS. THE SIGN IS + BECAUSE COEF(I,3) HAS GOT A
C     (-) SIGN AS CALCULATED IN SUBROUTINE HTCOEF.
      CONV(I,I)=CONV(I,I)+COEF(I,3)
C     FOR FAT LAYERS:
      CONV(I-1,25)=MET(I-1)/(ROBLD*COEF(I-1,3))
C     FOR MUSCLE LAYERS:
      CONV(I-2,25)=MET(I-2)/(ROBLD*COEF(I-2,3))
C     FOR CORE LAYERS:
      CONV(I-3,25)=MET(I-3)/(ROBLD*COEF(I-3,2))
C     SUBTRACT OFF COEF(I,3)*TAMB FOR THE PROPER OPERATION
C     OF THE HT TERM ON SKIN.
 220  CONV(I,25)=-COEF(I,3)*TAMB+MET(I)/(COEF(I,2)*ROBLD)
      CONV(1,25)=CONV(1,25)-RESP/(COEF(1,2)*ROBLD)
      RETURN
      END


      SUBROUTINE OUTP(X,BTEM,DERT,IHLF,KL,PRMT)
C     THIS SUBROUTINE SPECIFIES THE OUTPUT FORM DESIRED
C     FOR DETERMINING THE TEMPERATURE DISTRIBUTION FROM
C     CENTRAL RELATIONSHIP BETWEEN PARAMETERS SUCH AS
C     METABOLIC RATES, BLOW RATES, ETC.
      COMMON BETA(6),COEF(24,3),BFLO(24),ISKIN(6),MET(24),
```

```
     1COND(24,24),TAMB,SA(6),BRSP,B4(6),BR4(6),
     2OMET(24),OBFLO(24),ABFLO,VOLUME(24),SL,DTEMP
     3,OBTEM(24),WRIT,TMAT,ORESP,TIME
      DIMENSION BTEM(1),DERT(1),PRMT(1)
      DIMENSION CTEM5(120),CTEM6(120),CTEM7(120),CTEM8(120),
     1CTEM10(120),CTEM12(120),CTEM18(120)
      DIMENSION XT(120),PFLO1(120),APFLO(120),PFLO6(120),
     1PFLO9(120),PFLO10(120),PFLO17(120),PFLO18(120)
      DIMENSION PTEM1(120),PTEM5(120),PTEM6(120),PTEM7(120)
     1,PTEM8(120),PTEM9(120),PTEM10(120),PTEM12(120),
     2PTEM18(120)
      REAL MET
      XXI=X+0.005
      IX=XXI
      XI=IX
      IF ((XXI-XI).GE.0.009) RETURN
      X=IX
      ABFLO=0.
      DO 5 J=1,24
C     DO 5 J=1,KL
  5   ABFLO=ABFLO+BFLO(J)
      IF (X.LE.18.) GOTO 8
      TX=(X+0.005)/5.
      ITX=TX
      TIX=ITX
      IF ((TX-TIX).LE.0.009) GOTO 8
      GOTO 21
  8   WRITE(6,10) X,BFLO(1),ABFLO,BFLO(6),BFLO(9),
     1BFLO(10),BFLO(17),BFLO(18)
      WRITE(6,20) BTEM(1),BTEM(5),BTEM(6),BTEM(7),BTEM(8),
     1BTEM(9),BTEM(10),BTEM(12),BTEM(18)
  10  FORMAT(5X,F10.5,7E12.4)
  20  FORMAT(/5X,9F10.4)
  21  XI=X+11.
      IX=XI
      IF (X.NE.0.) GOTO 28
      DO 25 I=1,11
      IX=I
      AI=I
      XT(IX)=AI-11.
C     DATA STORED FROM TIME=-10 ON,IX=1,T=-10;IX=11,T=0
  23  PFLO1(IX)=BFLO(1)
      APFLO(IX)=ABFLO
      PFLO6(IX)=BFLO(6)
      PFLO9(IX)=BFLO(9)
      PFLO10(IX)=BFLO(10)
      PFLO17(IX)=BFLO(17)
      PFLO18(IX)=BFLO(18)
      PTEM1(IX)=BTEM(1)
      PTEM5(IX)=BTEM(5)
```

```
      PTEM6(IX)=BTEM(6)
      PTEM7(IX)=BTEM(7)
      PTEM8(IX)=BTEM(8)
      PTEM9(IX)=BTEM(9)
      PTEM10(IX)=BTEM(10)
      PTEM12(IX)=BTEM(12)
 25   PTEM18(IX)=BTEM(18)
      RETURN
 28   XT(IX)=X
      PFLO1(IX)=BFLO(1)
      APFLO(IX)=ABFLO
      PFLO6(IX)=BFLO(6)
      PFLO9(IX)=BFLO(9)
      PFLO10(IX)=BFLO(10)
      PFLO17(IX)=BFLO(17)
      PFLO18(IX)=BFLO(18)
      PTEM1(IX)=BTEM(1)
      PTEM5(IX)=BTEM(5)
      PTEM6(IX)=BTEM(6)
      PTEM7(IX)=BTEM(7)
      PTEM8(IX)=BTEM(8)
      PTEM9(IX)=BTEM(9)
      PTEM10(IX)=BTEM(10)
      PTEM12(IX)=BTEM(12)
      PTEM18(IX)=BTEM(18)
      IF (X.EQ.(TIME)) GOTO 30
      RETURN
 30   CONTINUE
C     IF WANT TO PUT OUTPUT ON CARDS, DELETE THE C'S FROM
C     THE FOLLOWING COMMENT CARDS.
C     N1=TIME+1
C 31  DO 32 M=1,N1
C     MI=M+10
C     WRITE CARD OUT FROM T=0,M=1,MI=11 ON
C     CTEM5(M)=PTEM5(MI)-OBTEM(5)
C     CTEM6(M)=PTEM6(MI)-OBTEM(6)
C     CTEM7(M)=PTEM7(MI)-OBTEM(7)
C     CTEM8(M)=PTEM8(MI)-OBTEM(8)
C     CTEM10(M)=PTEM10(MI)-OBTEM(10)
C     CTEM12(M)=PTEM12(MI)-OBTEM(12)
C32   CTEM18(M)=PTEM18(MI)-OBTEM(18)
C35   FORMAT(16F5.2)
C     N2=TIME+1
C     WRITE(7,35) (CTEM5(M),M=1,N2)
C     WRITE(7,35) (CTEM6(M),M=1,N2)
C     WRITE(7,35) (CTEM7(M),M=1,N2)
C     WRITE(7,35) (CTEM8(M),M=1,N2)
C     WRITE(7,35) (CTEM10(M),M=1,N2)
C     WRITE(7,35) (CTEM12(M),M=1,N2)
C     WRITE(7,35) (CTEM18(M),M=1,N2)
```

```
 40    CALL PRNT(XT,PFLO1,APFLO,PFLO6,PFLO9,PFLO10,PFLO17,
      1PFLO18,PTEM1,PTEM5,PTEM6,PTEM7,PTEM8,PTEM9,PTEM10,
      2PTEM12,PTEM18)
       RETURN
       END


       SUBROUTINE CLCOEF(TCOND1,TCOND2,TCOND3,TCOND4,ROCOR,
      1ROMUS,ROFAT,ROSKN,ROBLD,VOL,COR,XMUS,SKN,FAT,XL,R1,R2,
      2R3,XLL,R11,R22,R33,R4X)
C      THIS SUBROUTINE CALCULATES COEFFICIENTS WHICH ARE
C      NONVARYING, DESCRIBING AREA, VOLUME, AND PHYSICAL
C      PROPERTIES OF THE BODY, AND REDUCING TO EQUIVALENT
C      CYLINDERS.
       COMMON BETA(6),COEF(24,3),BFLO(24),ISKIN(6),MET(24),
      1COND(24,24),TAMB,SA(6),RESP,R4(6),R44(6),
      2OMET(24),CBFLO(24),ABFLO,VOLUME(24),SL,DTEMP
      3,OBTEM(24),WEIT,TMAT,ORESP,TIME
       DIMENSION VOL(6),COR(6),XMUS(6),SKN(6),FAT(6),XL(6),
      1R1(6),R2(6),R3(6)
       DIMENSION TCOND1(24),TCOND2(24),TCOND3(24),TCOND4(24),
      1XLL(6),R11(6),R22(6),R33(6),R4X(6)
       DIMENSION ROCOR(24),ROMUS(24),ROFAT(24),ROSKN(24)
C      THERE ARE 6*4=24  PARTS, IN (I,J), I IS REFERRED AS
C      THE PART CONCERNED, J IS THE POSITION OF THE TERM
C      IN THE EQUATION I.
       DO 110 K=1,6
 110   READ(5,120) XLL(K),R11(K),R22(K),R33(K),R4X(K)
 120   FORMAT(5F10.3)
       WRITE(6,140)
 140   FORMAT(/5X,'TCON1',5X,'TCON2',5X,'TCON3')
       DO 170 J=1,6
       I=4*J-3
C      VOL/SA=3.142*R**2/(2*3.142*L)=R/2
       R4(J)=2.*VOL(J)/SA(J)
       XL(J)=SA(J)/(2.*R4(J)*3.14159)
       R3(J)=SQRT(COR(J)+XMUS(J)+FAT(J))*R4(J)
       R2(J)=SQRT(COR(J)+XMUS(J))*R4(J)
       R1(J)=SQRT(COR(J))*R4(J)
       VOLUME(I)=(R1(J)**2*XL(J)*3.14159)
       VOLUME(I+1)=(R2(J)**2-R1(J)**2)*XL(J)*3.14159
       VOLUME(I+2)=(R3(J)**2-R2(J)**2)*XL(J)*3.14159
       VOLUME(I+3)=(R4(J)**2-R3(J)**2)*XL(J)*3.14159
C      IF WANT THE READ IN VALUES, DELETE  THE C'S FROM
C      THE FOLLOWING 5 CARDS.
C      XL(J)=XLL(J)
C      R1(J)=R11(J)
C      R2(J)=R22(J)
C      R3(J)=R33(J)
C      R4(J)=R4X(J)
```

```
C       R1**2+R2**2=RF2**2/2
  145   RR1=0.70711*R1(J)
        RR2=0.70711*SQRT(R1(J)**2+R2(J)**2)
        RR3=0.70711*SQRT(R2(J)**2+R3(J)**2)
        RR4=0.70711*SQRT(R3(J)**2+R4(J)**2)
        R44(J)=RR4
C       TCON1=AVERAGE THERMO COND OF R1 AND R2.
C       TCON2=AVERAGE THERMO COND OF R2 AND R3...ETC.
C       TCOND1=THERMAL CONDUCTIVITY OF R1.
        TCON1=(R1(J)**2*TCOND1(J)+(R2(J)**2-R1(J)**2)*
       1TCOND2(J))/R2(J)**2
        TCON2=((R2(J)**2-R1(J)**2)*TCOND2(J)+(R3(J)**2-
       1R2(J)**2)*TCOND3(J))/(R3(J)**2-R1(J)**2)
        TCON3=((R3(J)**2-R2(J)**2)*TCOND3(J)+(R4(J)**2-
       1R3(J)**2)*TCOND4(J))/(R4(J)**2-R2(J)**2)
        WRITE(6,150) TCON1,TCON2,TCON3
  150   FORMAT(4X,F6.4,4X,F6.4,4X,F6.4)
        COEF(I,1)=TCON1/R1(J)**2*2.*R1(J)/((RF2-RR1)*ROCOR(J))
C       ROCOR=PRODUCT OF DENSITY AND HEAT CAPACITY OF CORE
C       TISSUE.
C       ROMUS=PRODUCT OF DENSITY AND HEAT CAPACITY OF MUSCLE
C       LAYER.
C       ROBLD=PRODUCT OF DENSITY AND HEAT CAPACITY OF BLOOD.
C       ROFAT=PRODUCT OF DENSITY AND HEAT CAPACITY OF FAT
C       LAYER.
C       ROSKN=PRODUCT OF DENSITY AND HEAT CAPACITY OF SKIN
C       LAYER.
        COEF(I,2)=(R1(J)**2*XL(J)*3.14159)*ROCOR(J)/ROBLD
        COEF(I,3)=0.
        ROMID1=(ROCOR(J)*COR(J)+ROMUS(J)*XMUS(J))/
       1(COR(J)+XMUS(J))
        ROMID2=(ROMUS(J)*XMUS(J)+ROFAT(J)*FAT(J))/
       1(XMUS(J)+FAT(J))
        ROMID3=(ROFAT(J)*FAT(J)+ROSKN(J)*SKN(J))/
       1(FAT(J)+SKN(J))
        COEF(I+1,1)=TCON1/(R2(J)**2-R1(J)**2)*2.*R1(J)/
       1((RR2-RR1)*ROMUS(J))
        COEF(I+1,2)=TCON2/(R2(J)**2-R1(J)**2)*2.*R2(J)/
       1((RR3-RR2)*ROMUS(J))
        COEF(I+1,3)=(R2(J)**2-R1(J)**2)*XL(J)*3.14159
       1*ROMUS(J)/ROBLD
        COEF(I+2,1)=TCON2/(R3(J)**2-R2(J)**2)*2.*R2(J)/
       1((RR3-RR2)*ROFAT(J))
        COEF(I+2,2)=TCON3/(R3(J)**2-R2(J)**2)*2.*R3(J)/
       1((RR4-RR3)*ROFAT(J))
        COEF(I+2,3)=(R3(J)**2-R2(J)**2)*XL(J)*3.14159
       1*ROFAT(J)/ROBLD
        COEF(I+3,1)=TCON3/(R4(J)**2-R3(J)**2)*2.*R3(J)/
       1((RR4-RR3)*ROSKN(J))
        COEF(I+3,2)=(R4(J)**2-R3(J)**2)*XL(J)*3.14159
```

```
     1*ROSKN(J)/ROBLD
      COEF(I+3,3)=2.*R4(J)/((R4(J)**2-R3(J)**2)*POSKN(J))
 170  BETA(J)=(R4(J)-RR4)/TCOND4(J)
      RETURN
      END


      SUBROUTINE CPARAM(VOL,COR,XMUS,FAT,SKN,PCMT)
C     THIS SUBROUTINE CALCULATES THE PHYSICAL PARAMETERS
C     OF THE ANIMAL, SUCH AS WEIGHT, AREA, METABOLIC RATE
C     OF DIFFERENT PARTS OF THE BODY.
      COMMON BETA(6),COEF(24,3),BFLO(24),ISKIN(6),MET(24),
     1COND(24,24),TAMB,SA(6),RESP,R4(6),RF4(6),
     2OMET(24),OBFLO(24),ABFLO,VOLUME(24),SL,DTEMP
     3,OBTEM(24),WEIT,TMAT,ORESP,TIME
      DIMENSION PCWT(24),WTPT(6),PCAT(6),PCMT(24)
      DIMENSION COR(6),XMUS(6),FAT(6),SKN(6),VOL(6)
      REAL MET
C     CALCULATE WEIGHT OF EACH PART OF THE BODY IN GRAMS
      READ(5,100) WEIT
C     WEIT HERE IS GIVEN IN KGS.
 100  FORMAT(F10.4)
      READ(5,105) (COR(I),XMUS(I),FAT(I),SKN(I),I=1,6)
 105  FORMAT(4F10.5)
      READ(5,110) (PCWT(I),I=1,6)
 110  FORMAT(6F10.5)
      DO 120 I=1,6
 120  WTPT(I)=WEIT*PCWT(I)*1000.
C     PCWT IS THE SEGMENTAL WEIGHT AS A PERCENTAGE OF THE
C     BODY WEIGHT.
C     FIND VOLUME OF EACH SEGMENT.
      DO 125 I=1,6
 125  VOL(I)=WTPT(I)
C     CALCULATE THE AREA OF EACH SEGMENT OF THE BODY IN
C     SQUARE CMS.
      TAREA=0.097*WEIT**0.633
      TAREA=TAREA*10000.
      READ(5,110) (PCAT(I),I=1,6)
C     PCAT IS THE SEGMENTAL AREA AS A PERCENTAGE OF THE
C     TOTAL BODY SURFACE AREA.
      DO 140 I=1,6
 140  SA(I)=TAREA*PCAT(I)
C     RADIUS AND LENGTH WILL BE CALCULATED IN SUBROUTINE
C     CLCOEF.
C     CALCULATE METABOLIC RATE OF PARTS OF THE BODY IN
C     UNITS OF CAL/MIN BY EMPIRICAL FORMULA.
      TMAT=(186000.*WEIT**0.62957)/(24.*60.)
      RESP=TMAT*0.1
      ORESP=RESP
      READ(5,150) (PCMT(I),I=1,24)
```

```
  150  FORMAT(4F10.6)
       DO 155 I=1,24
  155  MET(I)=TMAT*PCMT(I)*0.01
C      SINCE THERE ARE 2 ARMS AND 2 LEGS, TO GET THE WEIGHT,
C      VOLUME, METABOLIC RATE, AND SURFACE AREA FOR EACH ARM
C      OF LEG, THE VALUE OBTAINED ABOVE FOR EACH SEGMENT
C      WOULD HAVE TO BE REDUCED BY HALF.
       DO 157 I=3,6
       WTPT(I)=WTPT(I)*0.5
       VOL(I)=VOL(I)*0.5
       SA(I)=SA(I)*0.5
       J=(I-1)*4
       MET(J+1)=MET(J+1)*0.5
       MET(J+2)=MET(J+2)*0.5
       MET(J+3)=MET(J+3)*0.5
  157  MET(J+4)=MET(J+4)*0.5
C      WRITE OUT THE ABOVE ESTIMATES.
       WRITE(6,160) WEIT
  160  FORMAT(/5X,'WEIGHT OF THE PIG IS',F10.4,2X,'KG')
       WRITE(6,165) TMAT
  165  FORMAT(/5X,'TOTAL BASAL METABOLIC RATE=',F10.3)
       WRITE(6,170)
  170  FORMAT(/1X,'VOL. OF',5X,'HEAD',6X,'TRUNK',5X,'THIGH',
      15X,'FOOT',6X,'ARM',7X,'HAND')
       WRITE(6,180) (VOL(I),I=1,6)
  180  FORMAT(10X,6F10.3)
       WRITE(6,190)
  190  FORMAT(/1X,'AREA OF',5X,'HEAD',6X,'TRUNK',5X,'THIGH',
      15X,'FOOT',6X,'ARM',7X,'HAND')
       WRITE(6,200) (SA(I),I=1,6)
  200  FORMAT(10X.6F10.3)
       WRITE(6,210)
  210  FORMAT(/1X,'METAB RATE OF',1X,'CORE',10X,'MUSCLE',
      19X,'FAT',12X,'SKIN')
       WRITE(6,220) (MET(I),I=1,24)
  220  FORMAT(10X,4F15.6)
       RETURN
       END


       SUBROUTINE CBFLOW(PCBL)
C      THIS SUBROUTINE ESTIMATES THE STEADY VALUES OF BLOOD
C      FLOW IN DIFFERENT PARTS OF THE BODY.
       COMMON BETA(6),COEF(24,3),BFLO(24),ISKIN(6),MET(24),
      1COND(24,24),TAMB,SA(6),RESP,R4(6),RF4(6),
      2OMET(24),OBFLO(24),ABFLO,VOLUME(24),SL,DTEMP
      3,OBTEM(24),WEIT,TMAT,ORESP,TIME
       DIMENSION PCBL(24)
       READ(5,100) (PCBL(I),I=1,24)
  100  FORMAT(4F10.6)
```

```
      WTO=3085.5*WEIT**0.17
      DO 150 I=3,6
      J=(I-1)*4
      PCBL(J+1)=PCBL(J+1)*0.5
      PCBL(J+2)=PCBL(J+2)*0.5
      PCBL(J+3)=PCBL(J+3)*0.5
  150 PCBL(J+4)=PCBL(J+4)*0.5
      DO 160 J=1,24
  160 BFLO(J)=WTO*PCBL(J)*0.01
      WRITE(6,200)
  200 FORMAT(/5X,'THE BLOOD FLOW RATES IN THE 24 DIFFERENT
     1PARTS ARE')
      WRITE(6,300) (BFLO(I),I=1,24)
  300 FORMAT(4F20.5)
      WRITE(6,500) WTO
  500 FORMAT(//3X,'TOTAL BLOOD FLOW IS',F10.3,'CC PER MIN')
      RETURN
      END


      SUBROUTINE CBFLO(T,ROBLD,PCBL)
C     THIS SUBROUTINE ESTIMATES THE STEADY VALUES OF BLOOD
C     FLOW IN DIFFERENT PARTS OF THE BODY.
      COMMON BETA(6),COEF(24,3),BFLO(24),ISKIN(6),MET(24),
     1COND(24,24),TAMB,SA(6),RESP,R4(6),RR4(6),
     2OMET(24),OBFLO(24),ABFLO,VOLUME(24),SL,DTEMP
     3,OBTEM(24),WEIT,TMAT,ORESP,TIME
      DIMENSION PCBL(24),T(24)
      REAL MET
C     ESTIMATING BLOOD FLOW IN THE HEAD, TRUNK, HAND,
C     AND FOOT.
      WTO=3085.5*WEIT**0.17
      READ(5,10) (PCBL(I),I=1,24)
   10 FORMAT(4F10.6)
      DO 100 I=3,6
      J=(I-1)*4
      PCBL(J+1)=PCBL(J+1)*0.5
      PCBL(J+2)=PCBL(J+2)*0.5
      PCBL(J+3)=PCBL(J+3)*0.5
  100 PCBL(J+4)=PCBL(J+4)*0.5
C     A AND B ARE INCREMENTS USED IN THE ITERATION OF
C     METABOLIC RATES.
C     C AND D ARE LIMITS THAT BOUND THE ITERATION OF BLOOD
C     FLOW RATES AND METABOLIC RATES.
C     P IS THE RATIO OF THE VALUE OF THE BLOOD FLOW RATE
C     BEING ITERATED TO THE READ IN VALUE.
      A=0.99
      B=1.05
      C=0.1
      D=0.25
```

```
      DO 105 J=1,24
105   BFLO(J)=WTO*PCBL(J)*0.01
      DO 245 J=1,6
      I=4*J-3
      IF (J.EQ.3) GOTO 245
      IF (J.EQ.5) GOTO 245
110   BFLO(I+3)=((T(I+2)-T(I+3))*COEF(I+3,1)+(T(I+3)-TAMB)
     1*COEF(I+3,3)+MET(I+3)/(COEF(I+3,2)*ROBLD))*COEF(I+3,
     22)/(T(I+3)-T(I))
      P=BFLO(I+3)/(WTO*PCBL(I+3)*0.01)
      IF (J-4) 115,140,140
115   IF (P-1.) 120,140,130
120   IF ((1.-P).LE.D) GOTO 140
      MET(I+3)=MET(I+3)*A
      GOTO 110
130   IF ((P-1.).LE.D) GOTO 140
      MET(I+3)=MET(I+3)*B
      GOTO 110
140   BFLO(I+2)=((T(I+1)-T(I+2))*COEF(I+2,1)+(T(I+3)-
     1T(I+2))*COEF(I+2,2)+MET(I+2)/(COEF(I+2,3)*ROBLD))
     2*COEF(I+2,3)/(T(I+2)-T(I))
      P=BFLO(I+2)/(WTO*PCBL(I+2)*0.01)
      IF(P-1.) 150,170,160
150   IF ((1.-P).LE.C) GOTO 170
      MET(I+2)=MET(I+2)*A
      GOTO 140
160   IF ((P-1.).LE.C) GOTO 170
      MET(I+2)=MET(I+2)*B
      GOTO 140
170   BFLO(I+1)=((T(I)-T(I+1))*COEF(I+1,1)+(T(I+2)-T(I+1))*
     1COEF(I+1,2)+MET(I+1)/(COEF(I+1,3)*ROBLD))*COEF(I+1,3)
     2/(T(I+1)-T(I))
      P=BFLO(I+1)/(WTO*PCBL(I+1)*0.01)
      IF (P-1.) 180,200,190
180   IF ((1.-P).LE.C) GOTO 200
      MET(I+1)=MET(I+1)*A
      GOTO 170
190   IF ((P-1.).LE.C) GOTO 200
      MET(I+1)=MET(I+1)*B
      GOTO 170
200   CONTINUE
      IF (J-2) 210,245,215
210   BFLO(I)=((T(I+1)-T(I))*COEF(I,1)+
     1(MET(I)-RESP)/(COEF(I,2)*ROBLD))
     2*COEF(I,2)/(T(I)-T(5))
      GOTO 216
215   BFLO(I)=((T(I+1)-T(I))*COEF(I,1)+
     1MET(I)/(COEF(I,2)*ROBLD))*COEF(I,2)/(T(I)-T(I-4))
216   P=(BFLO(I)-BFLO(I+1)-BFLO(I+2)-BFLO(I+3))
     1/(WTO*PCBL(I)*0.01)
```

```
      IF (P-1.) 220,240,230
  220 IF ((1.-P).LE.C) GOTO 240
      MET(I)=MET(I)*A
      GOTO 200
  230 IF ((P-1.).LE.C) GOTO 240
      MET(I)=MET(I)*B
      GOTO 200
  240 BFLO(I)=BFLO(I)-BFLO(I+1)-BFLO(I+2)-BFLO(I+3)
  245 CONTINUE
C      ESTIMATING THE BLOOD FLOW IN THE ARM AND THIGH.
      DO 380 J=3,5,2
      I=4*J-3
  250 BFLO(I+3)=((T(I+2)-T(I+3))*COEF(I+3,1)+(T(I+3)-TAMB)
     1*COEF(I+3,3)+(MET(I+3)/ROBLD+BFLO(I+7)*(T(I+7)-T(I+3)
     2))/COEF(I+3,2))*COEF(I+3,2)/(T(I+3)-T(I))
      P=BFLO(I+3)/(WTO*PCBL(I+3)*0.01)
      IF (P-1.) 260,280,270
  260 IF ((1.-P).LE.D) GOTO 280
      MET(I+3)=MET(I+3)*A
      GOTO 250
  270 IF ((P-1.).LE.D) GOTO 280
      MET(I+3)=MET(I+3)*B
      GOTO 250
  280 BFLO(I+2)=((T(I+1)-T(I+2))*COEF(I+2,1)+(T(I+3)-
     1T(I+2))*COEF(I+2,2)+(MET(I+2)/ROBLD+BFLO(I+6)*
     2(T(I+6)-T(I+2)))/COEF(I+2,3))*COEF(I+2,3)/(T(I+2)-
     3T(I))
      P=BFLO(I+2)/(WTO*PCBL(I+2)*0.01)
      IF (P-1) 290,310,300
  290 IF ((1.-P).LE.C) GOTO 310
      MET(I+2)=MET(I+2)*A
      GOTO 280
  300 IF ((P-1.).LE.C) GOTO 310
      MET(I+2)=MET(I+2)*B
      GOTO 280
  310 BFLO(I+1)=((T(I)-T(I+1))*COEF(I+1,1)
     1+(T(I+2)-T(I+1))*COEF(I+1,2)
     2+(MET(I+1)/ROBLD+BFLO(I+5)*(T(I+5)-T(I+1)))
     3/COEF(I+1,3))*COEF(I+1,3)/(T(I+1)-T(I))
      P=BFLO(I+1)/(WTO*PCBL(I+1)*0.01)
      IF (P-1.) 320,340,330
  320 IF ((1.-P).LE.C) GOTO 340
      MET(I+1)=MET(I+1)*A
      GOTO 310
  330 IF ((P-1.).LE.C) GOTO 340
      MET(I+1)=MET(I+1)*B
      GOTO 310
  340 BFLO(I)=((T(I+1)-T(I))*COEF(I,1)
     1+(MET(I)/ROBLD+BFLO(I+4)*(T(I+4)-T(I)))
     2/COEF(I,2))*COEF(I,2)/(T(I)-T(5))
```

```
      P=(BFLO(I)-BFLO(I+1)-BFLO(I+2)-BFLO(I+3)-BFLO(I+4)
     1-BFLO(I+5)-BFLO(I+6)-BFLO(I+7))/(WTO*PCBL(I)*0.01)
      IF (P-1.) 350,380,360
  350 IF ((1.-P).LE.C) GOTO 380
      MET(I)=MET(I)*A
      GOTO 340
  360 IF ((P-1.).LE.C) GOTO 380
      MET(I)=MET(I)*B
      GOTO 340
  380 BFLO(I)=BFLO(I)-BFLO(I+1)-BFLO(I+2)-BFLO(I+3)
     1-BFLO(I+4)-BFLO(I+5)-BFLO(I+6)-BFLO(I+7)
      BFLO(5)=0.
      MET(5)=ROBLD*(COEF(5,2)*COEF(5,1)*(T(5)-T(6))
     1+BFLO(1)*(T(5)-T(1))+BFLO(2)*(T(5)-T(2))+BFLO(3)*(T(5)
     2-T(3))+BFLO(4)*(T(5)-T(4))+BFLO(6)*(T(5)-T(6))
     3+BFLO(7)*(T(5)-T(7))+BFLO(8)*(T(5)-T(8))+2.*(
     4(BFLO(9)+BFLO(13))*(T(5)-T(9))+(BFLO(10)+BFLO(14))*
     5(T(5)-T(10))+(BFLO(11)+BFLO(15))*(T(5)-T(11))+(BFLO
     6(12)+BFLO(16))*(T(5)-T(12))+(BFLO(17)+BFLO(21))*(T(5)-
     7T(17))+(BFLO(18)+BFLO(22))*(T(5)-T(18))+(BFLO(19)+
     8BFLO(23))*(T(5)-T(19))+(BFLO(20)+BFLO(24))*(T(5)-
     9T(20))))
C     THIS IS AN EMPIRICAL EQUATION FOR ADJUSTING THE BODY
C     CORE METABOLIC RATE ACCORDING TO WEIGHT CHANGES OF
C     THE MODEL ANIMAL.
      EWTO=0.
      DO 390 I=1,8
  390 EWTO=EWTO+BFLO(I)
      DO 400 I=9,24
  400 EWTO=EWTO+2.*BFLO(I)
      BFLO(5)=WTO-EWTO
      WRITE(6,410)
  410 FORMAT(/5X,'THE ADJUSTED BLOOD FLOW RATES IN THE 24
     1DIFFERENT PARTS ARE')
      WRITE(6,420) (BFLO(I),I=1,24)
  420 FORMAT(4F20.5)
      WRITE(6,430) WTO
  430 FORMAT(/5X,'THE ADJUSTED TOTAL BLOOD FLOW IS',
     1F14.5,'CC PER MIN')
      EMET=0.
      DO 440 I=1,8
  440 EMET=EMET+MET(I)
      DO 450 I=9,24
  450 EMET=EMET+2.*MET(I)
      WRITE(6,460)
  460 FORMAT(/5X,'THE ADJUSTED METABOLIC RATES IN THE 24
     1DIFFERENT PARTS ARE')
      WRITE(6,420) (MET(I),I=1,24)
      WRITE(6,470) EMET
  470 FORMAT(//3X,'THE ADJUSTED TOTAL METABOLIC RATE IS'
```

```
     1,F13.5,'CAL PER MIN')
      RETURN
      END


      SUBROUTINE HTCOEF(HT,VOL,BTEM)
C     THIS SUBROUTINE CALCULATES HEAT TRANSFER COEFFICIENTS
C     AND MODIFIES BETA APPROPRIATELY.
      COMMON BETA(6),COEF(24,3),BFLO(24),ISKIN(6),MET(24),
     1COND(24,24),TAMB,SA(6),RESP,P4(6),BP4(6),
     2OMET(24),CBFLO(24),ABFLO,VOLUME(24),SL,DTEMP
     3,OBTEM(24),WEIT,TMAT,ORESP,TIME
      DIMENSION VOL(6),HT(6),TEMP(6)
      DIMENSION BTEM(24)
      DO 36 I=1,6
      J=I*4
      TEMP(I)=BTEM(J)
C     VOL,SA,TEMP,BETA ARE AVAILABLE FOR I OF 1 TO 6.
      HT(I)=HTX(VOL(I),SA(I),TEMP(I),TAMB)
      BETA(I)=1./(1.+BETA(I)*HT(I))
C     THE BETA STATEMENT IS PRESENT BECAUSE BETA IN THE
C     RIGHT HAND SIDE OF THE BETA STATEMENT, WHICH WAS
C     CALCULATED FROM SUBROUTINE CLCOEF IS JUST (P-RP)/RP,
C     WHICH IS NOT YET THE TRUE DEFINITION OF BETA.
 36   COEF(J,3)=-COEF(J,3)*BETA(I)*HT(I)
C     COEF(J,3)  IS THE -(2*P3)/(P3**2-P2**2)*(H*BETA)/
C     (DENSITY*CP)
C     BECAUSE CERTAIN PART OF THE TRUNK SURFACE RESTED ON
C     THE BENCH, SO COEF(8,3)=COEF(8,3)*0.9
      COEF(8,3)=COEF(8,3)*0.9
      RETURN
      END


      FUNCTION HTX(V,SA,BT,TA)
C     THIS CONTAINS THE EMPIRICAL CORRELATION USED FOR
C     THE HEAT TRANSFER COEFFICIENT CALCULATION.
      HRAD=0.87*1.355E-12*((BT+273.)**2+(TA+273.)**2)*
     1(BT+TA+2.*273.)
C     HCOV=(((BT-TA)*1.8*SA/(4.*V*0.03281))**0.25*0.4/7373.
      HCOV=0.750E-4*((BT-TA)*SA/(4.*V))**0.25
      HTX=(HRAD+HCOV)*60.
      RETURN
      END
```

```
      SUBROUTINE CMET(X,BTEM,EXP1,EXP2,EXP3)
C     THIS SUBROUTINE IS USED TO CALCULATE THE METABOLIC
C     RATE OF THE ANIMAL AS THE TEMPERATURE AND TIME
C     CHANGE.
      COMMON BETA(6),COEF(24,3),BFLO(24),ISKIN(6),MET(24),
     1COND(24,24),TAMB,SA(6),RESP,R4(6),FR4(6),
     2OMET(24),CBFLO(24),ABFLO,VOLUME(24),SL,DTEMP
     3,OBTEM(24),WEIT,TMAT,ORESP,TIME
      DIMENSION EXP1(24),EXP2(24),EXP3(24),BTEM(1),OOMET(24)
      REAL MET
      IF (BFLO(5).EQ.0.) GOTO 40
      IF ((BTEM(5)-DTEMP).GE.0.) GOTO 35
      IF (SL.GT.60.) GOTO 20
      IF ((BTEM(5)-43.7).GE.0.) GOTO 15
      DO 10 I=1,24
 10   MET(I)=OMET(I)*(1+EXP1(I))
      RETURN
 15   SL=100.
 20   DO 30 I=1,24
 30   MET(I)=OMET(I)*(1+EXP2(I))
      RETURN
 35   OX=X
      DO 37 I=1,24
 37   OOMET(I)=MET(I)
 40   DO 60 I=1,24
 60   MET(I)=OOMET(I)*2.7183**(-EXP3(I)*(X-OX))
      RETURN
      END


      SUBROUTINE CRESP(BTEM,DETA)
C     THIS SUBROUTINE CALCULATES THE HEAT LOSS DUE TO
C     RESPIRATION BY GAS EXCHANGE AND EVAPORATION AS A
C     FUNCTION OF TEMPERATURE.
      COMMON BETA(6),COEF(24,3),BFLO(24),ISKIN(6),MET(24),
     1COND(24,24),TAMB,SA(6),RESP,R4(6),FR4(6),
     2OMET(24),CBFLO(24),ABFLO,VOLUME(24),SL,DTEMP
     3,OBTEM(24),WEIT,TMAT,ORESP,TIME
      DIMENSION BTEM(1)
C     DETA, THE PROPORTIONAL CONSTANT, AND COUN=0 HAVE
C     BEEN SPECIFIED IN THE SUBROUTINE STPTUP.
C
      IF (BFLO(5).EQ.0.) RETURN
      IF (BTEM(5)-DTEMP) 20,20,40
 20   RESP=ORESP*(1.+DETA*(BTEM(5)-OBTEM(5)))
      RETURN
 40   RESP=0.
      RETURN
      END
```

```
      SUBROUTINE CFLOW(BTEM,ALFA)
C     THIS SUBROUTINE IS USED TO CALCULATE THE BLOOD FLOW
C     RATE OF VARIOUS LAYERS IN DIFFERENT SEGMENTS DURING
C     THE TRANSIENT CONDITIONS.
C     ALFA, THE PROPORTIONAL CONSTANT, AND THE
C     INITIAL CONDITIONS FOR BFLO AND BTEM HAVE BEEN
C     SPECIFIED IN THE SUBROUTINE STRTUP.
      COMMON BETA(6),COEF(24,3),BFLO(24),ISKIN(6),MET(24),
     1COND(24,24),TAMB,SA(6),RESP,R4(6),B4(6),
     2OMET(24),OBFLO(24),ABFLO,VOLUME(24),SL,DTEMP
     3,OBTEM(24),WEIT,TMAT,ORESP,TIME
      DIMENSION ALFA(24),BTEM(24)
C
      IF (BFLO(5).EQ.0.) GOTO 60
      IF (BTEM(5)-DTEMP) 20,20,40
 20   DO 35 J=1,6
      I=4*J-3
      IF (I.EQ.5) GOTO 30
      IF (I.EQ.13) GOTO 28
      IF (I.EQ.21) GOTO 28
      AAB=ABS((BTEM(I)-OBTEM(I))/(OBTEM(5)-OBTEM(I)))
      BFLO(I)=OBFLO(I)*(1.+ALFA(I)*ABS(AAB))
      GOTO 30
 28   BFLO(I)=OBFLO(I)*(1.+ALFA(I)
     1*((BTEM(I)-OBTEM(I))/(OBTEM(I-4)-OBTEM(I))))
 30   ABB=ABS((BTEM(I+1)-OBTEM(I+1))/(OBTEM(I)-OBTEM(I+1)))
      BFLO(I+1)=OBFLO(I+1)*(1.+ALFA(I+1)*ABS(ABB))
      BFLO(I+2)=OBFLO(I+2)*(1.+ALFA(I+2)
     1*((BTEM(I+1)-BTEM(I+2))/(OBTEM(I+1)-OBTEM(I+2))-1.))
 35   BFLO(I+3)=OBFLO(I+3)*(1.+ALFA(I+3)
     1*((BTEM(I+1)-BTEM(I+3))/(OBTEM(I+1)-OBTEM(I+3))-1.))
      IF (BFLO(I+2).LE.0.) BFLO(I+2)=0.
      IF (BFLO(I+3).LE.0.) BFLO(I+3)=0.
      GOTO 60
 40   DO 50 I=1,24
 50   BFLO(I)=0.
 60   CONTINUE
      RETURN
      END


      SUBROUTINE PRNT(XT,PFLO1,APFLO,PFLO6,PFLO9,PFLO10,
     1PFLO17,PFLO18,PTEM1,PTEM5,PTEM6,PTEM7,PTEM8,PTEM9,
     2PTEM10,PTEM12,PTEM18)
C     THIS SUBROUTINE IS USED TO PLOT OUT THE VALUES OF
C     VARIABLES DESIRED IN THE FORM OF GRAPHS.
      COMMON BETA(6),COEF(24,3),BFLO(24),ISKIN(6),MET(24),
     1COND(24,24),TAMB,SA(6),RESP,R4(6),B4(6),
     2OMET(24),OBFLO(24),ABFLO,VOLUME(24),SL,DTEMP
     3,OBTEM(24),WEIT,TMAT,ORESP,TIME
```

```
      DIMENSION XT(120),PFLO1(120),APFLO(120),PFLO6(120),
     1PFLO9(120),PFLO10(120),PFLO17(120),PFLO18(120)
      DIMENSION PTEM1(120),PTEM5(120),PTEM6(120),PTEM7(120)
     1,PTEM8(120),PTEM9(120),PTEM10(120),PTEM12(120),
     2PTEM18(120)
      NTERM=TIME+10
C     CALL GRAPH(NTERM,XT,PFLO1,1,2,5.0,8.,10.,-10.,1500.,
C    10.,'TIME(MIN);','ML PER MIN ;','STRESS PIG;',
C    2'PFLO1;')
C     CALL GRAPHS(NTERM,XT,APFLO,2,2,'APFLO;')
C     CALL GRAPHS(NTERM,XT,PFLO6,3,2,'PFLO6;')
C     CALL GRAPHS(NTERM,XT,PFLO9,4,2,'PFLO9;')
C     CALL GRAPHS(NTERM,XT,PFLO10,5,2,'PFLO10;')
C     CALL GRAPHS(NTERM,XT,PFLO17,7,2,'PFLO17;')
C     CALL GRAPHS(NTERM,XT,PFLO18,6,2,'PFLO18;')
      CALL GRAPH(NTERM,XT,PTEM5,1,2,11.,6.,10.,-10.,2.,34.,
     1'TIME(MIN);','TEMP(DEGREE C);','STRESS PIG;',
     2'PTEM5;')
      CALL GRAPHS(NTERM,XT,PTEM6,3,2,'PTEM6;')
      CALL GRAPHS(NTERM,XT,PTEM7,4,2,'PTEM7;')
      CALL GRAPHS(NTERM,XT,PTEM8,8,2,'PTEM8;')
      CALL GRAPHS(NTERM,XT,PTEM9,2,2,'PTEM9;')
      CALL GRAPHS(NTERM,XT,PTEM10,5,2,'PTEM10;')
      CALL GRAPHS(NTERM,XT,PTEM12,6,2,'PTEM12;')
      CALL GRAPHS(NTERM,XT,PTEM18,7,2,'PTEM18;')
      RETURN
      END
```

APPENDIX B. TEMPERATURE DATA OF MHS ANIMALS

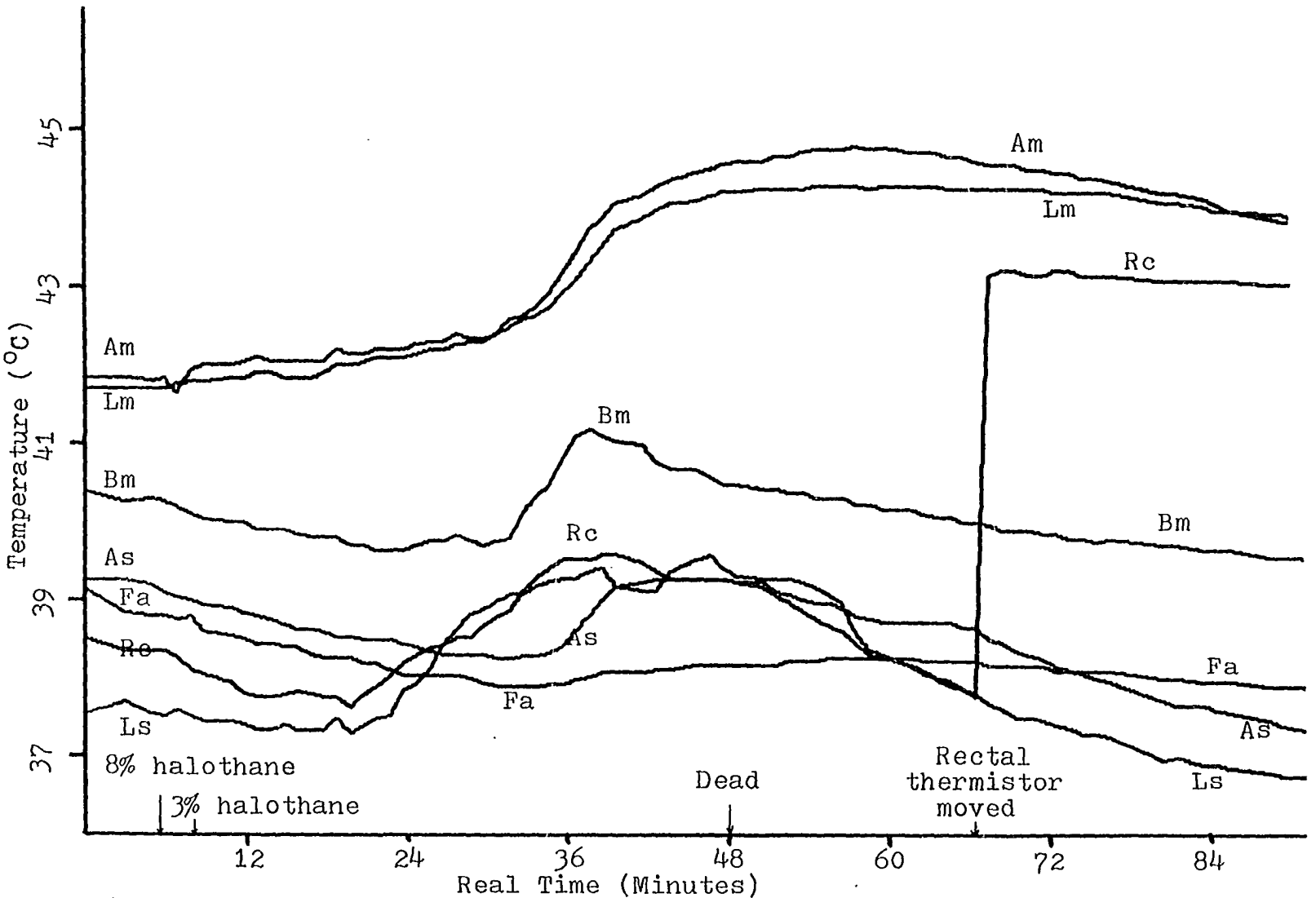

Figure 20. Temperature variation of MHS pig 1

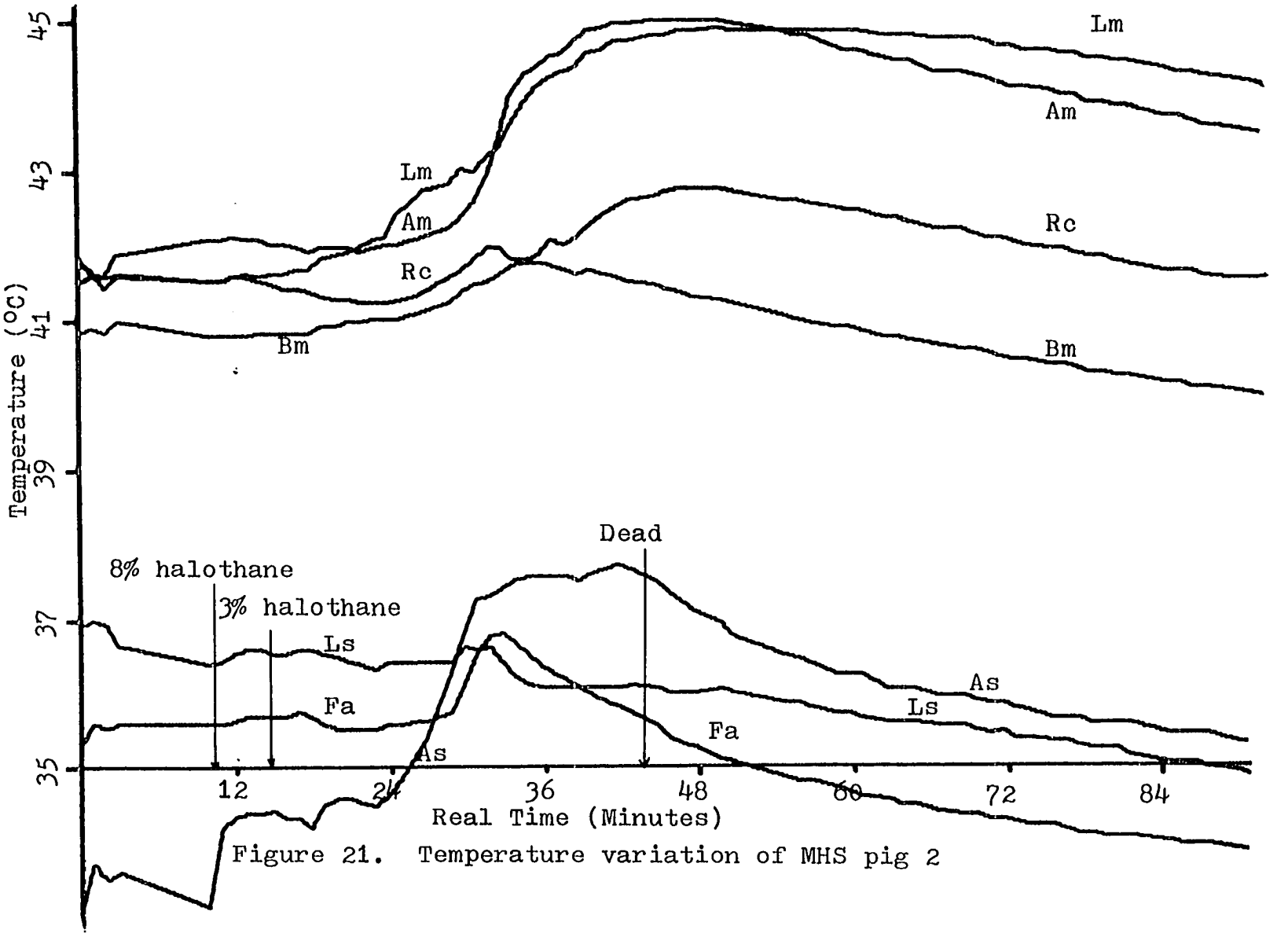

Figure 21. Temperature variation of MHS pig 2

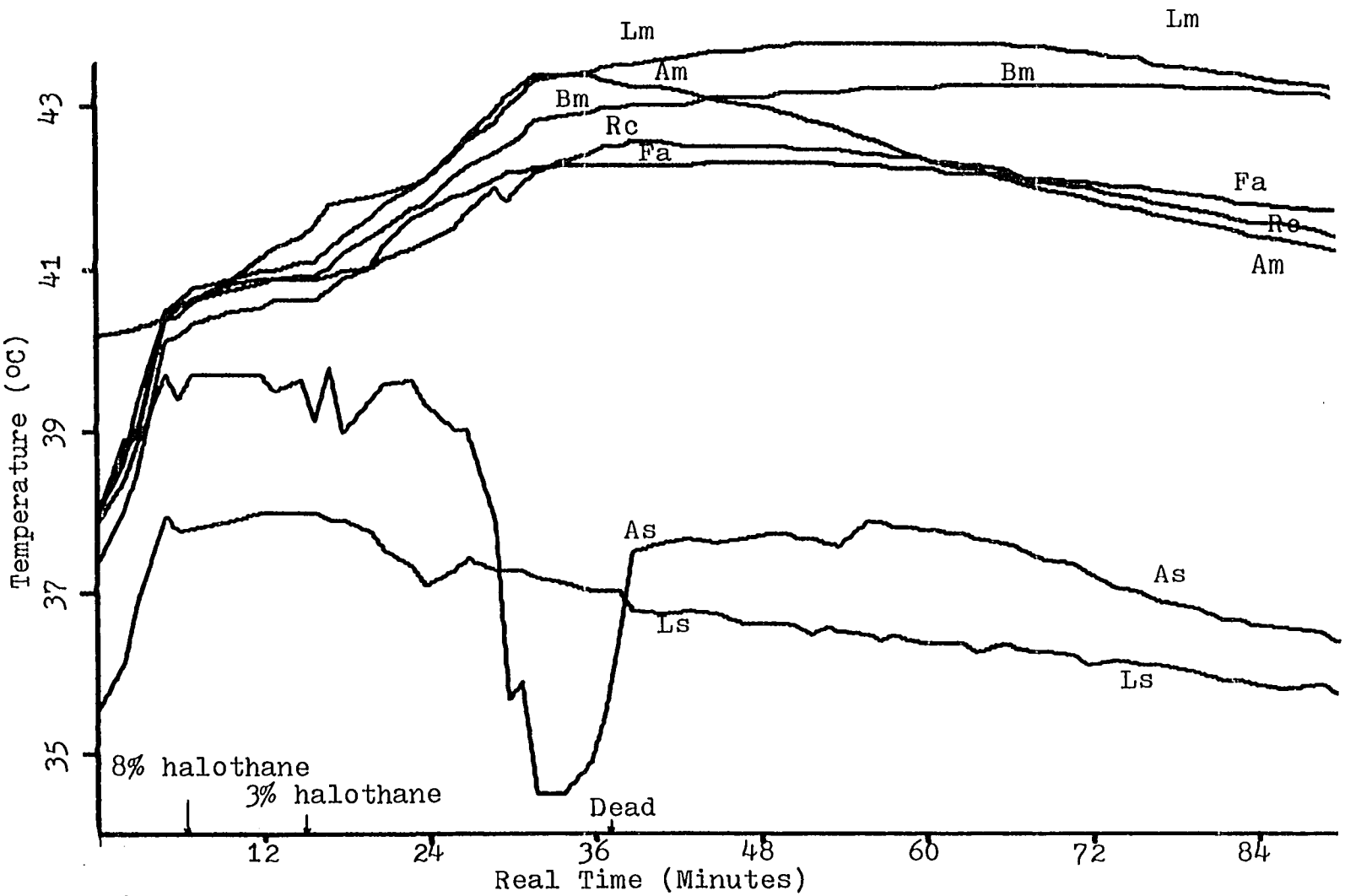

Figure 22. Temperature variation of MHS pig 3

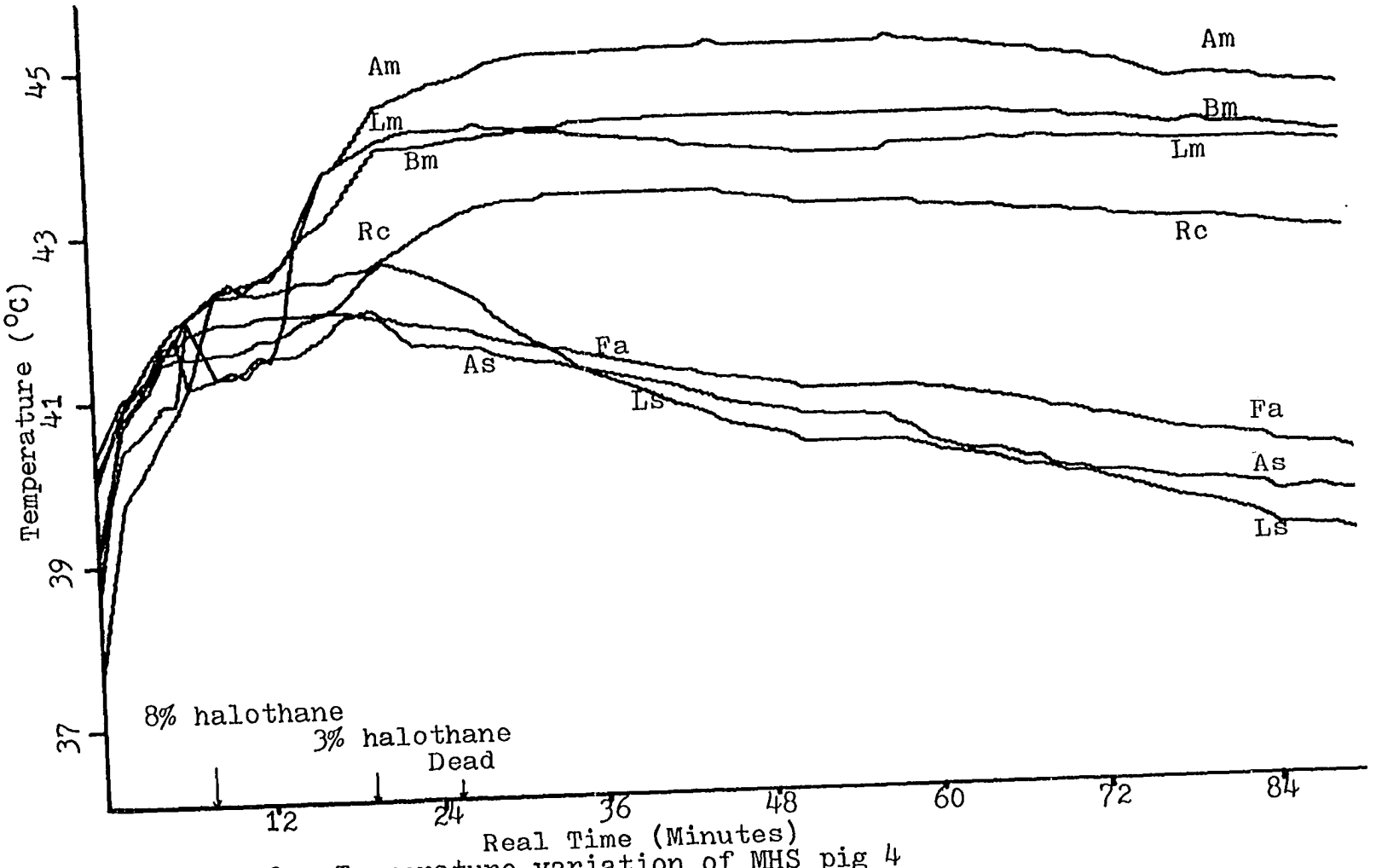

Figure 23. Temperature variation of MHS pig 4

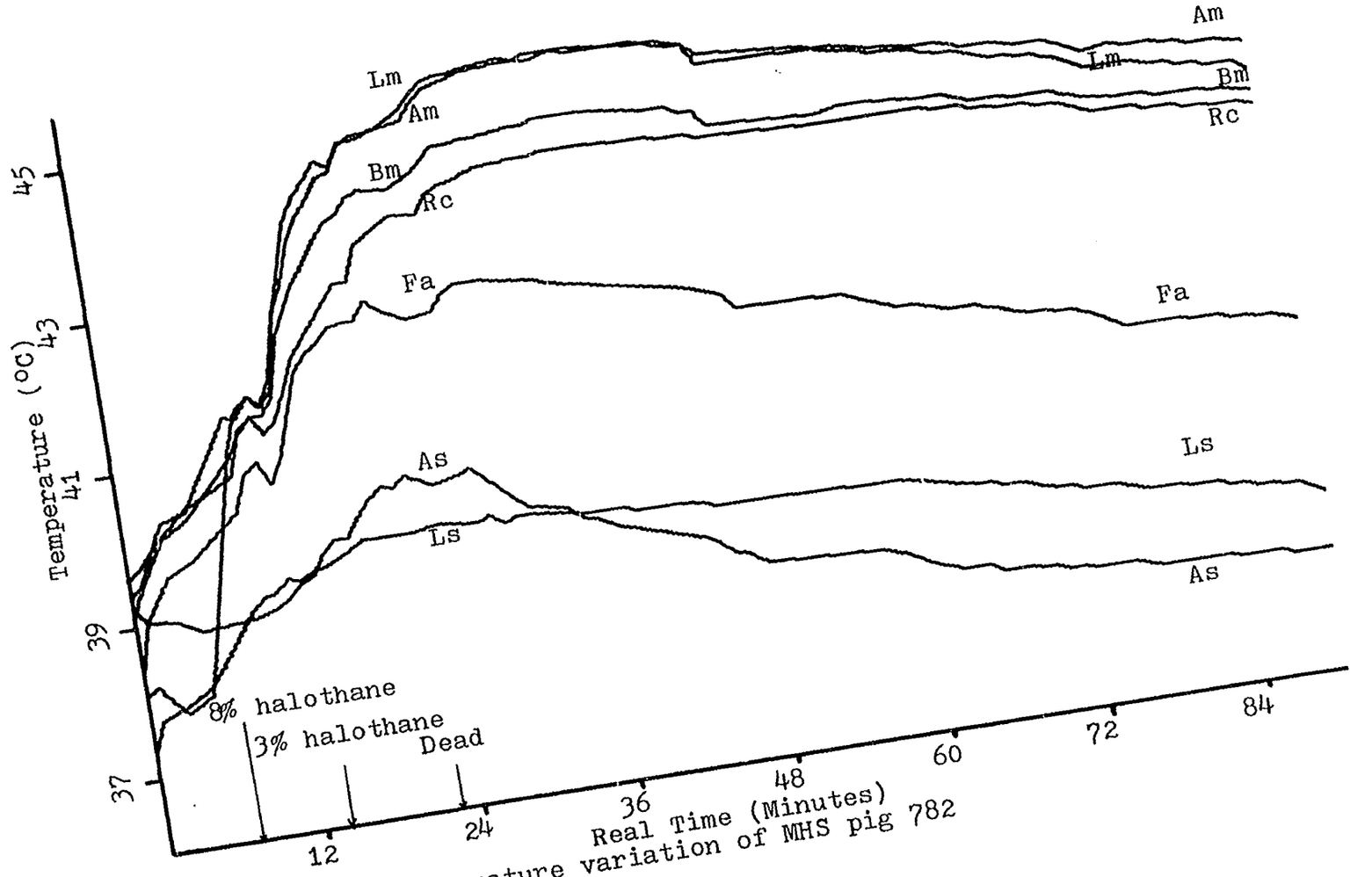

Figure 24. Temperature variation of MHS pig 782

APPENDIX C. BLOOD FLOW DATA OF MHS ANIMALS

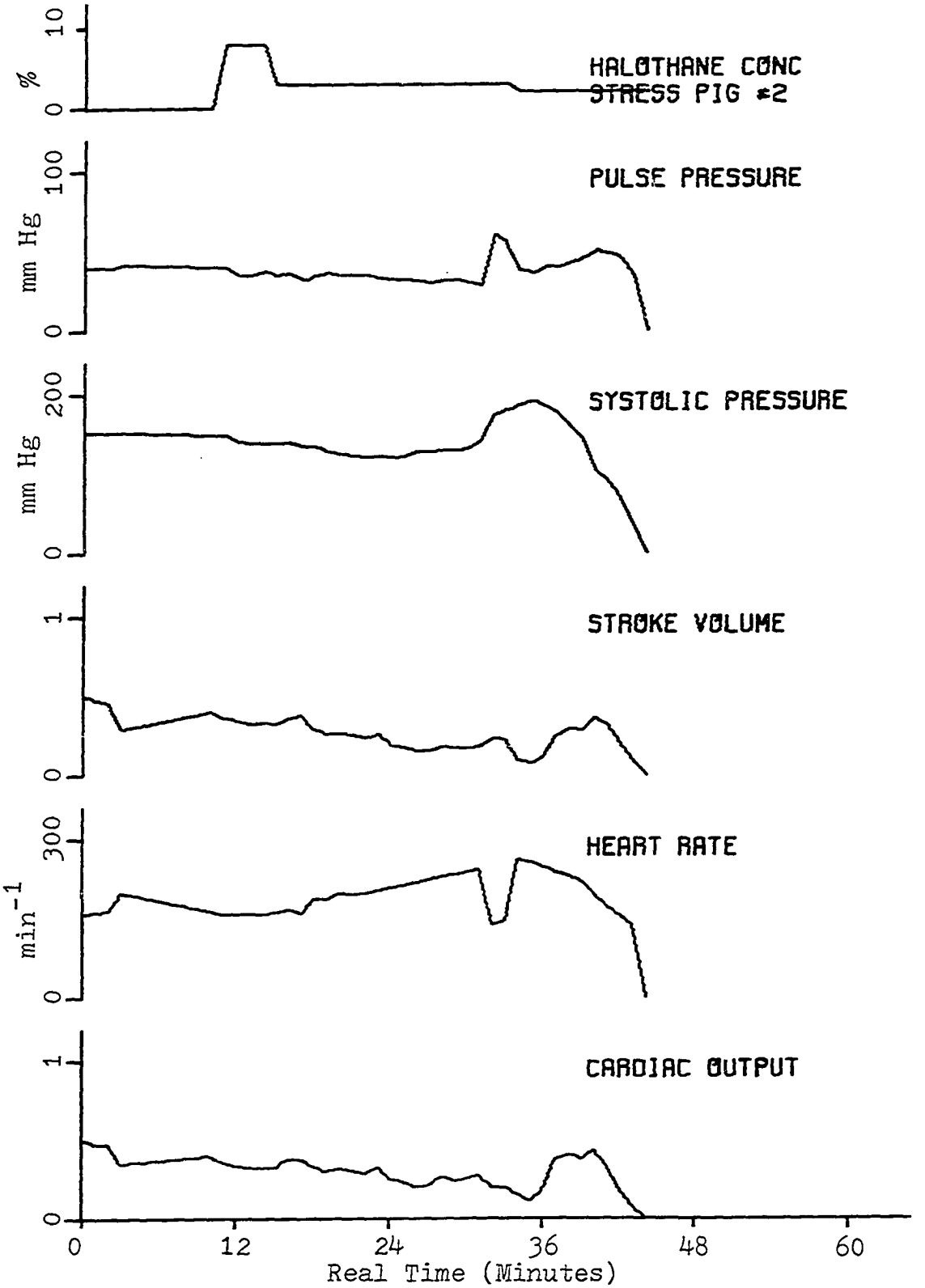

Figure 25. Blood flow information for MHS pig 2

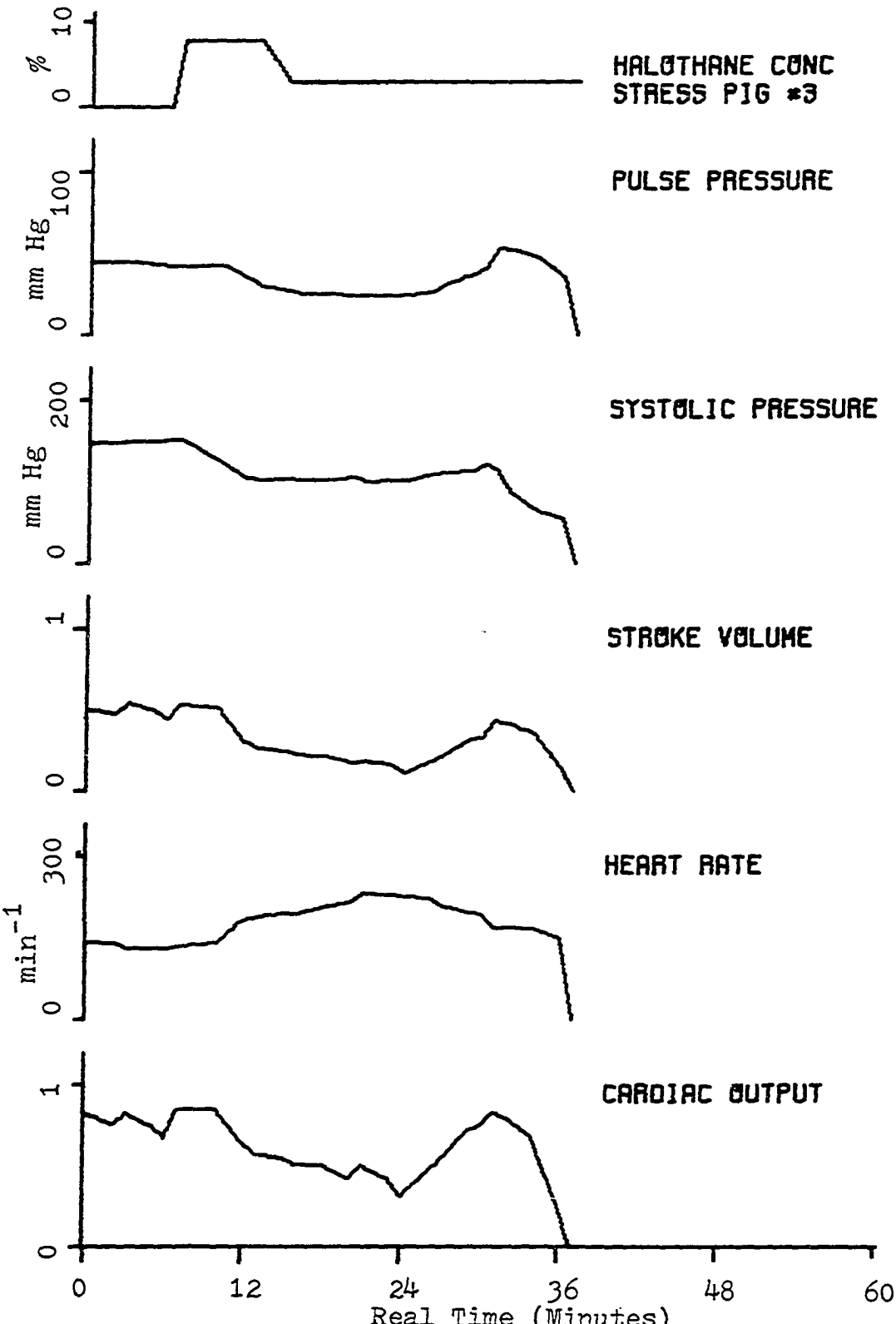

Figure 26. Blood flow information for MHS pig 3

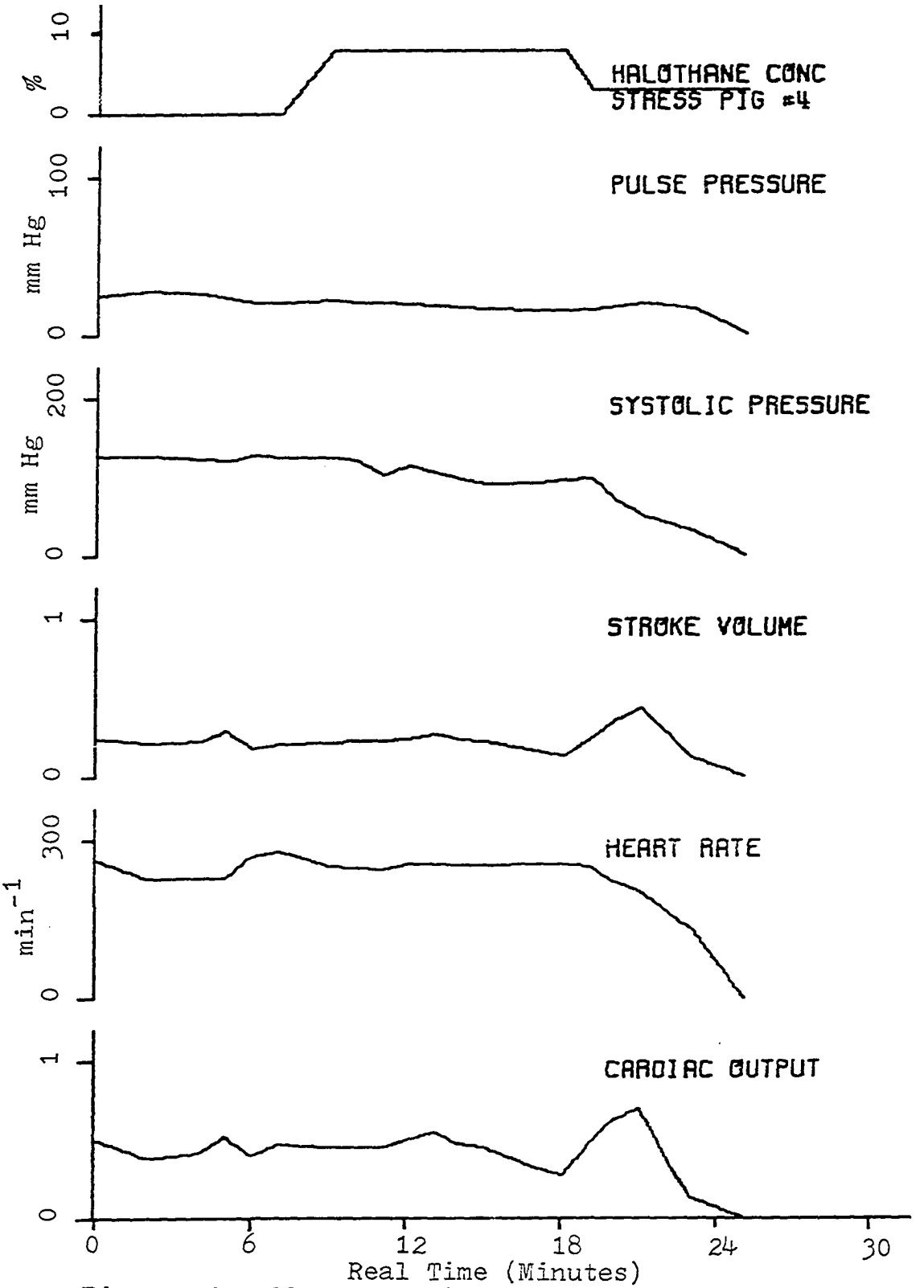

Figure 27. Blood flow information for MHS pig 4

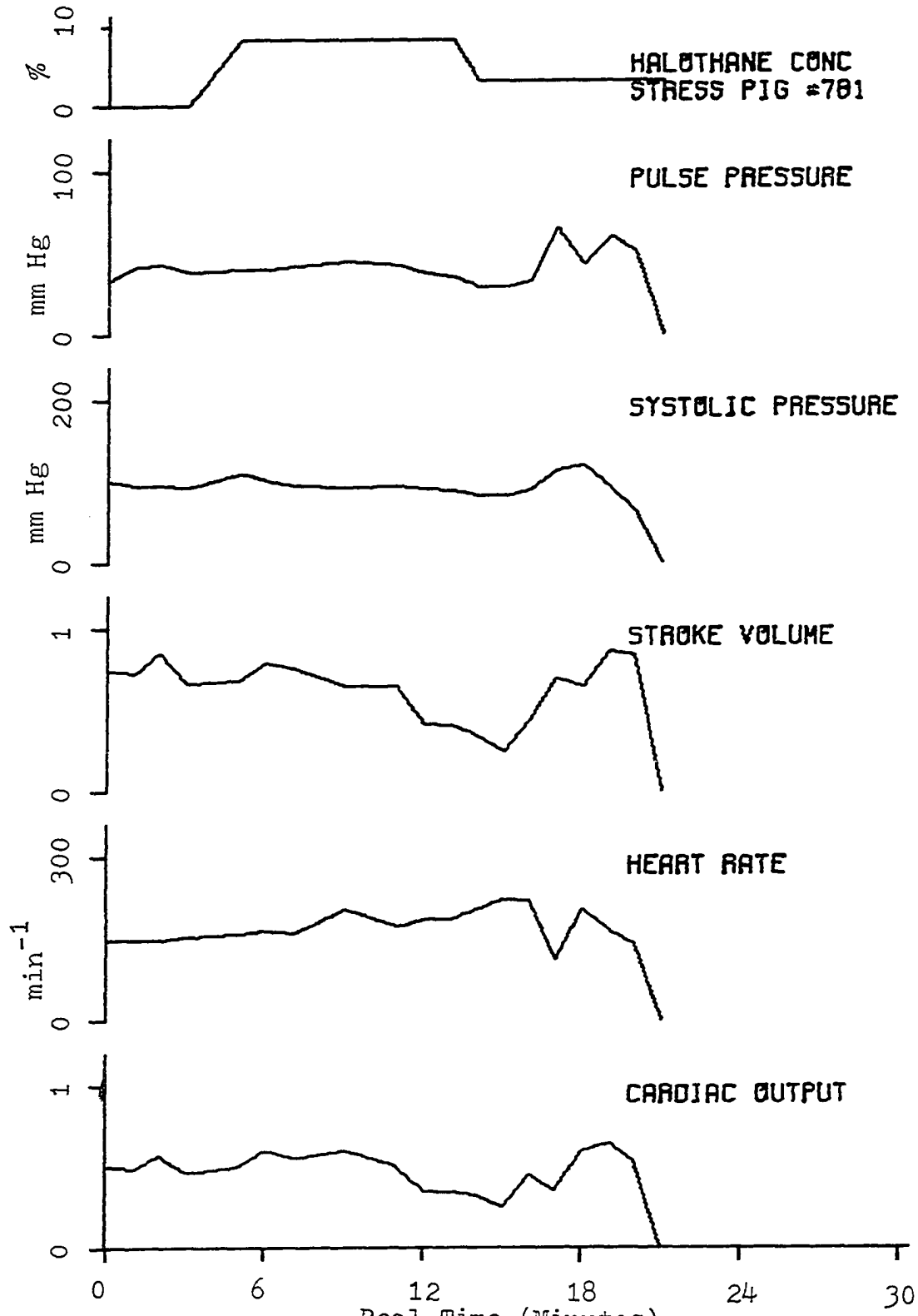

Figure 28. Blood flow information for MHS pig 781

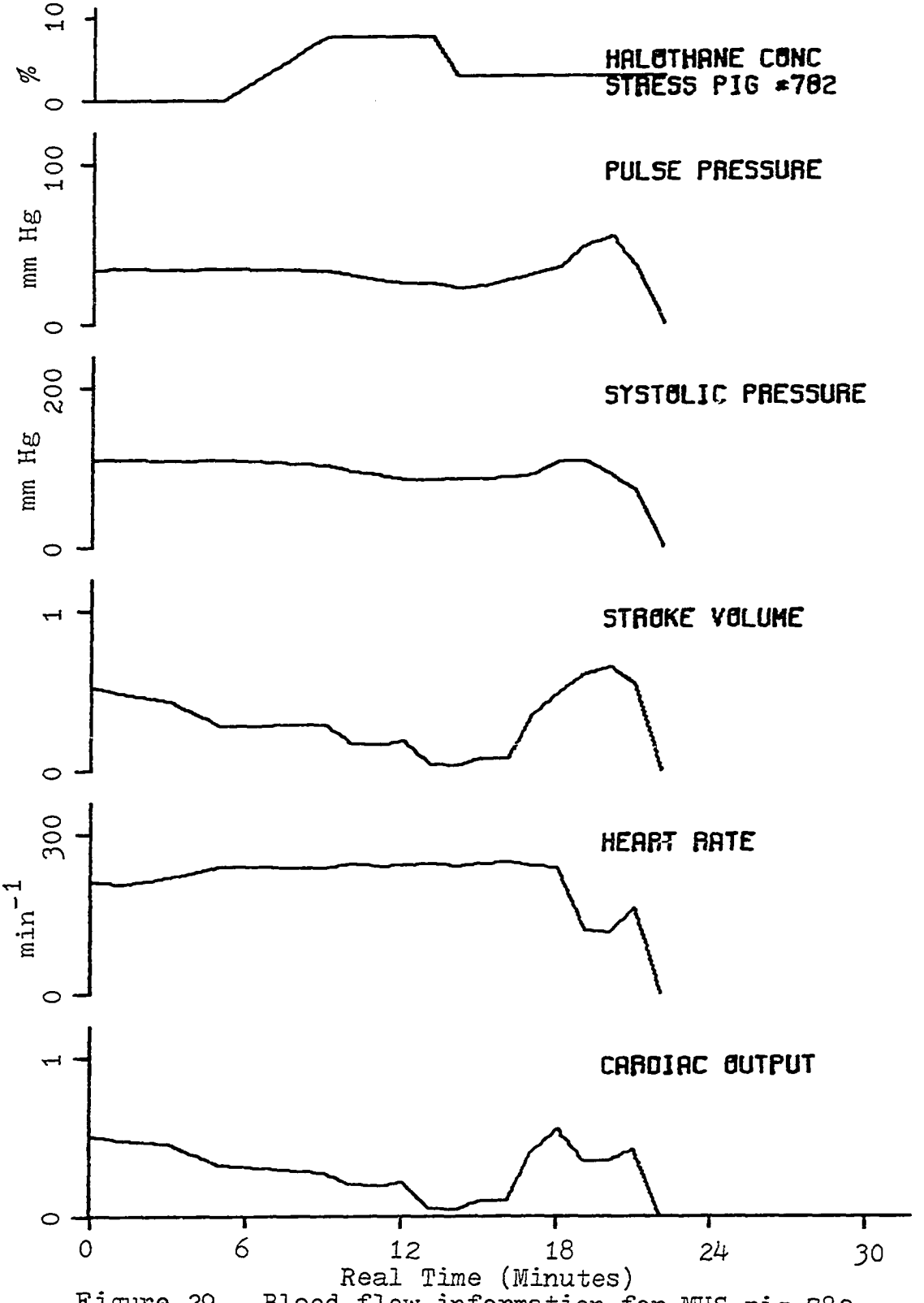

Figure 29. Blood flow information for MHS pig 782

APPENDIX D. BODY COMPOSITION OF THE SWINE[a]

Pig number			1	3	4
Head			12.0	15.9	13.4
Gut			18.5	24.0	15.3
Carcass without head and gut			115.85	125.0	102.2
One side of Carcass			57.15	60.15	52.9
	Ham		14.7	15.8	13.6
		Fat	2.5	1.3	0.85
		Muscle	8.9	10.5	9.75
		Bone	1.8	2.0	1.7
		Skin	1.5	2.0	1.3
	Loin		15.1	18.35	15.3
		Fat	4.1	4.5	2.8
		Muscle	7.7	9.55	8.0
		Bone	2.4	2.5	3.7
		Skin	0.9	1.8	0.8
	Shoulder		12.95	13.7	13.2
		Fat	1.81	1.1	0.4
		Muscle	8.12	8.9	8.6
		Bone	2.0	2.5	2.85
		Skin	1.0	1.2	1.35
	Belly		12.3	10.3	6.8
		Fat	4.0	1.7	0.6
		Muscle	5.9	5.9	4.1
		Bone	1.1	1.6	1.2
		Skin	1.3	1.1	0.9
	Two feet		2.1	2.1	2.0
		Fat	0.1	0.1	0.13
		Muscle	0.5	0.3	0.16
		Bone	0.9	1.1	1.31
		Skin	0.6	0.6	0.4

[a]Weights are in lbs.

APPENDIX E. THE DIFFERENTIAL EQUATIONS

Head

$$\frac{dT_1}{dt} = \frac{2}{r_1}\frac{k_1}{\rho C_{p_1}}\frac{T_2-T_1}{R_2-R_1} + \frac{w_1+w_2+w_3+w_4}{V_1}\frac{\rho C_{p_b}}{\rho C_{p_1}}(T_5-T_1)$$

$$+ \frac{\dot{M}_1}{\rho C_{p_1} V_1} - \frac{RESP}{\rho C_{p_1} V_1}$$

$$\frac{dT2}{dt} = \frac{2r_1}{r_2^2-r_1^2}\frac{k_1}{\rho C_{p_2}}\frac{T_1-T_2}{R_2-R_1} + \frac{2r_2}{r_2^2-r_1^2}\frac{k_2}{\rho C_{p_2}}\frac{T_3-T_2}{R_3-R_2}$$

$$+ \frac{w_2}{V_2}\frac{\rho C_{p_b}}{\rho C_{p_2}}(T_1-T_2) + \frac{\dot{M}_2}{\rho C_{p_2} V_2}$$

$$\frac{dT_3}{dt} = \frac{2r_2}{r_3^2-r_2^2}\frac{k_2}{\rho C_{p_3}}\frac{T_2-T_3}{R_3-R_2} + \frac{2r_3}{r_3^2-r_2^2}\frac{k_3}{\rho C_{p_3}}\frac{T_4-T_3}{R_4-R_3}$$

$$+ \frac{w_3}{V_3}\frac{\rho C_{p_b}}{\rho C_{p_3}}(T_1-T_3) + \frac{\dot{M}_3}{\rho C_{p_3} V_3}$$

$$\frac{dT_4}{dt} = \frac{2r_3}{r_4^2-r_3^2}\frac{k_3}{\rho C_{p_4}}\frac{T_3-T_4}{R_4-R_3} + \frac{w_4}{V_4}\frac{\rho C_{p_b}}{\rho C_{p_4}}(T_1-T_4)$$

$$- \frac{2r_4}{r_4^2-r_3^2}\frac{h\beta}{\rho C_{p_4}}(T_4-T_a) + \frac{\dot{M}_4}{\rho C_{p_4} V_4}$$

Trunk

$$\frac{dT_5}{dt} = \frac{2}{r_5}\frac{k_5}{\rho C_{p_5}}\frac{T_6-T_5}{R_6-R_5} + \frac{w_1}{V_5}\frac{\rho C_{p_b}}{\rho C_{p_5}}(T_1-T_5) + \frac{\rho C_{p_b} w_2 (T_2-T_5)}{\rho C_{p_5} V_5}$$

$$+ \frac{w_3}{V_5}\frac{\rho C_{p_b}}{\rho C_{p_5}}(T_3-T_5) + \frac{w_4}{V_5}\frac{\rho C_{p_b}}{\rho C_{p_5}}(T_4-T_5)$$

$$+ \frac{w_6}{V_5}\frac{\rho C_{p_b}}{\rho C_{p_5}}(T_6-T_5) + \frac{w_7}{V_5}\frac{\rho C_{p_b}}{\rho C_{p_5}}(T_7-T_5)$$

$$+ \frac{w_8}{V_5}\frac{\rho C_{p_b}}{\rho C_{p_5}}(T_8-T_5) + \frac{2(w_9+w_{13})}{V_5}\frac{\rho C_{p_b}}{\rho C_{p_5}}(T_9-T_5)$$

$$+ \frac{2(w_{10}+w_{14})}{V_5}\frac{\rho C_{p_b}}{\rho C_{p_5}}(T_{10}-T_5) + \frac{2(w_{11}+w_{15})}{V_5}\frac{\rho C_{p_b}}{\rho C_{p_5}}(T_{11}-T_5)$$

$$+ \frac{2(w_{12}+w_{16})}{V_5}\frac{\rho C_{p_b}}{\rho C_{p_5}}(T_{12}-T_5) + \frac{2(w_{17}+w_{21})}{V_5}\frac{\rho C_{p_b}}{\rho C_{p_5}}(T_{17}-T_5)$$

$$+ \frac{2(w_{18}+w_{22})}{V_5}\frac{\rho C_{p_b}}{\rho C_{p_5}}(T_{18}-T_5) + \frac{2(w_{19}+w_{23})}{V_5}\frac{\rho C_{p_b}}{\rho C_{p_5}}(T_{19}-T_5)$$

$$+ \frac{2(w_{20}+w_{24})}{V_5}\frac{\rho C_{p_b}}{\rho C_{p_5}}(T_{20}-T_5) + \frac{\mathbb{M}_5}{\rho C_{p_5} V_5}$$

$$\frac{dT_6}{dt} = \frac{2r_5}{r_6^2-r_5^2}\frac{k_5}{\rho C_{p_6}}\frac{(T_5-T_6)}{(R_6-R_5)} + \frac{2r_6}{r_6^2-r_5^2}\frac{k_6}{\rho C_{p_6}}\frac{(T_7-T_6)}{(R_7-R_6)}$$

$$+ \frac{w_6}{V_6}\frac{\rho C_{p_b}}{\rho C_{p_6}}(T_5-T_6) + \frac{\mathbb{M}_6}{\rho C_{p_6} V_6}$$

$$\frac{dT_7}{dt} = \frac{2r_6}{r_7^2-r_6^2}\frac{k_6}{\rho c_{p_7}}\frac{T_6-T_7}{R_7-R_6} + \frac{2r_7}{r_7^2-r_6^2}\frac{k_7}{\rho c_{p_7}}\frac{T_8-T_7}{R_8-R_7}$$

$$+ \frac{w_7}{V_7}\frac{\rho c_{p_b}}{\rho c_{p_7}}(T_5-T_7) + \frac{\mathbb{M}_7}{\rho c_{p_7} V_7}$$

$$\frac{dT_8}{dt} = \frac{2r_7}{r_8^2-r_7^2}\frac{k_7}{\rho c_{p_8}}\frac{T_7-T_8}{R_8-R_7} + \frac{w_8}{V_8}\frac{\rho c_{p_b}}{\rho c_{p_8}}(T_5-T_8)$$

$$- \frac{2r_8}{r_8^2-r_7^2}\frac{h\beta}{\rho c_{p_8}}(T_8-T_a) + \frac{\mathbb{M}_8}{\rho c_{p_8} V_8}$$

Hind leg

$$\frac{dT_9}{dt} = \frac{2}{r_9}\frac{k_9}{\rho c_{p_9}}\frac{T_{10}-T_9}{R_{10}-R_9} + \frac{\sum_9^{16} w_i}{V_9}\frac{\rho c_{p_b}}{\rho c_{p_9}}(T_5-T_9)$$

$$+ \frac{w_{13}}{V_9}\frac{\rho c_{p_b}}{\rho c_{p_9}}(T_{13}-T_9) + \frac{\mathbb{M}_9}{\rho c_{p_9} V_9}$$

$$\frac{dT_{10}}{dt} = \frac{2r_9}{r_{10}^2-r_9^2}\frac{k_9}{\rho c_{p_{10}}}\frac{T_9-T_{10}}{R_{10}-T_9} + \frac{w_{10}}{V_{10}}\frac{\rho c_{p_b}}{\rho c_{p_{10}}}(T_9-T_{10})$$

$$+ \frac{w_{14}}{V_{10}}\frac{\rho c_{p_b}}{\rho c_{p_{10}}}(T_{14}-T_{10}) + \frac{2r_{10}}{r_{10}^2-r_9^2}\frac{k_{10}}{\rho c_{p_{10}}}\frac{T_{11}-T_{10}}{R_{11}-R_{10}}$$

$$+ \frac{\mathbb{M}_{10}}{\rho c_{p_{10}} V_{10}}$$

$$\frac{dT_{11}}{dt} = \frac{2r_{10}}{r_{11}^2-r_{10}^2}\frac{k_{10}}{\rho C_{p_{11}}}\frac{T_{10}-T_{11}}{R_{11}-R_{10}} + \frac{2r_{11}}{r_{11}^2-r_{10}^2}\frac{k_{11}}{\rho C_{p_{11}}}\frac{T_{12}-T_{11}}{R_{12}-R_{11}}$$

$$+\frac{w_{11}}{V_{11}}\frac{\rho C_{p_b}(T_9-T_{11})}{\rho C_{p_{11}}} + \frac{w_{15}}{V_{11}}\frac{\rho C_{p_b}(T_{15}-T_{11})}{\rho C_{p_{11}}} + \frac{\dot{M}_{11}}{\rho C_{p_{11}} V_{11}}$$

$$\frac{dT_{12}}{dt} = \frac{2r_{11}}{r_{12}^2-r_{11}^2}\frac{k_{11}}{\rho C_{p_{12}}}\frac{T_{11}-T_{12}}{R_{12}-R_{11}} - \frac{2r_{12}}{r_{12}^2-r_{11}^2}\frac{h\beta\,(T_{12}-T_a)}{\rho C_{p_{12}}}$$

$$+\frac{w_{12}}{V_{12}}\frac{\rho C_{p_b}(T_9-T_{12})}{\rho C_{p_{12}}} + \frac{w_{16}}{V_{12}}\frac{\rho C_{p_b}(T_{16}-T_{12})}{\rho C_{p_{12}}} + \frac{\dot{M}_{12}}{\rho C_{p_{12}} V_{12}}$$

Hind foot

$$\frac{dT_{13}}{dt} = \frac{2}{r_{13}}\frac{k_{13}}{\rho C_{p_{13}}}\frac{T_{14}-T_{13}}{R_{14}-R_{13}} + \frac{\sum_{13}^{16} w_i}{V_{13}}\frac{\rho C_{p_b}}{\rho C_{p_{13}}}(T_9-T_{13})$$

$$+ \frac{\dot{M}_{13}}{\rho C_{p_{13}} V_{13}}$$

$$\frac{dT_{14}}{dt} = \frac{2r_{13}}{r_{14}^2-r_{13}^2}\frac{k_{13}}{\rho C_{p_{14}}}\frac{T_{13}-T_{14}}{R_{14}-R_{13}} + \frac{2r_{14}}{r_{14}^2-r_{13}^2}\frac{k_{14}}{\rho C_{p_{14}}}\frac{T_{15}-T_{14}}{R_{15}-R_{14}}$$

$$+\frac{w_{14}}{V_{14}}\frac{\rho C_{p_b}}{\rho C_{p_{14}}}(T_{13}-T_{14}) + \frac{\dot{M}_{14}}{\rho C_{p_{14}} V_{14}}$$

$$\frac{dT_{15}}{dt} = \frac{2r_{14}}{r_{15}^2-r_{14}^2}\frac{k_{14}}{\rho C_{p_{15}}}\frac{T_{14}-T_{15}}{R_{15}-R_{14}} + \frac{2r_{15}}{r_{15}^2-r_{14}^2}\frac{k_{15}}{\rho C_{p_{15}}}\frac{T_{16}-T_{15}}{R_{16}-R_{15}}$$

$$+\frac{w_{15}}{V_{15}}\frac{\rho C_{p_b}}{\rho C_{p_{15}}}(T_{13}-T_{15}) + \frac{\dot{M}_{15}}{\rho C_{p_{15}} V_{15}}$$

$$\frac{dT_{16}}{dt} = \frac{2r_{15}}{r_{16}^2-r_{15}^2}\frac{k_{15}}{\rho C_{p_{16}}}\frac{T_{15}-T_{16}}{R_{16}-R_{15}} + \frac{w_{16}}{V_{16}}\frac{\rho C_{p_b}}{\rho C_{p_{16}}}(T_{13}-T_{16})$$

$$- \frac{2r_{16}}{r_{16}^2-r_{15}^2}\frac{h\beta}{\rho C_{p_{16}}}(T_{16}-T_a) + \frac{\mathbb{M}_{16}}{\rho C_{p_{16}} V_{16}}$$

Front leg

$$\frac{dT_{17}}{dt} = \frac{2}{r_{17}}\frac{k_{17}}{\rho C_{p_{17}}}\frac{T_{18}-T_{17}}{R_{18}-R_{17}} + \frac{\sum_{17}^{24} w_i}{V_{17}}\frac{\rho C_{p_b}}{\rho C_{p_{17}}}(T_5-T_{17})$$

$$+ \frac{w_{21}}{V_{17}}\frac{\rho C_{p_b}}{\rho C_{p_{17}}}(T_{21}-T_{17}) + \frac{\mathbb{M}_{17}}{\rho C_{p_{17}} V_{17}}$$

$$\frac{dT_{18}}{dt} = \frac{2r_{17}}{r_{18}^2-r_{17}^2}\frac{k_{17}}{\rho C_{p_{18}}}\frac{T_{17}-T_{18}}{R_{18}-R_{17}} + \frac{2r_{18}}{r_{18}^2-r_{17}^2}\frac{k_{18}}{\rho C_{p_{18}}}\frac{T_{19}-T_{18}}{R_{19}-R_{18}}$$

$$+ \frac{w_{18}}{V_{18}}\frac{\rho C_{p_b}}{\rho C_{p_{18}}}(T_{17}-T_{18}) + \frac{w_{22}}{V_{18}}\frac{\rho C_{p_b}}{\rho C_{p_{18}}}(T_{22}-T_{18}) + \frac{\mathbb{M}_{18}}{\rho C_{p_{18}} V_{18}}$$

$$\frac{dT_{19}}{dt} = \frac{2r_{18}}{r_{19}^2-r_{18}^2}\frac{k_{18}}{\rho C_{p_{19}}}\frac{T_{18}-T_{19}}{R_{19}-R_{18}} + \frac{2r_{19}}{r_{19}^2-r_{18}^2}\frac{k_{19}}{\rho C_{p_{19}}}\frac{T_{20}-T_{19}}{R_{20}-R_{19}}$$

$$+ \frac{w_{19}}{V_{19}}\frac{\rho C_{p_b}}{\rho C_{p_{19}}}(T_{17}-T_{19}) + \frac{w_{23}}{V_{19}}\frac{\rho C_{p_b}}{\rho C_{p_{19}}}(T_{23}-T_{19}) + \frac{\mathbb{M}_{19}}{\rho C_{p_{19}} V_{19}}$$

$$\frac{dT_{20}}{dt} = \frac{2r_{19}}{r_{20}^2-r_{19}^2}\frac{k_{19}}{\rho C_{p_{20}}}\frac{T_{19}-T_{20}}{R_{20}-R_{19}} - \frac{2r_{20}}{r_{20}^2-r_{19}^2}\frac{h\beta}{\rho C_{p_{20}}}(T_{20}-T_a)$$

$$+ \frac{w_{20}}{V_{20}}\frac{\rho C_{p_b}}{\rho C_{p_{20}}}(T_{17}-T_{20}) + \frac{w_{24}}{V_{20}}\frac{\rho C_{p_b}}{\rho C_{p_{20}}}(T_{24}-T_{20}) + \frac{\mathbb{M}_{20}}{\rho C_{p_{20}} V_{20}}$$

Front foot

$$\frac{dT_{21}}{dt} = \frac{2}{r_{21}} \frac{k_{21}}{\rho C_{p_{21}}} \frac{T_{22}-T_{21}}{R_{22}-R_{21}} + \frac{\sum_{21}^{24} w_i}{V_{21}} \frac{\rho C_{p_b}}{\rho C_{p_{21}}} (T_{17}-T_{21}) + \frac{\mathbb{M}_{21}}{\rho C_{p_{21}} V_{21}}$$

$$\frac{dT_{22}}{dt} = \frac{2r_{21}}{r_{22}^2-r_{21}^2} \frac{k_{21}}{\rho C_{p_{22}}} \frac{T_{21}-T_{22}}{R_{22}-R_{21}} + \frac{2r_{22}}{r_{22}^2-r_{21}^2} \frac{k_{22}}{\rho C_{p_{22}}} \frac{T_{23}-T_{22}}{R_{23}-R_{22}} + \frac{w_{22}}{V_{22}} \frac{\rho C_{p_b}}{\rho C_{p_{22}}} (T_{21}-T_{22}) + \frac{\mathbb{M}_{22}}{\rho C_{p_{22}} V_{22}}$$

$$\frac{dT_{23}}{dt} = \frac{2r_{22}}{r_{23}^2-r_{22}^2} \frac{k_{22}}{\rho C_{p_{23}}} \frac{T_{22}-T_{23}}{R_{23}-R_{22}} + \frac{2r_{23}}{r_{23}^2-r_{22}^2} \frac{k_{23}}{\rho C_{p_{23}}} \frac{T_{24}-T_{23}}{R_{24}-R_{23}} + \frac{w_{23}}{V_{23}} \frac{\rho C_{p_b}}{\rho C_{p_{23}}} (T_{21}-T_{23}) + \frac{\mathbb{M}_{23}}{\rho C_{p_{23}} V_{23}}$$

$$\frac{dT_{24}}{dt} = \frac{2r_{23}}{r_{24}^2-r_{23}^2} \frac{k_{23}}{\rho C_{p_{24}}} \frac{T_{23}-T_{24}}{R_{24}-R_{23}} - \frac{2r_{24}}{r_{24}^2-r_{23}^2} \frac{h\beta}{\rho C_{p_{24}}} (T_{24}-T_a) + \frac{w_{24}}{V_{24}} \frac{\rho C_{p_b}}{\rho C_{p_{24}}} (T_{21}-T_{24}) + \frac{\mathbb{M}_{24}}{\rho C_{p_{24}} V_{24}}$$